

**A SELF-REDUCING RANGE-FINDER WITH
AN AUTOMATIC REGISTRATION SYSTEM**

PRINTED IN THE NETHERLANDS BY W. D. MEINEMA N.V., DELFT

NETHERLANDS GEODETIC COMMISSION

PUBLICATIONS ON GEODESY

NEW SERIES

VOLUME 3

NUMBER 1

A SELF-REDUCING RANGE-FINDER
WITH AN AUTOMATIC
REGISTRATION SYSTEM

BY

DR. IR. M. J. M. BOGAERTS

1969

RIJKSCOMMISSIE VOOR GEODESIE, KANAALWEG 4, DELFT, NETHERLANDS

CONTENTS

1	INTRODUCTION	7
1.1	Automation with the bearing and distance method	7
1.2	Principle of optical distance measurement	9
1.3	Optical distance-measuring instruments having an automatic registration system	10
2	PRINCIPLE OF THE NEW OPTICAL DISTANCE-MEASURING EQUIPMENT	13
3	OPTICAL SECTION	17
3.1	Distance measurement and reduction of the distances measured to the horizontal	17
3.2	Path of the rays through the optical elements used	21
3.3	Calculation of the anticipated deviations in the measuring result	34
3.4	Height measurement	43
3.5	The telescope and image separation	45
4	SOME CONCEPTS IN SWITCHING ALGEBRA	47
5	CODED DISKS	50
5.1	Analogous-digital conversion of a rotation	50
5.2	The use of a progressive-binary code (Gray code)	52
5.3	Angular measurement	54
5.4	Measurement of distance and height	57
5.5	Production of the coded disks	60
5.6	Investigation of the accuracy of the coded disks	66
6	ELECTRONIC SECTION	75
6.1	Brief survey of the electronic section	75
6.2	The logical switching circuits used	78
6.3	The input of basic data by means of thumb-wheel switches	80
6.4	The registering section and the magnetic-tape memory	82
6.5	The reading section and the punch	89
7	COMPUTING PROGRAMMES	94
7.1	The pre-programme of tacheometry	94
7.2	The main programme of tacheometry	96
7.3	The programmes for checking the detail survey, for the area calculation and mapping	97
8	CONCLUSIONS	102
	REFERENCES	105
	SUMMARY	107
	SAMENVATTING	109

1 INTRODUCTION

1.1 Automation *) with the bearing and distance method

During the period from 1963 to 1966 experiments were conducted in the Geodetic Institute of the Delft University of Technology with a view to ascertaining by what methods the observations recorded with present-day optical distance-measuring equipment could be processed automatically to the best advantage.

This investigation consisted of the following three items:

1. Finding a data carrier for the observations whereby automatic operation could be put into service as early as possible in the process.
2. Automatically processing the data obtainable with the various types of optical distance-measuring instruments into coordinates in the rectangular x, y, z coordinate system.
3. Automating, with the aid of these coordinates, the operations of checking the measurements, calculating the areas of the plots surveyed and making drawings of these plots together with the buildings on them.

The formulation of the computing programmes for the computers IBM 1620 and IBM 360 proved no easy task. The following conditions had to be taken into account:

- The large number of possibilities that may occur in a traverse measurement (different cases of eccentric set-ups at substations, traversing with check bearings, etc.).
- The numbering of the traverse points in a network of traverses.
- The large number of errors for which the traverse measurement has to be tested.
- The great variety of optical distance-measuring appliances. The observations to be processed with the computing programmes designed may originate from double-image tacheometers, range-finders, stadia line and diagram tacheometers. Among the first three types there are self-reducing and non-reducing distance-measuring appliances. For determination of the height differences, stadia readings may be taken or readings on a vertical circle with a grade or tangent division.

All the difficulties were finally overcome. A series of four computing programmes was produced. In the *Pre-Programme of Tacheometry* the observations collected in the field are made suitable for processing in the *Main Programme of Tacheometry*. In this second programme the closing errors of the traverses are calculated, the traverse measurements checked and finally the coordinates of all the control points calculated. With the aid of the programme *Check Programme of Tape Measurements* the detail measurement is checked for measuring errors and it is investigated whether the area calculation of all the plots surveyed can be carried out.

In the programme *Area Calculation and Drawing*, the areas of the plots are finally computed and the drawing instructions for the electronic drawing machine recorded, if desired, on a punched tape, on punched cards or on magnetic tape.

*) According to the definition of Prof. Dr. Ir. C. J. D. M. VERHAGEN automation is the systematic adoption of self-acting systems which, for a certain period, can function entirely or to a large extent without human intervention.

As these programmes may also be used for the new distance-measuring equipment which is described in this thesis, these programmes will be dealt with in greater detail in chapter 7. The original *Pre-Programme of Tacheometry* undergoes a change due to the very varied input of data.

A very troublesome problem was that of finding a good data carrier for the observations. The most cumbersome method for this is to record the observations on punched documents. These data are punched at a later stage, after which further automatic processing is effected. It is clear that a method of this kind involves considerable drawbacks. Punching takes up much time. A punch typist can at the utmost punch 10 000 letters or digits per hour, but with punched documents that are not so well filled in this number at once drops by thousands. Moreover, in the case of punching that is put out to a service bureau the waiting times have to be considered. Punching may cost much money as compared with the other operations, but the greatest drawback is undoubtedly the source of errors which it introduces. Experience has shown that an average of three out of every thousand touches are erroneous.

All these drawbacks impelled us to search for a data carrier which could be put into service more directly in the automated process. This was found in the shape of the *mark-sensing* card. On this card a mark is placed against the figures with a pencil provided with an electrographite lead. A transfer interpreter scans the cards with block brushes. When a conductive graphite line is passed in course of scanning, a hole is punched in this card or in an accompanying card. In this way punched cards are obtained which can be further processed in an electronic computer.

The frequent objection that mark-sensing cards are not easily legible and are on this account unsuitable for use in measurements in which checks have to be made in the field, has already been sufficiently superseded by experience. In [42] a description is given of the system in which these mark-sensing cards are used.

Compared with the processing of the data on the conventional field sheets, the adoption of mark-sensing cards was a substantial improvement. Nevertheless there were still some practical drawbacks attaching to this method, viz.:

- On one side of the card only 27 lines (each with 12 positions) can be marked. For this reason a large number of cards is necessary for a survey.
- A special pencil is required for marking the card.
- The cards are not proof against rain, creasing, etc.
- Great care has to be taken in erasing erroneously placed lines.
- The card has to be filled up on a hard background. If the card is pressed slightly during the placing of a mark, the transfer interpreter cannot observe this mark by means of its scanning mechanism.

Within the framework of the investigation efforts were made to find a new way of registration which meets the aforementioned drawbacks. The data sheets that are read by the *Optical Mark Page Reader IBM 1232* were found very suitable for tacheometry. On each of the two sides of the data sheet a maximum of 1000 positions can be marked with an ordinary lead pencil. The data sheets were read with an apparatus containing a number of lamps and photo-electric cells. A lamp emits a ray of light which is reflected by the paper to the corresponding photo-electric cell. The paper slides along under the luminous sources in the page reader. When the ray passes a black pencil mark it is no longer reflected but is absorbed. This yields a signal for the punch which is coupled to the page reader to make

a punched hole in a card. In this way two punched cards are made of each data sheet. These data sheets, which are described in detail in [2], offer the further advantage that shrinkage due to rain and the like, creasing of the forms and erasing does not cause any errors in the punch.

The data sheets are found to be highly serviceable in practice. An improvement may be possible in future if use is made of a data carrier on which the digits recorded are read by means of a scanning system. See [3]. It is probable that in this direction no efforts need be made towards further automation of the recording of observations obtained with optical distance-measuring equipment.

An important point in this research is that no alteration at all was needed in the existing optical distance-measuring equipment itself. The measuring data of all the instruments can be processed by the calculating and drawing programmes via this system.

Meanwhile it has been established from measuring experience that for efficient working the field party should consist of five persons. The members of this field party have the following functions: 1 partyleader, 1 operator, 1 booker and 2 staff men. If the observations obtained with optical distance-measuring equipment can be registered automatically, the booker in the field party is redundant and the party may be reduced to 4 persons. This aspect of automation of the measuring method is considered so important that some manufacturers of geodetic instruments have already begun to construct optical distance-measuring equipment with automatic registration.

In the present thesis a description is given of a new optical distance-measuring instrument which is equipped with an automatic registration system and which deviates in various respects from existing instruments.

1.2 Principle of optical distance measurement

In order that some of the possibilities of automatic registration in connection with optical distance-measuring instruments may be further examined, the principle of optical distance measurement will first be dealt with more fully from this viewpoint.

With all the existing forms of optical distance-measuring equipment the measurements are taken according to the method of survey by bearing and distance. As a rule a bearing, a distance and, in some cases, a height difference is measured between two points with an optical distance-measuring instrument. From the first two values the x and y coordinates of the point are determined and, with the measured height difference, the z coordinate.

a. The bearing measurement

With optical distance-measuring instruments, as with a theodolite, the bearing measurement is taken by reading the graduated scale on a horizontal circle.

b. The distance measurement

For distance measurement the basis taken with all optical distance-measuring instruments is a parallactic triangle.



Fig. 1.1

The distance l to be measured is given by the formulae:

$$l = b \cot \delta \quad \text{or} \quad l = \frac{1}{2} b \cotg \frac{1}{2} \delta \quad \dots \dots \dots (1.1)$$

In these formulae, b is a survey staff intercept on a horizontal or vertical survey staff. As δ is of the order of $1/100$ radian, the two formulae may for the purpose of mathematical calculations be equated with each other.

A factor which complicates distance measurement is the reduction of a trigonometric slope distance to its horizontal projection. As the surveyor is usually only concerned with the latter quantity, an automatic reduction mechanism is incorporated in most optical distance-measuring equipment. If the measurement is to a point at an angle of inclination α , this means that with a vertical survey staff the horizontal distance $l = \frac{1}{2} \cot \frac{1}{2} \delta \cdot b \cdot \cos^2 \alpha$ and with a horizontal survey staff $l = \frac{1}{2} \cot \frac{1}{2} \delta \cdot b \cdot \cos \alpha$. See [27].

As a rule a measurement with an optical distance-measuring instrument is not carried beyond 100 m. If the distance is greater, atmospheric disturbance affects the accuracy too much. Still, there are optical distance-measuring instruments in existence with which measurements up to 600 m can be effected, but their accuracy is not very high.

The relative accuracy of distance measurement with optical distance-measuring equipment lies between $1 : 10^4$ and $1 : 10^3$, which means that the standard deviation lies between 1 cm and 1 dm per 100 m.

With most distance-measuring instruments the accuracy with which the horizontal circle can be read is balanced against the accuracy with which the distance can be measured.

c. Measurement of height difference

Measurement of the height difference between the position of the instrument and the target resolves itself into three distinct operations:

1. determination of the height of the apex of the parallax triangle;
2. determination of the height of the point of observation on the survey staff;
3. measurement of the height difference between the quantities mentioned under (1) and (2).

The height difference mentioned under (3) can be determined from a reading on a survey staff or on the vertical circle of the instrument. This circle may be provided with a grade or tangent division. In many cases (e.g., with cadastral measurements), no height difference is determined.

1.3 Optical distance-measuring instruments having an automatic registration system

Optical distance-measuring instruments may be divided into two groups. Starting from figure 1.1 and the formula $l = b \cot \delta$, it is found that for a given survey staff intercept b the measurement of the parallax angle δ gives the desired l , whereas for a given δ the length l is found from the measurement of a survey staff intercept b . The optical distance-measuring instrument belonging to the first group consists of a theodolite (variable δ) and a survey

staff of fixed intercept, which is usually 2 m. The second group of optical distance-measuring equipment consists of an instrument equipped with a construction by means of which an invariable parallactic angle δ can be formed (by means of a prism, diagram, etc.), with which instrument a variable survey staff intercept b can be measured.

It is not surprising that with automation of registration the best examples are to be found with theodolites and not with distance-measuring instruments of variable survey staff intercept. Automation in the case of theodolites offers some advantages:

- There is no difference whatever between observation of the angles in the traverse and the parallactic angles. The same horizontal circle may be used for the registration of both quantities.
- With a theodolite and a subtense bar the reduced distance can at once be measured.
- A theodolite with an automatic registration system can be used for other purposes as well.

The principles of some theodolites equipped with an automatic registration system will now be stated in brief.

The first representative of this group is a code theodolite made by the firm of FENNEL. This second theodolite is provided with a horizontal circle with a coded scale of graduations. After aiming at the target the position is photographed on a 35 mm film. Registration is digital up to 0.1 grade. The remaining analogous part is obtained by imaging two diametrical positions of circles on the strip of film. A graduation of one image serves as index for the other.

The station number, detail number, etc. having been set on an indicator, are included in coded form on the photograph taken. This theodolite is used in conjunction with a processing instrument, the Z 84 of the firm of ZUSE, which converts the data of the film into a punched tape.

A second theodolite is the *Digigon* of the firm of BREITHAUPT. This instrument is equipped with a horizontal circle provided with 5000 black and white lines. The rotational movements of the circle are converted into periodic pulses via a lamp and a photo-electric cell. This *Winkelschrittgeber* is manufactured by the firm of LEITZ. A so-called interpolator which can subdivide the pulses into units of 10 decimilligrades is likewise incorporated in the instrument. A calculator which can add and subtract must be fitted to the theodolite. In order to arrive at automatic registration a punched-tape apparatus is fitted to this calculator.

The third instrument dealt with is the *Kern Registering Tacheometer*. In registering the observations with this instrument the same coded film strip is used as with the Fennel theodolite. The data on this strip are also processed into a punched tape in the Zuse Z 84. As regards angular measurement the two theodolites may be considered identical. In distance measurement an important difference occurs. The instrument is equipped with a subtense bar. By rotating a Boscovic prism system contained in the telescope two targets on the survey staff can be set in coincidence. According to the firm of KERN it is not possible, on account of various technical difficulties, to make the total range of the prism system so great that with one base a measuring range of from 2.5 to 150 m can be obtained. For this reason, marks for different distances are made on the survey staff. In this way three subtense bars of different lengths are obtained. In order to tell what base has been used, the position of the central focussing lens is included in the photograph.

A few more examples may be mentioned of these theodolites, in which the automatic registration is effected in different ways. These instruments, however, are still in the stage of research.

Notwithstanding the fact that the automation of the registration system is easier than in optical distance-measuring equipment with a variable staff intercept, the measuring process with the first-mentioned group of instruments takes longer than with the second group. Great care must be exercised in mounting a subtense bar, both for horizontal setting and for positioning perpendicular to the measuring direction. In the case of measurement with a variable parallactic angle at least two observations must be carried out. For the purpose of reading a staff intercept this number is only one.

In the past it has also been found that an optical detail survey has hardly ever been carried out with a theodolite and subtense bars, but with instruments having a fixed parallactic angle.

2 PRINCIPLE OF THE NEW OPTICAL DISTANCE-MEASURING EQUIPMENT

If it is desired to provide an optical distance-measuring instrument with an automatic registration system and one does not wish to use the theodolite in conjunction with the subtense bar, the choice will obviously be in favour of a range-finder. With a range-finder the apical angle δ of the parallax triangle is usually formed with the aid of a prism system (Todis of Breithaupt, BRT 006, Teletop of Zeiss, etc.). The survey staff on which the distance is read forms part of the instrument itself. The apex of the parallax triangle is situated at the point to be determined. In this case, when designing an automatic registration system one need not in principle reckon with a survey staff which is placed by a staff man on the points to be determined.

Fig. 2.1 represents the part of the new optical distance-measuring equipment which is used in the field. The field instrument equipment consists of a self-reducing range-finder provided with three coded disks and a cabinet in which the automatic registration of the measuring data is effected. The system furthermore comprises an electronic instrument for reading the memory element in which the observations are stored and a card-punching machine (see figure 2.2).

The measuring data to be finally collected in the form of punched cards undergo several arithmetical processing operations by means of the four calculating programmes mentioned in section 1.1. These programmes are discussed in detail in chapter 7.

Apart from the mechanical section there are three important parts to be differentiated in the field instrument equipment: the optical system, the coded disks and the electronic machinery. These parts are dealt with at length in chapters 3, 5 and 6.

By means of the optical part a direct distance-measurement can be effected between the setting-up at a station and the target, which are not situated at the same level. Moreover, the horizontal distance and the height difference between these two points can be measured. The distance between the shiftable pentaprisms on the base rail (see Nos. 1 and 2 in figure 2.1) is a measure for these three quantities.

The optical part consists of a number of pentaprisms and triangular prisms and a telescope in which a Fresnel prism for image separation is incorporated. The principle of distance and height measurement is dealt with in sections 3.1 and 3.4.

The movement of the shiftable pentaprisms is transmitted by means of a toothed bar and a number of gear wheels to a rotatable coded disk. This optical coded disk is provided with a special binary code, the so-called *Gray code*. Owing to the fact that the disk has 13 tracks, it is divided into $2^{13} = 8192$ sectors. The disk is read with the aid of a small lamp and 13 photo-electric cells. In section 5.4 the method of distance and height measurement with this disk is further elucidated.

The angular measurement is registered with the aid of the two other coded disks (see section 5.3). In this device the main disk is divided into $2^{10} = 1024$ sectors. There is also a track of lines on this disk.

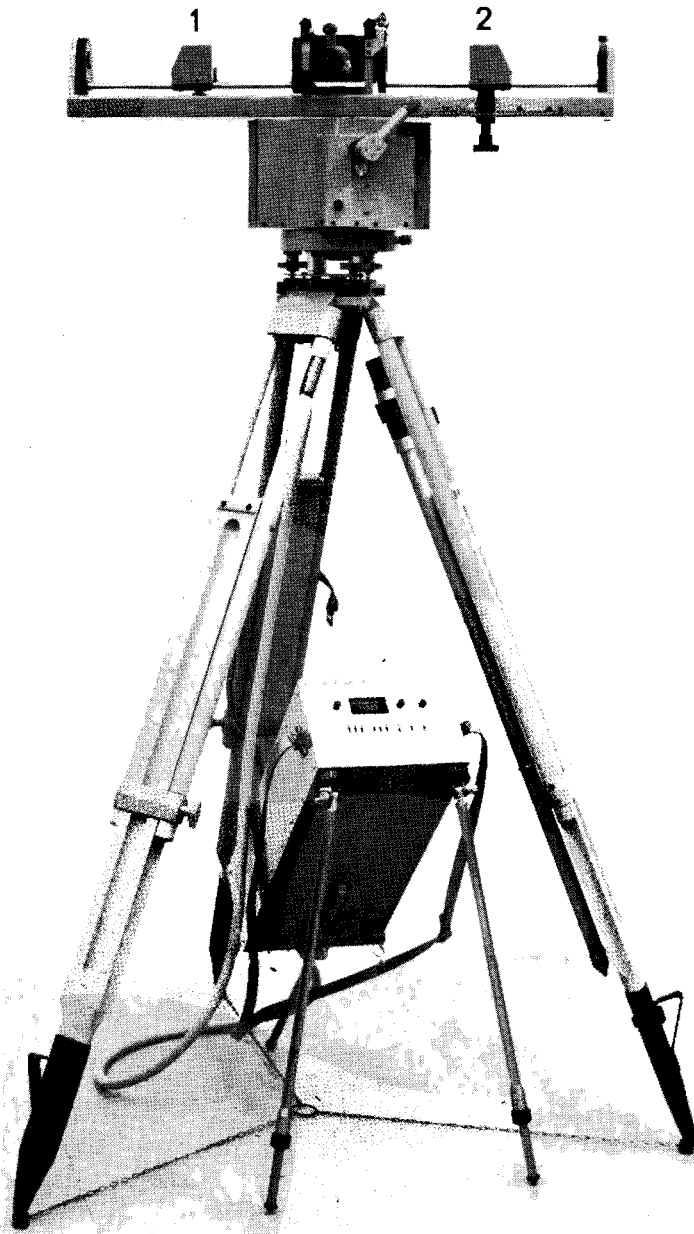


Fig. 2.1

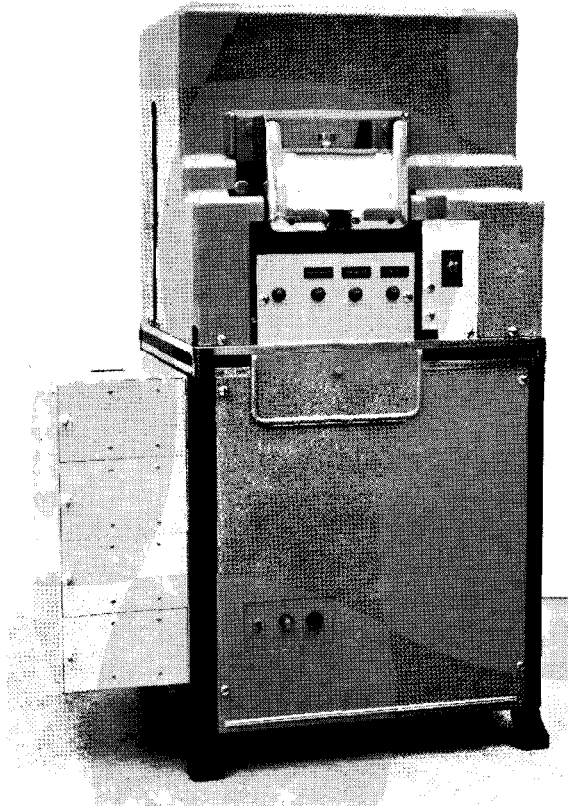


Fig. 2.2

In the case of an observation of bearing, one of the lines of this track must coincide with a reference mark. It was intended that this reference mark should be situated in a flexible piece of image-transmitting fibre glass optics. By means of this it is possible to bring about a setting in coincidence at any position around the instrument. This is necessary because, unlike what is usual in theodolites, in this instrument the horizontal circle, the coded disk, rotates and the reading index remains stationary.

The piece of fibre glass optics is rigidly connected to the reading mechanism, which here again consists of a lamp and a number of photo-electric cells. On account of the very long delivery time of the fibre optics, this reference mark is mounted for the time being in a rotatable viewing glass (see figure 5.8).

The setting in coincidence serves a twofold purpose. In the first place the reading mechanism is set in a position at which all the photo-electric cells are removed as far as possible from the black-to-white transitions. In this way no contradictions can occur in the reading.

In the second place the second coded disk, which acts as a micrometer, is shifted with respect to the reading mechanism. This micrometer disk has six tracks, i.e. $2^6 = 64$ sectors. In this way a total of $2^{16} = 65\,536$ units is made available for the angular measurement over

a complete circle. The observation of bearing can thus be carried out with an accuracy somewhat less than 1 centigrade.

Besides the variable measuring data obtained by means of the coded disks, a number of basic data must also be registered for each point. These data consist for instance of the station number, the target number, the code for traverse, detail or height measurement, the number of the repetition measurement, the error. These basic data are set on thumb-wheel switches. This system is further elaborated in section 6.3.

The basic and the variable measuring data have to be registered in an easily accessible store. For this purpose a Philips cassette tape recorder has been selected. Data which have to be stored in binary form on magnetic tape must be presented in series. As the data from the coded disks and the thumb-wheel switches have to be presented in parallel, a certain amount of electronic equipment is required for their translation. This equipment consists mainly of a shift register of 80 positions for translating the parallel signals into series.

Furthermore, provision is made for automatic numbering of the detail points per station. This numbering, which may run up to 99, is also shown on the instrument by means of two indicators. The store with the registering section is dealt with in section 6.4.

The observations which are collected in the store by means of the field instruments must be made suitable for automatic processing in the computer. The equipment required for this purpose consists of a reading unit of the magnetic tape and a card punch. An equipment of this kind at the office can process the data of a large number of instruments with automatic processing. For the processing of the data obtained with the prototype a comparatively simple system has been evolved consisting of a reading section which at the same time serves as a controlling unit for a Bull PC 80 card punch, incidentally an older type. The ideal solution is presumably that of translating the data of the magnetic tape from the cassette into a magnetic tape which can be processed by the computer. This admittedly involves the difficulty of the input of basic data for the entire measurement, such as coordinates of the basic points, tolerances, etc. In the case of processing with punched cards only a few additional cards bearing these data need be introduced.

3 OPTICAL SECTION

Incorporated in the instrument is, along with a prism system for distance measurement, also a mechanism for reducing the distances to the horizontal plane. In an instrument that is provided with automatic registration, a reduction mechanism of this kind is not necessary because, a coded disk may also be provided for the vertical angular measurement. By calculation in the computer the trigonometric slope distances can be reduced. As, when using a coded disk for the vertical angular measurement, one can in principle work in just the same way as with the horizontal circle, such a disk has been omitted in the construction of the prototype. Moreover, it has been found that by a certain arrangement of the optical elements, the trigonometric slope distance as well as the reduced horizontal distance and the height difference between two points can be measured.

3.1 Distance measurement and reduction of the distances measured to the horizontal

As set forth in the introduction, the principle of optical distance measurement is based on the measuring of a number of elements of the parallactic triangle. With the instrument designed the distance to be measured is $l = x \cdot \frac{1}{2} \cot \frac{1}{2} \delta$, in which δ is the fixed parallactic angle and x the staff intercept to be measured (see figure 3.1).

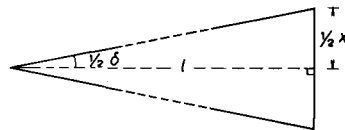


Fig. 3.1

The instrument is constructed as a range-finder. In this instrument the apex of the parallactic triangle is situated at the point to be determined. The staff intercept x is measured on the instrument itself. In figure 3.2a the top plan view of the optical section is shown and in figure 3.2b the front view.

The instrument comprises the following optical parts:

- Four pentaprisms 1, 2, 3 and 4.
- Two triangular prisms 5 and 6.
- An objective 7 and an eye-piece 9 (see section 3.5).
- Fresnel biprism 8 (see section 3.5).

The pentaprisms 1 and 2 can be slid along a rule. The distance between these two prisms is the staff intercept x . The maximum length of x is 50 cm. Prisms 3 and 4, which are rigidly fixed to each other, serve to bring the rays from the field object into the telescope.

The triangular prisms 5 and 6 serve to form the parallactic angle δ . The deviation γ which each of the prisms imparts to the rays of light passing through them is equal to half of angle δ .

The maximum distance l to be measured may be taken as 100 m. For a maximum length of x of 50 cm this means that the multiplication constant A is equal to 200.

Since

$$l = A \cdot x = x \cdot \frac{1}{2} \cot \frac{1}{2} \delta = \frac{1}{2} x \cdot \cot \gamma, \cot \gamma = 400 \text{ or } \gamma = 1/400 \text{ radian} \dots (3.1)$$

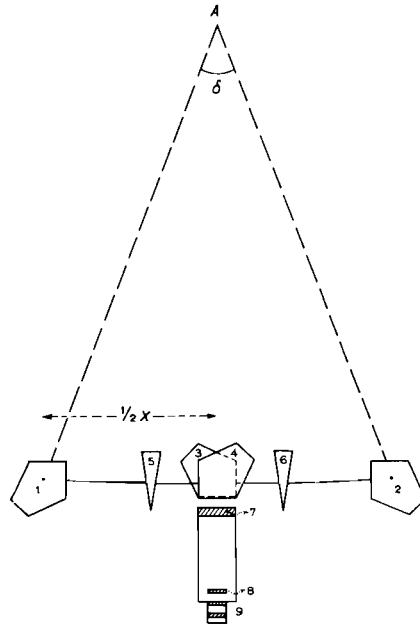


Fig. 3.2a

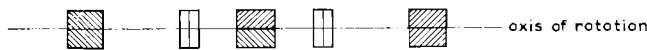


Fig. 3.2b

From $l = A \cdot x$ we obtain for the standard deviation in the distance l : $\sigma_l = A \cdot \sigma_x$. Hence it follows that if the object in view is to obtain a smaller σ_l , then A for instance may be taken at a lower value and hence the deviation γ of the prisms at a higher value. If we select for instance $A = 100$, then $\gamma = 1/200$ radian. The maximum distance that can then be measured is 50 m. If with $A = 100$ one still wishes to measure distances up to 100 m, a specially adapted staff will have to be used. See figure 3.3.

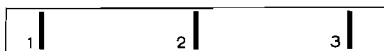


Fig. 3.3

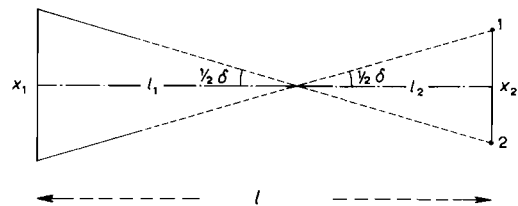


Fig. 3.4

The staff is provided with three targets, whose mid points are situated 25 cm apart. If for instance targets 1 and 2 are set in coincidence in the visual field, then 25 m must be added to the distance measured.

It follows from figure 3.4 that the distance to be measured is $l = l_1 + l_2$.

$$l_1 = x_1 \cdot \frac{1}{2} \cotg \frac{1}{2} \delta \quad (x_1 = \text{staff intercept read})$$

$$l_2 = x_2 \cdot \frac{1}{2} \cotg \frac{1}{2} \delta \quad (x_2 = \text{distance between targets 1 and 2})$$

$$l = (x_1 + x_2) \cdot \frac{1}{2} \cotg \frac{1}{2} \delta = 100(x_1 + x_2) \dots \dots \dots (3.2)$$

When targets 1 and 3 are set in coincidence 50 m is therefore added.

This system may be further extended by the use of a smaller constant A and a longer staff. In order to know, with a view to automatic registration, which targets have been set in coincidence, the position of the internal focussing lens, for instance, may be included in the store, via a certain code.

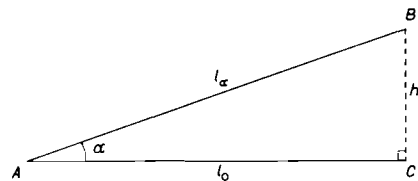


Fig. 3.5

In figure 3.5 point A is the station of the instrument, B the station of the target. AC is the horizontal projection of AB . The figure gives the relation between l_α , l_0 and h .

From

$$l_0 = l_\alpha \cos \alpha \text{ we obtain } Ax_0 = Ax_\alpha \cos \alpha \text{ or } x_0 = x_\alpha \cos \alpha \dots \dots \dots (3.3)$$

$$h = l_\alpha \sin \alpha, \text{ so that } h = Ax_\alpha \sin \alpha \dots \dots \dots (3.4)$$

Here x_α is the staff intercept to be determined when measuring at an angle of inclination of α grades. When measuring the trigonometric slope distance l_α all the optical elements are rotated through an angle α . In this case $l_\alpha = \frac{1}{2} x_\alpha \cotg \frac{1}{2} \delta$.

For determination of the horizontal distance l_0 the staff intercept x_α of figure 3.6 must be reduced to $x_\alpha \cos \alpha$.

In figures 3.6 and 3.7 U and W are the points of intersection of the rays of light which are refracted through 100° in the pentaprisms. V_1 and V_2 in the triangular prisms are the points of intersection of the incident and emerging rays. If the instrument is not provided with the two triangular prisms, the emerging rays RU and TW will be perpendicular to the staff UW of the instrument. RT is parallel to UW . It has been assumed in this case that the whole optical system (including the telescope) has an angle of inclination α . When the triangular prisms are placed in position in such a way that the refracting edges also form an angle α with the vertical, then the two rays of light each acquire a deviation of $\frac{1}{2} \delta$. RU changes into SU and TW into SW . Here $RS = ST = \frac{1}{2} x_\alpha$.

How this reduction is brought about, is made clear with the aid of figure 3.7. If for instance the left triangular prism is rotated perpendicularly to UW , then the ray V_1S describes a conical surface. The refraction of this beam via U in the left-hand pentaprism is not essential to this argument regarding the principle of reduction. We consider the base of the cone to be the circle with radius $RS = \frac{1}{2} x_\alpha$ perpendicular to the direction RU .

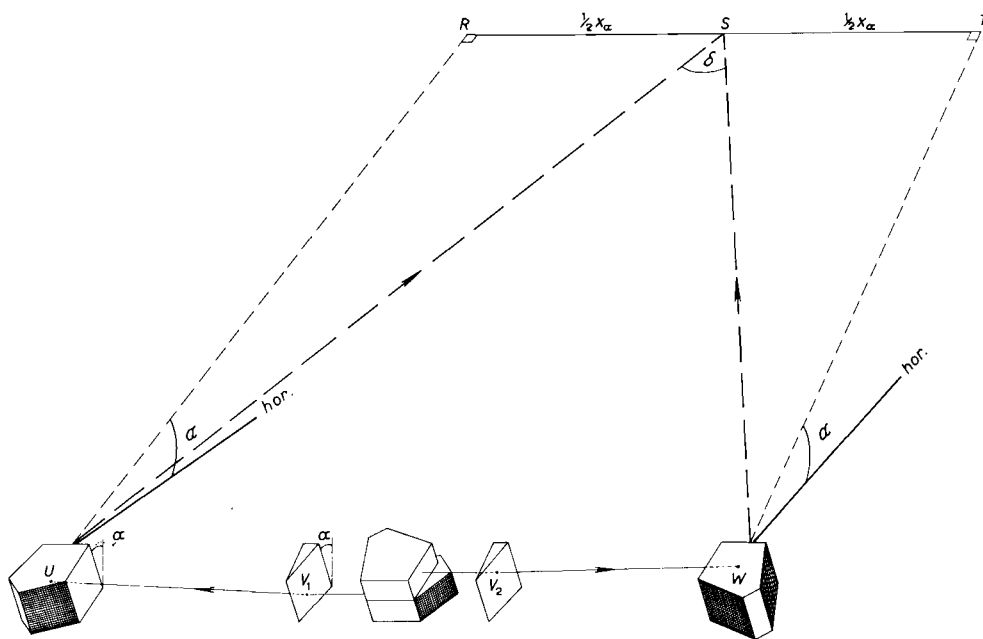


Fig. 3.6

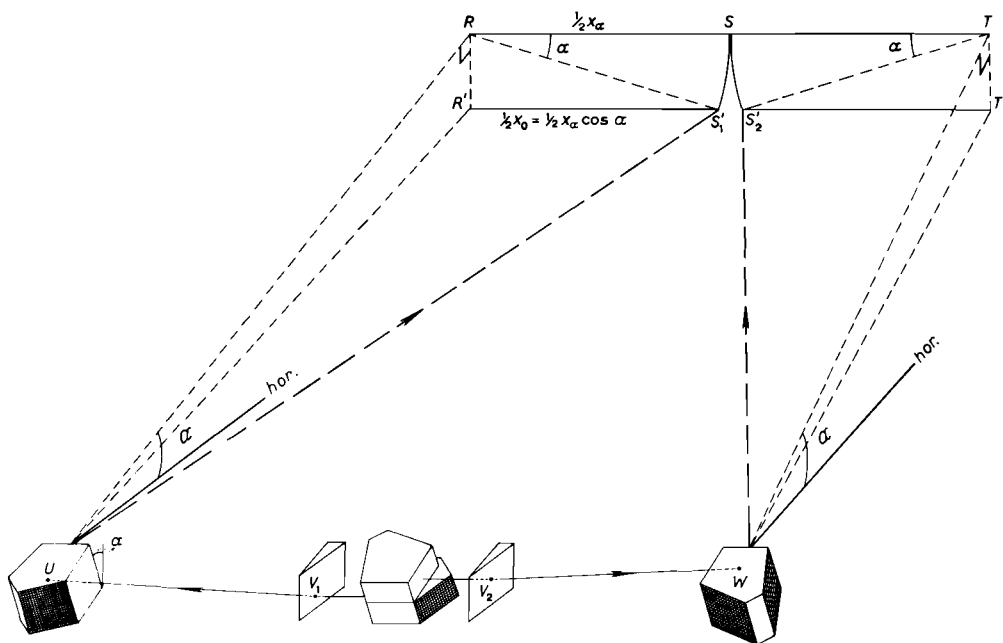


Fig. 3.7

If the triangular prism is turned through an angle α , that is, *that the refracting edge comes into a vertical position*, then the lateral deviation of the ray V_1R is not $RS = \frac{1}{2}x_\alpha$ but $R'S_1' = \frac{1}{2}x_\alpha \cos \alpha = \frac{1}{2}x_0$. In the same way it can be said for the right-hand part that the lateral deviation TS changes into $T'S_2' = \frac{1}{2}x_0$.

In order to set the images of S_1' and S_2' in coincidence with each other, the outer pentaprisms must be shifted inwards in such a way that the distance UW is no longer x_α but $x_\alpha \cos \alpha$. In this way the reduction is brought about.

In this connection the most important conclusion is that for the purpose of reduction the refracting edges of the triangular prisms should continue to be vertical. This is easy to achieve by not fixing the prisms to the rotating optical system but fixing them rigidly to the part of the instrument that can be rotated in the horizontal direction only.

Although the foregoing indicates the principle of distance measurement and reduction, there are still a number of problems left unsolved in regard to precision of measurement. Definite mathematical and arithmetical solutions to the following problems will be given in the sections below:

- By rotation of the pentaprisms the loci of the points of intersection U and W of the rays of light will undergo a change. What is the effect of this upon distance measurement?
- What requirements as to precision have to be satisfied in the construction of the optical components?
- To what extent may the prisms show a deformation?
- How is the result of distance measurement affected by altering the position of the triangular prism between the pentaprisms?

In order to answer these questions, simulation computations were carried out with the aid of the formulae developed in section 3.2. First of all a base model was calculated with the aid of these formulae. This is the ideal instrument provided with optical elements having no deviations.

Furthermore, a mathematical model of the instrument was designed in the form of an Algol programme for the TR-4 computer. By means of this it is possible to simulate deformations in the basic model in every conceivable way. The prisms can be moved into any desired position, and all the refractive and reflecting surfaces can be rotated and shifted in position. These deformations will give rise to errors, the magnitudes of which can be calculated. As the instrument is symmetrical, only the right-hand half will be included in the present investigation.

3.2 Path of the rays through the optical elements used

In calculating the path of the rays through the basic model and the various optical components taken singly, three different systems of formulation may be used. These systems are the matrix method, the vector method and the method with the conventional trigonometric formulae. In the calculations use was made of the last two systems. In studying the path of the rays through a separate pentaprism the matrix method is found suitable.

The three systems of formulation will be dealt with briefly by reference to the refraction and reflection of a ray of light.

The matrix method

In geodetic literature the matrix method for plane surfaces is seldom used, although this simple method was introduced as early as 1929 by T. SMITH. See [28] en [35]. The method is paraxial. The ray must impinge upon the refractive surface at an angle with the normal which is generally smaller than 1 gr. The relation between the coordinates of the image point (x', y', z') and of the point of light (x, y, z) is given by:

$$\begin{pmatrix} x' \\ y' \\ z' \\ 1 \end{pmatrix} = \begin{pmatrix} 1 + \mu L^2 & \mu LM & \mu LN & -a\mu L \\ \mu LM & 1 + \mu M^2 & \mu MN & -a\mu M \\ \mu LN & \mu MN & 1 + \mu N^2 & -a\mu N \\ 0 & 0 & 0 & 1 \end{pmatrix} \begin{pmatrix} x \\ y \\ z \\ 1 \end{pmatrix} \dots \dots \dots (3.5)$$

L, M and N are directional cosines of the normal to the refractive surface, a is the distance of the point of light from this surface. The relation between the indices of refraction is given by μ , where $\mu = (n'/n) - 1$. In the case of reflection it is found that $\mu = -2$.

If we are only concerned with the direction of the ray of light the matrices are more simple. If the directional cosines of the incident ray are $\cos \alpha, \cos \beta$ and $\cos \gamma$, and those of the emerging ray are $\cos \alpha', \cos \beta'$ and $\cos \gamma'$, then the matrix equation is:

$$\begin{pmatrix} \cos \alpha' \\ \cos \beta' \\ \cos \gamma' \end{pmatrix} = \begin{pmatrix} 1 + \mu L^2 & \mu LM & \mu LN \\ \mu LM & 1 + \mu M^2 & \mu MN \\ \mu LN & \mu MN & 1 + \mu N^2 \end{pmatrix} \begin{pmatrix} \cos \alpha \\ \cos \beta \\ \cos \gamma \end{pmatrix} \dots \dots \dots (3.6)$$

If there is a larger number of refractive and reflecting surfaces in the path of the rays, the relation of the incident and emerging rays of the optical system is obtained by premultiplying successively the matrices containing the directional cosines L, M and N of the surfaces starting with the matrix of the first surface.

With the aid of figure 3.8 it is easily found that the relation between the incident ray and the emerging ray of a *pentaprism* is:

$$\begin{pmatrix} \cos \alpha' \\ \cos \beta' \\ \cos \gamma' \end{pmatrix} = \begin{pmatrix} 0 & +1 & 0 \\ -1 & 0 & 0 \\ 0 & 0 & +1 \end{pmatrix} \begin{pmatrix} \cos \alpha \\ \cos \beta \\ \cos \gamma \end{pmatrix} \dots \dots \dots (3.7)$$

From this it follows that:

$$\left. \begin{matrix} \cos \alpha' = \cos \beta \\ \cos \beta' = -\cos \alpha \\ \cos \gamma' = \cos \gamma \end{matrix} \right\} \dots \dots \dots (3.8)$$

The directions of the two rays may be represented by two unit vectors:

$$\left. \begin{matrix} \bar{a} = \bar{i} \cos \alpha + \bar{j} \cos \beta + \bar{k} \cos \gamma \\ \text{and } \bar{b} = \bar{i} \cos \alpha' + \bar{j} \cos \beta' + \bar{k} \cos \gamma' \end{matrix} \right\} \dots \dots \dots (3.9)$$

If ϵ is the angle between the rays, then we obtain for the inner product of the unit vectors:

$$\left. \begin{aligned} \bar{a} \cdot \bar{b} &= ab \cos \epsilon = \cos \epsilon \\ \cos \epsilon &= \cos \alpha \cos \beta - \cos \beta \cos \alpha + \cos^2 \gamma \\ \cos \epsilon &= \cos^2 \gamma \end{aligned} \right\} \dots \dots \dots (3.10)$$

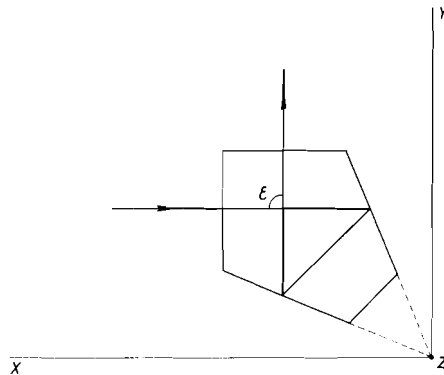


Fig. 3.8

As γ is the angle which the incident ray forms with the Z axis, the following conclusions may be drawn from the above formula.

- The rotation of the prism around the Z axis does not cause any change in γ . The angle ϵ remains invariable.
- On rotation around the X axis there is no change in γ , so that here again ϵ remains invariable.
- Only on rotation of the pentaprism around the Y axis does angle γ vary. The angle ϵ between the incident and the emerging rays varies according to the formula $\cos \epsilon = \cos^2 \gamma$.

The vector method

In the Algol programme in which a mathematical model for the distance-measuring instrument has been designed, certain procedures are included. In one of the most important procedures in this programme, the procedure "refraction", the vector method was used. See [7].

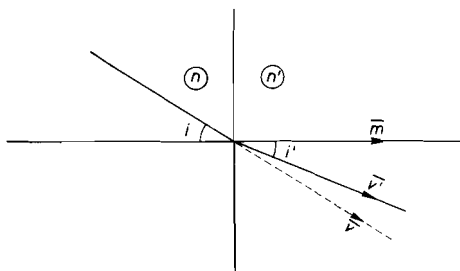


Fig. 3.9

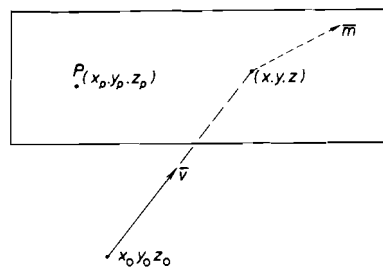


Fig. 3.10

In figure 3.9 \bar{m} = normal to the refractive surface.
 \bar{v} = directional vector of the unrefracted ray.
 \bar{v}' = directional vector of the refracted ray.

These three vectors are situated in one and the same plane, so that:

$$\bar{v}' = a\bar{v} + b\bar{m} \dots \dots \dots (3.11)$$

With the aid of the inner product of \bar{m} and \bar{v}' , the inner product of \bar{v} and \bar{v}' , and Snell's law, the values of a and b are calculated.

For refraction we have:

$$\left. \begin{aligned} a &= N \\ b &= -N \cos i + \sqrt{1 - N^2 + N^2 \cos^2 i} \end{aligned} \right\} \dots \dots \dots (3.12)$$

For reflection we have:

$$\left. \begin{aligned} a &= 1 \\ b &= -2 \cos i \end{aligned} \right\} \dots \dots \dots (3.13)$$

In these formulae:

$$N = \frac{n}{n'} \text{ and } \cos i = m_x v_x + m_y v_y + m_z v_z \dots \dots \dots (3.14)$$

For the calculation of the point of intersection (x, y, z) of the ray of light with the refractive surface, the following derivation is applicable. See figure 3.10.

The refractive surface is given by a point P (x_p, y_p, z_p) and the normal \bar{m} . The equation of this plane is:

$$m_x(x - x_p) + m_y(y - y_p) + m_z(z - z_p) = 0 \dots \dots \dots (3.15)$$

The ray is given by a point (x_0, y_0, z_0) and the directional vector \bar{v} . The equation of the ray of light is:

$$\bar{x} = \bar{x}_0 + \lambda \bar{v} \dots \dots \dots (3.16)$$

For each point on \bar{v} the following equations apply:

$$\left. \begin{aligned} x &= x_0 + \lambda v_x \\ y &= y_0 + \lambda v_y \\ z &= z_0 + \lambda v_z \end{aligned} \right\} \dots \dots \dots (3.17)$$

After substitution of these values in the equation of the plane we can solve λ thus:

$$\lambda = \frac{m_x(x_p - x_0) + m_y(y_p - y_0) + m_z(z_p - z_0)}{m_x v_x + m_y v_y + m_z v_z} \dots \dots \dots (3.18)$$

This λ , substituted in equation (3.17), gives the point of intersection of the ray with the plane.

The conventional trigonometric formulae

For the designing of the basic model the trigonometric formulae were used. In figure 3.11 yz is the refractive surface and xy a principal plane. The incident ray is not situated in the xy plane.

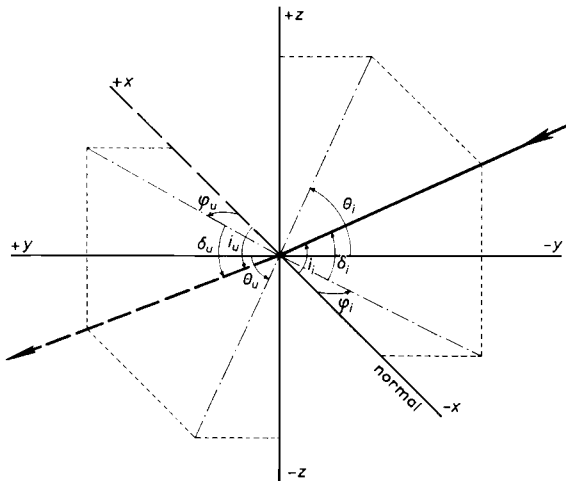


Fig. 3.11

The angles θ_u, i_u, φ_u and δ_u of the emerging ray are expressed in the corresponding quantities of the incident ray. As the ray is refracted in the plane that passes through this ray and the normal, we find:

$$\theta_u = \theta_i = \theta \dots \dots \dots (3.19)$$

According to Snell's law of refraction:

$$\sin i_u = \frac{n_1}{n_2} \sin i_i \dots \dots \dots (3.20)$$

Since $n_1 \approx 1$ (index of refraction of air), the factor n_1/n_2 will henceforth be given by $1/n$.

We find furthermore from figure 3.11 that:

$$\tan i_i = \frac{\tan \varphi_i}{\cos \theta}; \quad \tan i_u = \frac{\tan \varphi_u}{\cos \theta}; \dots \dots \dots (3.21)$$

$$\cos i_i = \cos \varphi_i \cos \delta_i; \quad \cos i_u = \cos \varphi_u \cos \delta_u \dots \dots \dots (3.22)$$

With the aid of the foregoing formulae we can express φ_u and δ_u in terms of the angles θ , i_i , φ_i and δ_i of the incident ray.

$$\sin^2 i_i = \frac{\tan^2 i_i}{1 + \tan^2 i_i} = \frac{\tan^2 \varphi_i}{\cos^2 \theta + \tan^2 \varphi} \dots \dots \dots (3.23)$$

Similarly:

$$\sin^2 i_u = \frac{\tan^2 \varphi_u}{\cos^2 \theta + \tan^2 \varphi_u} \dots \dots \dots (3.24)$$

From which follows, with Snell's law of refraction:

$$\frac{\tan^2 \varphi_i}{\cos^2 \theta + \tan^2 \varphi_i} = \frac{n^2 \tan^2 \varphi_u}{\cos^2 \theta + \tan^2 \varphi_u} \dots \dots \dots (3.25)$$

Hence:

$$\boxed{\tan^2 \varphi_u = \frac{\tan^2 \varphi_i \cos^2 \theta}{n^2(\cos^2 \theta + \tan^2 \varphi_i) - \tan^2 \varphi_i}} \dots \dots \dots (3.26)$$

From (3.21) and (3.22) we obtain:

$$\cos^2 \delta_i = \frac{\cos^2 \theta (\tan^2 \varphi_i + 1)}{\cos^2 \theta + \tan^2 \varphi_i} \quad \text{and} \quad \cos^2 \delta_u = \frac{\cos^2 \theta (\tan^2 \varphi_u + 1)}{\cos^2 \theta + \tan^2 \varphi_u} \dots \dots \dots (3.27)$$

After further development this gives:

$$\boxed{\cos^2 \delta_u = 1 - \frac{\tan^2 \varphi_i (1 - \cos^2 \theta)}{n^2(\cos^2 \theta + \tan^2 \varphi_i)}} \dots \dots \dots (3.28)$$

Since in calculating the basic model the loci of certain points of intersection of the rays are important, it is necessary to state a few further data regarding the path of the rays through a pentaprism.

Taking as basis an ideal pentaprism it may be assumed that the path of the rays through this pentaprism can be obtained simply by reflecting the pentaprism twice, whereupon the path of the rays follows as if the light is passing through a plano-parallel glass plate. See figure 3.12.

Each ray entering the prism will thus apparently emerge from this prism in the same direction.

The apparent thickness d of the prism is equal to AA' .

$$AA' = (2 + \sqrt{2})AB = d \dots \dots \dots (3.29)$$

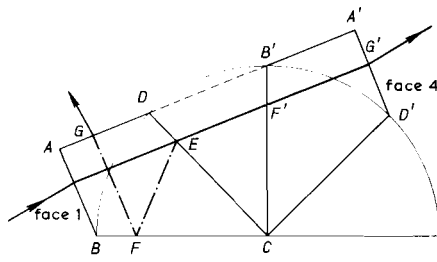


Fig. 3.12

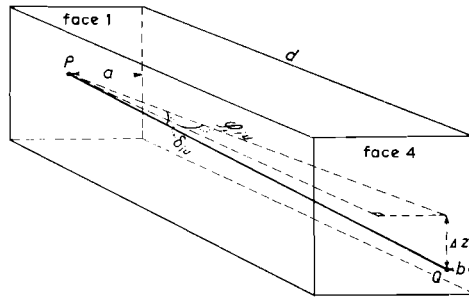


Fig. 3.13

From the foregoing reasoning we can find the place at which the ray of light emerges from the pentaprism. See figure 3.13. The ray enters on face 1 at point *P* and emerges at point *Q* on face 4. We obtain from the figure:

$$b = a - d \tan \varphi_{1u} \dots \dots \dots (3.30)$$

$$\Delta z = \frac{d}{\cos \varphi_{1u}} \cdot \tan \delta_{1u} \dots \dots \dots (3.31)$$

Since the incident ray on face 1 is parallel to the ray emerging from face 4, the following is applicable:

$$\varphi_{4u} = \varphi_{1i} \quad \text{and} \quad \theta_4 = \theta_1 \dots \dots \dots (3.32)$$

φ_{4u} is the angle which the projection of the ray upon the *x, y* plane forms with the +*y* axis and θ_4 the angle which the projection of the ray upon the *x, z* plane forms with the -*x* axis.

For the construction of the basic model it is necessary to define two coordinate systems (see figure 3.14) and to investigate the transformations of the rays of light from the one system to the other.

The coordinate system of the entire optical system is the system of *X, Y* and *Z* axes. The *X* axis coincides with the axis of rotation of the system. Perpendicular to it in the horizontal plane is the *Y* axis. The vertical is the *Z* axis. This system is a dextrorotatory system.

The path of the rays in the instrument (see figure 3.2a) is assumed to issue from the telescope, through prisms 3 and 4, via the triangular prisms 5 and 6 and through prisms 1 and 2 to point *A*. In the case of measurement at an angle of inclination α the refractive edges of the triangular prisms remain vertical. In this case the path of the rays through pentaprisms 1 and 2 will therefore differ from that obtaining in the case of measurement in the horizontal position.

As agreed in section 3.1, only the right-hand part of the optical system will be dealt with. On the pentaprism situated on the extreme right a dextrorotatory system of coordinates (*x, y, z*) is selected, the *x* axis of which coincides with the axis of rotation (perpendicular to face 1). In the horizontal position of this prism the *y* and *z* axes are parallel to the *Y* and *Z* axes of the entire system.

If the distance between the origins in figure 3.14 is h and the x, y, z system is rotated through an angle α around the X axis with respect to the X, Y, Z system, then the known transformation formulae will be as follows:

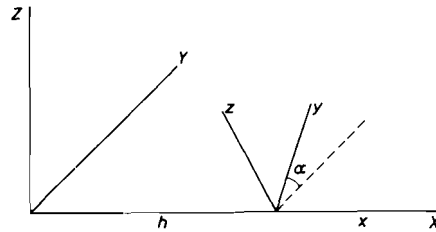


Fig. 3.14

$$\left. \begin{aligned} x &= X - h \\ y &= Y \cos \alpha + Z \sin \alpha \\ z &= -Y \sin \alpha + Z \cos \alpha \end{aligned} \right\} \dots \dots \dots (3.33)$$

$$\left. \begin{aligned} X &= x + h \\ Y &= y \cos \alpha - z \sin \alpha \\ Z &= y \sin \alpha + z \cos \alpha \end{aligned} \right\} \dots \dots \dots (3.34)$$

In the X, Y, Z system all the angles are indicated with a prime. These angles are defined analogously to those in the x, y, z system.

Transformation of the incident ray

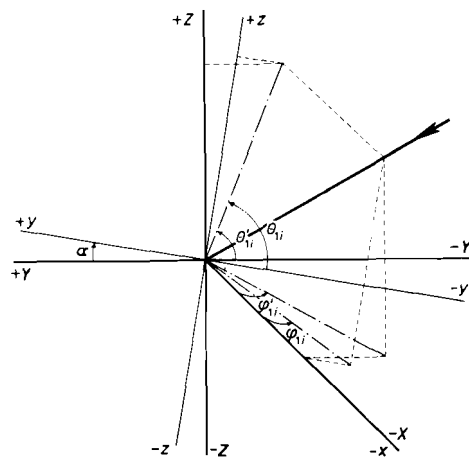


Fig. 3.15

As shown by figure 3.15, the incident ray on face 1 (y, z plane) of the pentaprism is given by:

$$\theta'_1 = \theta_1 - \alpha \dots \dots \dots (3.35)$$

$$\tan \varphi'_{1i} = \tan \varphi_{1i} \frac{\cos \theta'_1}{\cos \theta_1} \dots \dots \dots (3.36)$$

On development this gives:

$$\tan \varphi'_{1i} = \tan \varphi_{1i} (\cos \alpha + \tan \theta_1 \sin \alpha) \dots \dots \dots (3.37)$$

Transformation of the emerging ray

From figure 3.16 we find that the emerging ray on face 4 (*x, z* plane) of the pentaprism is given by:

$$y_A = -x_A \cot \varphi_{4u}; \quad Y_A = -x_A \cot \varphi'_{4u}; \quad z_A = +x_A \tan \theta_4; \quad Z_A = +x_A \tan \theta'_4 \quad (3.38)$$

It follows from the transformation formulae (3.33) and (3.34) that:

$$\left. \begin{aligned} x_A \cot \varphi'_{4u} &= x_A \cot \varphi_{4u} \cos \alpha + x_A \tan \theta_4 \sin \alpha \\ + x_A \tan \theta_4 &= -x_A \cot \varphi_{4u} \sin \alpha + x_A \tan \theta_4 \cos \alpha \end{aligned} \right\} \dots \dots \dots (3.39)$$

Hence:

$$\tan \varphi'_{4u} = \frac{\tan \varphi_{4u}}{\cos \alpha + \tan \theta_4 \sin \alpha} \dots \dots \dots (3.40)$$

and

$$\tan \theta'_4 = \frac{\tan \theta_4 \cos \alpha \tan \varphi_{4u} - \sin \alpha}{\tan \varphi_{4u}} \dots \dots \dots (3.41)$$

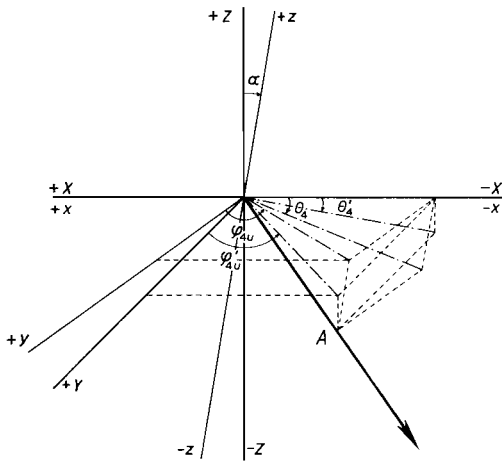


Fig. 3.16

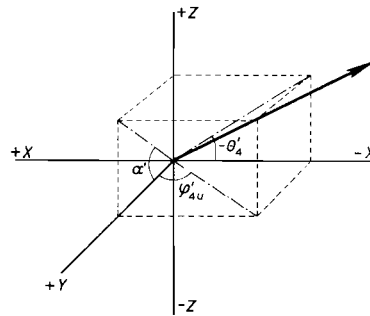


Fig. 3.17

With (3.32), (3.35) and (3.37) the quantities $\tan \varphi'_{4u}$ and $\tan \theta'_4$ can be further derived.

$$\tan \varphi'_{4u} = \frac{\tan \varphi'_{1i}}{\cos^2 \alpha + \tan(\theta'_1 + \alpha) \sin \alpha \cos \alpha + \tan(\theta'_1 + \alpha) \sin \alpha \tan \varphi'_{1i}} \dots \dots \dots (3.42)$$

$$\tan \theta'_4 = \frac{\tan(\theta'_1 + \alpha) \cos \alpha \tan \varphi'_{1i} - \sin \alpha \cos \alpha - \tan(\theta'_1 + \alpha) \sin^2 \alpha}{\tan \varphi'_{1i}} \dots \dots \dots (3.43)$$

In order to obtain a complete insight into the path of the rays through the instrument we also have to derive the formula for angle α' . This is the angle which the projection of the ray emerging from face 4 on to the Y, Z plane forms with the $+Y$ axis.

From figure 3.17 we obtain:

$$\tan \alpha' = -\tan \varphi'_{4u} \tan \theta'_4 \dots \dots \dots (3.44)$$

Hence:

$$\tan \alpha' = \frac{\sin \alpha + \tan(\theta'_1 + \alpha) \sin \alpha \tan \alpha - \tan(\theta'_1 + \alpha) \tan \varphi'_{1i}}{\cos \alpha + \tan(\theta'_1 + \alpha) \sin \alpha + \tan(\theta'_1 + \alpha) \tan \alpha \tan \varphi'_{1i}} \dots \dots \dots (3.45)$$

Recapitulation

The following angles, among others, were involved in the foregoing derivations.

x, y, z system	X, Y, Z system
α = the angle through which the x, y, z system has been rotated with respect to the X, Y, Z system around the X axis.	α' = the angle which the projection upon the Y, Z plane of the ray emerging from face 4 forms with the $+Y$ axis.
i_{1i} = the angle which the incident ray on face 1 forms with the $-x$ axis.	i'_{1i} = the angle which the incident ray on face 1 forms with the $-X$ axis.
φ_{1i} = the angle which the projection upon the x, y plane of the incident ray on face 1 forms with the $-x$ axis.	φ'_{1i} = the angle which the projection upon the XY plane of the incident ray on face 1 forms with the $-X$ axis.
δ_{1i} = the angle which the incident ray on face 1 forms with its projection upon the x, y plane.	
θ_1 = the angle which the projection of the ray upon the y, z plane forms with the $-y$ axis.	θ'_1 = the angle which the projection of the ray upon the Y, Z plane forms with the $-Y$ axis.
φ_{4u} = the angle which the projection upon the x, y plane of the emerging ray forms with the $+y$ axis.	φ'_{4u} = the angle which the projection upon the X, Y plane of the emerging ray forms with the $+Y$ axis.
θ_4 = the angle which the projection upon the x, z plane of the ray forms with the $-x$ axis.	θ'_4 = the angle which the projection upon the X, Z plane of the ray forms with the $-X$ axis.

Method of determining the point of intersection of the horizontal projection of the ray of light with the X axis

If point T in figure 3.18 is the origin of the system of coordinates X, Y, Z and if TS coincides with the $+X$ axis, then the horizontal distance to the point to be determined is:

$$l = (p + q + x_S) \cot \varphi'_{4u} \dots \dots \dots (3.46)$$

where $p + q + x_S = X_S$, whilst p is the distance from the point at which the ray is refracted in the triangular prism to face 1 of the pentaprism 3. From this formula we first solve x_S .

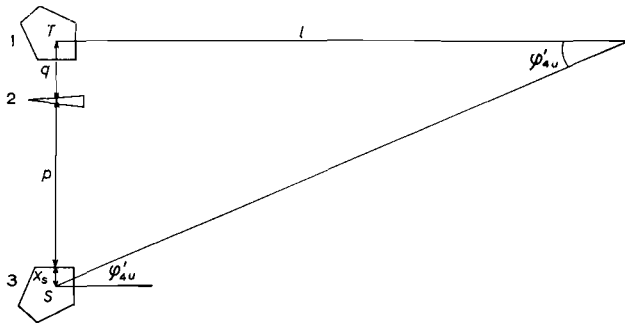


Fig. 3.18

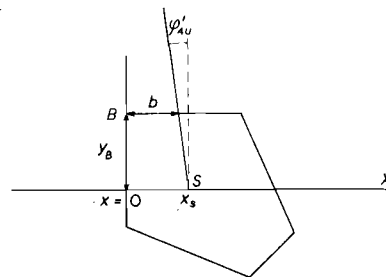


Fig. 3.19

Figure 3.19 shows a horizontal cross-section through the extreme right prism (prism No. 3 in figure 3.18). We find from the figure:

$$x_S = b + Y_B \tan \varphi'_{4u} \dots \dots \dots (3.47)$$

For the further derivation of x_S it is assumed that the ray of light falls from the telescope via the middle pentaprism (No. 1 in figure 3.18) parallel to the X axis on to the triangular prism (No. 2). This assumption is correct, as this prism No. 1 is rigidly coupled to the telescope. The rays will therefore invariably fall from the telescope on to the pentaprism at the same angle (practically a right-angle).

According to the assumptions for a pentaprism as given in dealing with the matrix method in this section, the emerging ray will remain perpendicular to the incident ray. Moreover, as the triangular prism keeps its refractive edge vertical, the plane that is formed by the refracted ray and the extension of the unrefracted ray is perpendicular to face 1 of pentaprism No. 3. This means that $\theta_1 = \alpha$ and $\theta_1' = 0$.

There are here two distinct cases.

1. The unrefracted ray is situated above the X axis.
2. The unrefracted ray is situated below the X axis.

In figure 3.20, which gives a view of face 1 of prism No. 3, point 1 is the position at which the X axis meets the plane; point 2 indicates the extension of the unrefracted ray, whilst point 3 is the position at which the ray falls on to the pentaprism.

The situation on face 1 of the pentaprism is shown in detail in figure 3.21.

From figures 3.13 and 3.21 we find:

$$Y_B = r \cos \alpha + e \sin \alpha + \Delta z \sin \alpha - t \sin \alpha \dots \dots \dots (3.48)$$

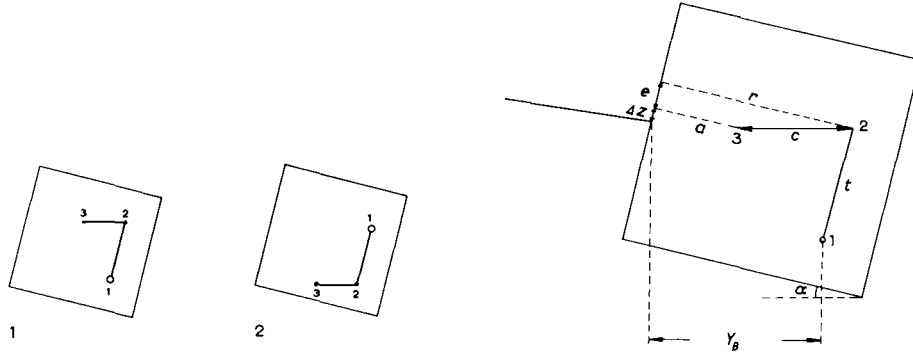


Fig. 3.20

Fig. 3.21

Since $c = p \tan \phi'_{1i}$, it follows that $e = p \tan \phi'_{1i} \sin \alpha$. Moreover, $a = r - p \tan \phi'_{1i} \cos \alpha$.

With (3.30), (3.31) and (3.47) we obtain:

$$X_S = r - p \tan \phi'_{1i} \cos \alpha - d \tan \phi_{1u} + Y_B \tan \phi'_{4u} \dots \dots \dots (3.49)$$

in which:

$$Y_B = r \cos \alpha + p \tan \phi'_{1i} \sin^2 \alpha + \frac{d}{\cos \phi_{1u}} \tan \delta_{1u} \sin \alpha - t \sin \alpha \dots \dots \dots (3.50)$$

From (3.46) it follows that:

$$l = (p + q) \cot \phi'_{4u} + x_S \cot \phi'_{4u} \dots \dots \dots (3.51)$$

$$x_S \cot \phi'_{4u} = r \cot \phi'_{4u} - p \cot \phi'_{4u} \tan \phi'_{1i} \cos \alpha - d \cot \phi'_{4u} \tan \phi_{1u} + Y_B \dots \dots \dots (3.52)$$

In this formula the quantities ϕ'_{4u} and ϕ_{1u} are expressed in terms of ϕ'_{1i} and α .

With $\theta_1 = \alpha$ and $\theta'_1 = 0$, we obtain from (3.42):

$$\cot \phi'_{4u} = \cot \phi'_{1i} + \tan \alpha \sin \alpha \dots \dots \dots (3.53)$$

For $\theta_1 = \alpha$, we obtain with (3.26) and (3.37):

$$\tan^2 \phi_{1u} = \frac{\tan^2 \phi'_{1i} \cos^2 \alpha}{n^2 (1 + \tan^2 \phi'_{1i}) - \tan^2 \phi'_{1i}} = \frac{\sin^2 \phi'_{1i} \cos^2 \alpha}{n^2 - \sin^2 \phi'_{1i}} = \frac{1}{n^2} \frac{\sin^2 \phi'_{1i} \cos^2 \alpha}{1 - \frac{\sin^2 \phi'_{1i}}{n^2}} \dots \dots \dots (3.54)$$

$$\tan^2 \phi_{1u} = \frac{1}{n^2} \sin^2 \phi'_{1i} \cos^2 \alpha \left(1 + \frac{\sin^2 \phi'_{1i}}{n^2} + \dots \right) \dots \dots \dots (3.55)$$

$$\tan \varphi_{1u} = \frac{1}{n} \sin \varphi'_{1i} \cos \alpha + \frac{1}{2n^3} \sin^3 \varphi'_{1i} \cos \alpha + \dots \dots \dots (3.56)$$

Since $\varphi'_{1i} \leq 1/100$ radian, $\sin^3 \varphi'_{1i} \leq 0.000\ 001$. This term may be neglected, whilst $\tan \varphi'_{1i}$ may be equated with $\sin \varphi'_{1i}$.

$$\tan \varphi_{1u} = \frac{1}{n} \tan \varphi'_{1i} \cos \alpha \dots \dots \dots (3.57)$$

From (3.28) we find:

$$\sin^2 \delta_{1u} = \frac{\tan^2 \varphi_{1i} (1 - \cos^2 \theta_1)}{n^2 (\cos^2 \theta_1 + \tan^2 \varphi_{1i})} \dots \dots \dots (3.58)$$

With (3.37) and $\theta_1 = \alpha$, it follows from this that:

$$\sin^2 \delta_{1u} = \frac{\tan^2 \varphi'_{1i} \cos^2 \alpha \sin^2 \alpha}{n^2 (\cos^2 \alpha + \tan^2 \varphi'_{1i} \cos^2 \alpha)} \dots \dots \dots (3.59)$$

$$\sin \delta_{1u} = \frac{1}{n} \sin \varphi'_{1i} \sin \alpha \dots \dots \dots (3.60)$$

Here again $\tan \varphi'_{1i}$ is equated with $\sin \varphi'_{1i}$, whilst furthermore $\sin \delta_{1u} = \tan \delta_{1u}$.

$$\tan \delta_{1u} = \frac{1}{n} \tan \varphi'_{1i} \sin \alpha \dots \dots \dots (3.61)$$

With (3.50), (3.52), (3.53), (3.57) and (3.61) the formula for x_s resolves itself after some simplifications into:

$$x_s \cot \varphi'_{4u} = r \cot \varphi'_{1i} + r \tan \alpha \sin \alpha - \left(p + \frac{d}{n} - r \right) \cos \alpha - t \sin \alpha \quad (3.62)$$

In the derivation of formula (3.62) the term $(d/n) \sin^2 \alpha \tan \varphi'_{1i} (1/\cos \varphi_{1u} - 1)$ was neglected, since this term is less than 0.000 001.

It follows from (3.51) and (3.53) that:

$$l = (p + q) \cot \varphi'_{1i} + (p + q) \tan \alpha \sin \alpha + x_s \cot \varphi'_{4u} \dots \dots \dots (3.63)$$

For the case in which the unrefracted ray is situated above the X axis the following is applicable

$$l = (p + q + r) (\cot \varphi'_{1i} + \tan \alpha \sin \alpha) - \left(p + \frac{d}{n} - r \right) \cos \alpha - t \sin \alpha \dots \dots (3.64)$$

For the case in which the unrefracted ray is situated below the X axis, the factor $-t \sin \alpha$ changes into $+t \sin \alpha$. As found from figure 3.2b, the axis of rotation passes through the separating surface of the two middle pentaprisms. The factor $-t \sin \alpha$ of one half of the optical system will neutralize the factor $+t \sin \alpha$ of the other half. In the rest of the derivations this factor may be neglected.

3.3 Calculation of the anticipated deviations in the measuring result

In the previous section the path of the rays through an ideal pentaprism was calculated. With the aid of this calculation the formula was developed for the distance l_α , which is measured at an angle of inclination α .

$$l_\alpha = (p+q+r)(\cot \varphi'_{ii} + \tan \alpha \sin \alpha) - \left(p + \frac{d}{n} - r\right) \cos \alpha \quad \dots \quad (3.65)$$

If measurement is effected with the telescope in a horizontal position, the angle of inclination thus being $\alpha = 0$, we obtain for the measured distance l_0 :

$$l_0 = (p+q+r) \cot \varphi'_{ii} - \left(p + \frac{d}{n} - r\right) \quad \dots \quad (3.66)$$

The difference between l_α and l_0 is:

$$\Delta l = (p+q+r) \tan \alpha \sin \alpha + \left(p + \frac{d}{n} - r\right) (1 - \cos \alpha) \quad \dots \quad (3.67)$$

If the variable p occurs only in the first term of the right-hand side, the following will apply:

$$\Delta l = (p+q+r) (\tan \alpha \sin \alpha + 1 - \cos \alpha) - \left(q - \frac{d}{n} + 2r\right) (1 - \cos \alpha) \quad (3.68)$$

For the theoretical basic model, with which all the deformed models of the instrument (see section 3.1) are compared, $(p+q+r)$ is equated with $c \cdot x$, where $x = l_0/A$, see (3.1).

This basic model is selected in such a manner that if $x = 0$ is applicable, then $\Delta l = 0$, from which we obtain:

$$q = \frac{d}{n} - 2r \quad \dots \quad (3.69)$$

The formula for Δl is now:

$$\Delta l = c \cdot x \left(1 - \frac{\cos 2\alpha}{\cos \alpha}\right) \quad \dots \quad (3.70)$$

This means that with the basic model, when measurement is effected at an angle of inclination α , a slight correction must still be applied.

For instance, with an angle of inclination of 15 grades and a distance of 50 metres with a multiplication constant of 100, the correction is found to be 21 mm. It will be seen in the following that this correction may in practically all cases be made nil by giving the optical components a certain slight deformation.

If (3.69) is substituted in the formula for l_0 (3.66), then:

$$l_0 = (p + q + r)(\cot \phi'_{1i} - 1) = c \cdot x(\cot \phi'_{1i} - 1) \dots \dots \dots (3.71)$$

From $l_0 = A \cdot x$, it follows that $c(\cot \phi'_{1i} - 1) = A$. Here $\cot \phi'_{1i}$ is the cotangent of the angle of deviation of the triangular prism, whilst c is the scale factor on the base rail.

Although with the actual instrument this is a practical impossibility, the theoretical basic model has a zero position which is indicated in figure 3.22. In the instrument prism 3 cannot be slid back further along the base rail than to the position of prism 2. For the measurement of smaller distances a solution can be found by using a specially constructed measuring mark.

The applicable equation for this zero position is $p + q = -r$. The breaking point of the ray is situated at a distance q from the origin of the system of coordinates.

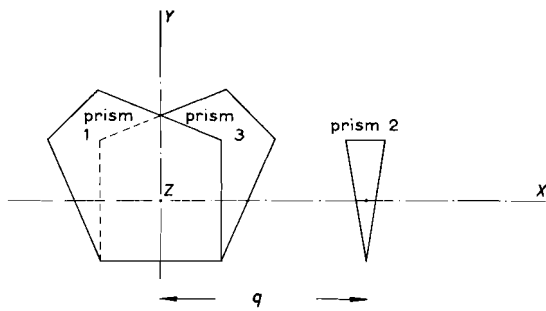


Fig. 3.22

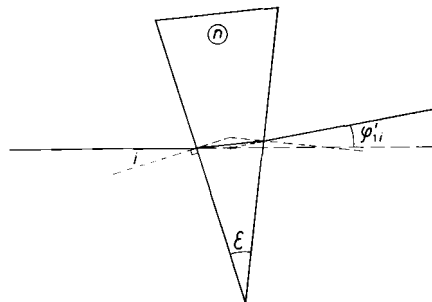


Fig. 3.23

As in the case of other double-image tacheometers, the triangular prisms must be at the position of minimum deviation. The position of the prism is such that a ray of light falling parallel to the X axis acquires the minimum deviation.

For the prism in figure 3.23 which is in the position of minimum deviation, the angle of incidence $i = \frac{1}{2}\epsilon + \frac{1}{2}\phi'_{1i}$. As, moreover, according to Snell's law the equation $\sin i = n \sin \frac{1}{2}\epsilon$ is applicable, we obtain:

$$\sin(\frac{1}{2}\epsilon + \frac{1}{2}\phi'_{1i}) = n \sin \frac{1}{2}\epsilon \dots \dots \dots (3.72)$$

or

$$\epsilon = 2 \arctan \frac{\sin \frac{1}{2}\phi'_{1i}}{n - \cos \frac{1}{2}\phi'_{1i}} \dots \dots \dots (3.73)$$

As the small angle φ'_{1i} is governed by the equation $\cot \varphi'_{1i} = \frac{1}{2} \cot \frac{1}{2} \varphi'_{1i}$, we obtain for the quantity $\frac{1}{2} \varphi'_{1i}$ in formula (3.73) the equation:

$$\frac{1}{2} \varphi'_{1i} = \arctan \frac{1}{2 \cot \varphi'_{1i}} \dots \dots \dots (3.74)$$

For the Algol computing programme it is necessary to establish all the refractive and reflecting surfaces of the optical elements. Along with these surfaces two other surfaces are of importance, viz. the surface that emits the rays of light (X, Z plane) and the surface that receives these rays (Y, Z plane).

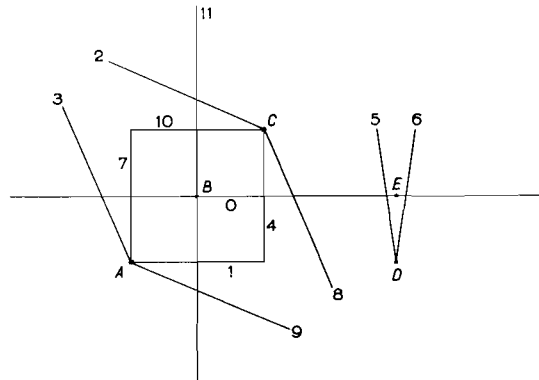


Fig. 3.24

In dealing with the vector method it has already been stated that a plane is determined by a point and the normal to that plane. See formula (3.15). In figure 3.24 all the planes are denoted by their new numbers. The points which determine these planes are designated by the letters A, B, C and D . In the deformations to be given to the basic model, points A, B, C and D serve as points of rotation for the planes, whilst points B and E will serve the same purpose for the prisms. At the zero position the points which determine the planes coincide with the points of rotation.

In studying the data for planes 5 and 6 in table 3.1, we find that the triangular prism is not yet in the position of minimum deviation. In the computing programme this is done automatically by rotating the prism around point E through an angle of $\frac{1}{2} \varphi'_{1i}$. The components along the coordinate axes of the normals to the planes are given in table 3.1. With the aid of rotations around the points of rotation and translations, the planes and the entire prisms can be given any desired position. The rotations and translations may take place within the computing programme around axes which are parallel to the X, Y and Z axis. For this purpose the following rules were adopted for the calculations.

- All the points of rotation remain fixed in the zero position of the basic model as indicated in figure 3.24. These points of rotation are not translated.
- Only the entire prisms and the planes with their normals and the fixing points can be transformed according to the given rotation and translation.

In view of the fixed position of the points of rotation it is advisable, when deforming the

Table 3.1

face	m_x	m_y	m_z	face	m_x	m_y	m_z
0	0	+1	0	6	$\cos \frac{1}{2}\epsilon$	$-\sin \frac{1}{2}\epsilon$	0
1	0	+1	0	7	+1	0	0
2	$\sin 25$	$\cos 25$	0	8	$\cos 25$	$\sin 25$	0
3	$-\cos 25$	$-\sin 25$	0	9	$-\sin 25$	$-\cos 25$	0
4	+1	0	0	10	0	+1	0
5	$\cos \frac{1}{2}\epsilon$	$\sin \frac{1}{2}\epsilon$	0	11	-1	0	0

basic model, to observe the following order of succession: rotation of the planes – translation of the planes – rotation of the prisms – translation of the prisms. The “measurement” with the mathematical model in the computing programme is carried out in the following manner.

First of all prism No. 3 (see figure 3.22) is slid along the base rail. Then prisms No. 1 and 3 are rotated through different angles around the X axis. For each of these measuring positions a ray of light is transmitted via all the optical elements from the fixing point for plane 0 (see figure 3.24) in the direction of the normal to this plane. The point of intersection of this ray with plane 11 is determined. The error is the difference between the distance measured on the base rail and the Y coordinate of the above-mentioned point of intersection with plane 11.

As the incident ray must continue to occupy the same position with respect to prism No. 1, plane 0 rotates automatically with this prism around the X axis. In the instrument the base rail need not be parallel to the X axis. During measurement in a horizontal position, there will, in case of translation of prism 3 along the base rail, not only be a translation along the X axis but also a shift along the Y and the Z axis. In the data tape for the computing programme to be introduced, the extent of the two latter translations will be indicated by two so-called coupling factors.

By reference to a greatly simplified flow diagram, the computing programme will now be briefly described. See figure 3.25.

First of all the basic model of the instrument is stored in the memory element. Corresponding to one serial number there is an unlimited number of instructions which are called by means of the addresses 1, 2, 3 and 4. These instructions are the deformations which are made in the instrument. These addresses are self-evident from figure 3.25. In address 5 the translation of prism No. 3 along the base rail is effected and prisms Nos. 1 and 3 are rotated through an angle α around the X axis in the same way as is done in an ordinary measurement. The error can now be determined for every position of the instrument. Before a new serial number is read, the basic model is restored to the original position.

The computer stops the calculations via address 6, after the total computing time has been determined. Three procedures are included in the programme:

- In the procedure *rotation* a number of planes can be rotated around a given axis. For instance, in the case of rotation of a prism, all the planes are rotated simultaneously.
- In the procedure *translation* a number of planes can be translated along a given axis.
- By means of the procedure *refraction*, the refracted ray of light is calculated as well as the distance from the refractive surface. In this procedure use is made of the vector method already described for the calculation of refraction and reflection by plane surfaces.

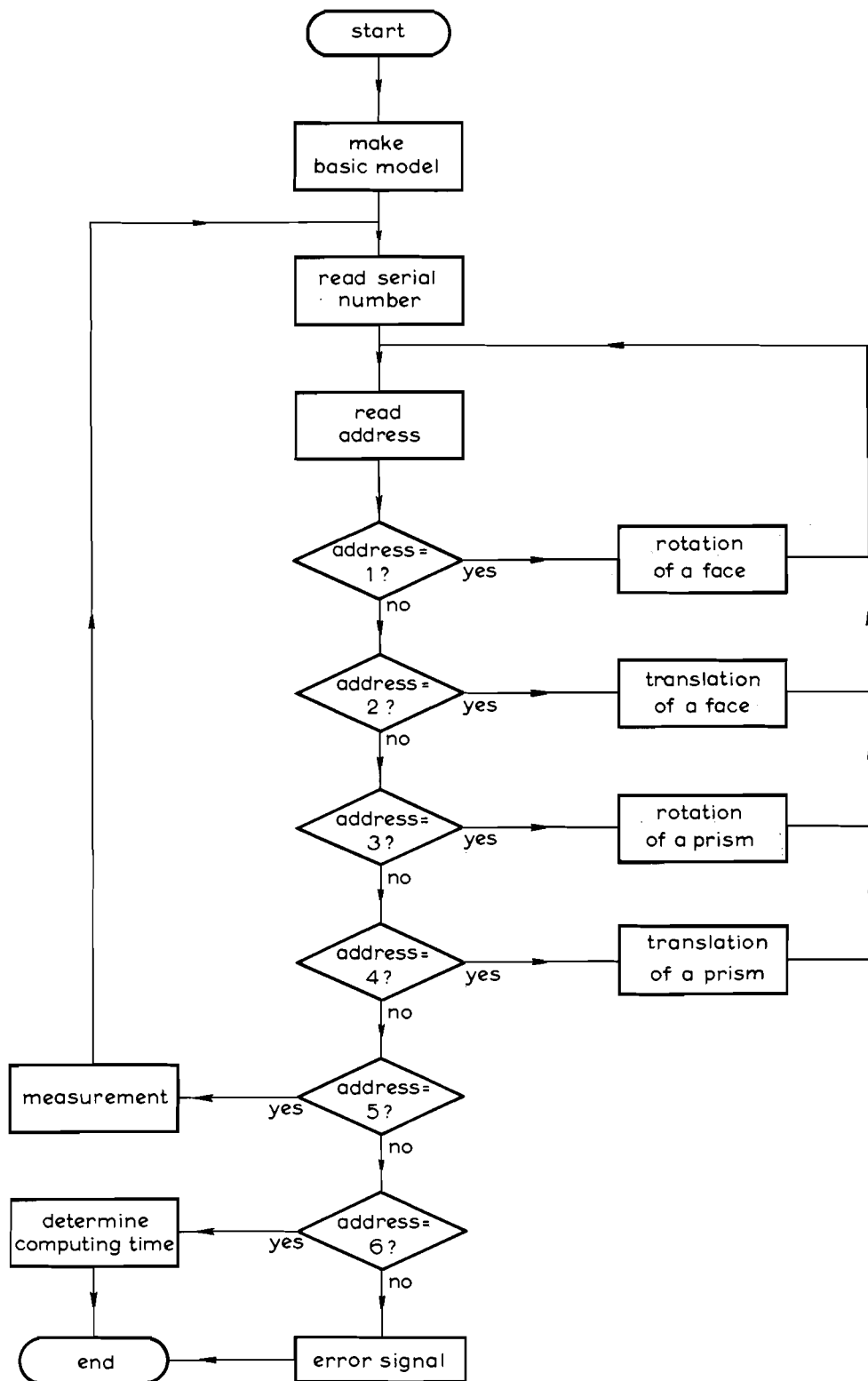


Fig. 3.25

At a later stage a further procedure "Snell" was added to the programme, by means of which it is also possible to calculate optical systems in which one or more spherical surfaces are included. Formula (3.70), $\Delta l = c \cdot x(1 - \cos 2\alpha / \cos \alpha)$, indicates how great an error is made with the basic model of the instrument at an angle of inclination α . In this formula the factor $c \cdot x$ may be equated with s . This is the length of the shift of the pentaprism along the base rail.

$$\Delta l_1 = s \left(1 - \frac{\cos 2\alpha}{\cos \alpha} \right) \dots \dots \dots (3.75)$$

Although this deviation is slight, it was investigated with the aid of the computing programme whether this term might not be made practically nil by a small deformation of one of the optical components.

By means of the computing programme the measuring error is found by calculating the point of intersection of the ray with the YZ plane, which is plane II in figure 3.24.

If the triangular prism rotates together with the pentaprisms, i.e. if the instrument does not reduce the distance, then the ray will describe a circle on the YZ plane. In that case the error is:

$$\Delta l_2 = A \cdot s (\cos \alpha - 1) \dots \dots \dots (3.76)$$

A is the multiplication constant.

The two formulae (3.75) and (3.76) are illustrated in figure 3.26.

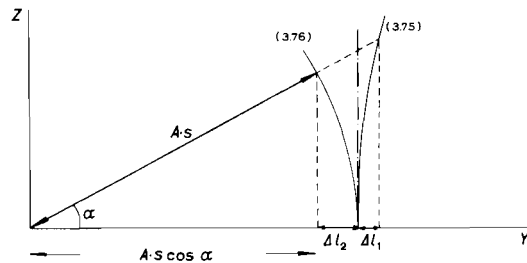


Fig. 3.26

As can be seen from the figure, the curves are situated on either side of the line at which the measuring error is nil. It should be possible virtually to eliminate the error according to (3.75) by causing the rays of light to traverse a triangular prism with a very small angle of refraction, which rotates together with the pentaprisms. This can be achieved by causing face 4 of prism 1 to rotate around the Z axis (see figures 3.24).

For each angle of inclination α there should be such a ratio between Δl_1 and Δl_2 that the error Δl_1 is eliminated.

$$\frac{|\Delta l_1|}{|\Delta l_2|} = a_\alpha \dots \dots \dots (3.77)$$

from which we obtain:

$$a_x = \frac{s \left(1 - \frac{\cos 2\alpha}{\cos \alpha} \right)}{A \cdot s(1 - \cos \alpha)} \dots \dots \dots (3.78)$$

If the total multiplication constant of the instrument is 100, the deviation of the ray of light in the right-hand part will be equal to $1/200$ radian, so that in (3.78) we find $A = 200$. For $\alpha = 30$ grades this gives $a_x = 0.015612$.

From this it follows that the part of the deviation that must not be subject to the reduction $0.015612 \times 1/200$ radian must be equal to 50 dmgr. According to this calculation face 4 of prism No. 1 would be rotated around the Z axis through an angle of 50 dmgr.

For different angles of inclination α the quantities a and b will assume different values. Moreover, the calculation of a and b according to the above formulae will be merely an approximation, since Δl_1 and Δl_2 will influence each other. In the mathematical derivation for the basic model in this chapter it has been assumed that the ray of light which falls upon the triangular prism is parallel to the X axis. In the case of rotation of face 4 this is no longer the case. A mathematical derivation of the new path of the rays is highly complicated, for which reason the errors have been precisely worked out in the computing programme for different rotations of face 4 whose magnitudes are in the vicinity of 50 dmgr.

Figure 3.27 gives a survey of the errors which occur for a distance of 40 m. These errors are generally proportional to the distance. The figure shows that a rotation of 44 dmgr produces the smallest deviations in the measuring result. This is based on the consideration that a measurement at an elevation of more than 30 grades is very exceptional.

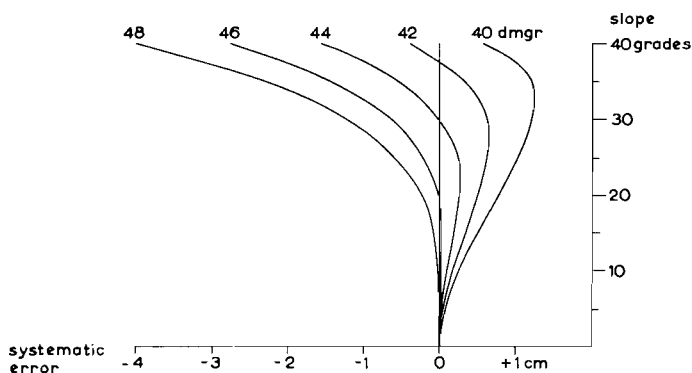


Fig. 3.27

In view of the questions posed at the end of section 3.1, several calculations were made by means of the computing programme for this deformed basic model, in which face 4 was given a rotation of 44 dmgr. As it is not feasible to discuss all results of the calculations, only a few of these results will be further examined in the following.

In order to ascertain what standards of accuracy are required when incorporating the optical components, the errors were determined when the prisms 1, 2 and 3 rotate singly around the three axes. The calculations were carried out for different translations of prism 3 and for the different angles of inclination α . In figure 3.28 the results are plotted in a graph for rotations of the prisms through $+0.1$ and -0.1 grade for a translation of prism 3 of

200 mm, which corresponds to a measurement over a distance of 40 m. The largest error is given by the rotation of prism No. 3 around the Y axis through -0.1 grade. In the case of rotation of the pentaprisms around the Z axis an addition constant is introduced according to the graphs.

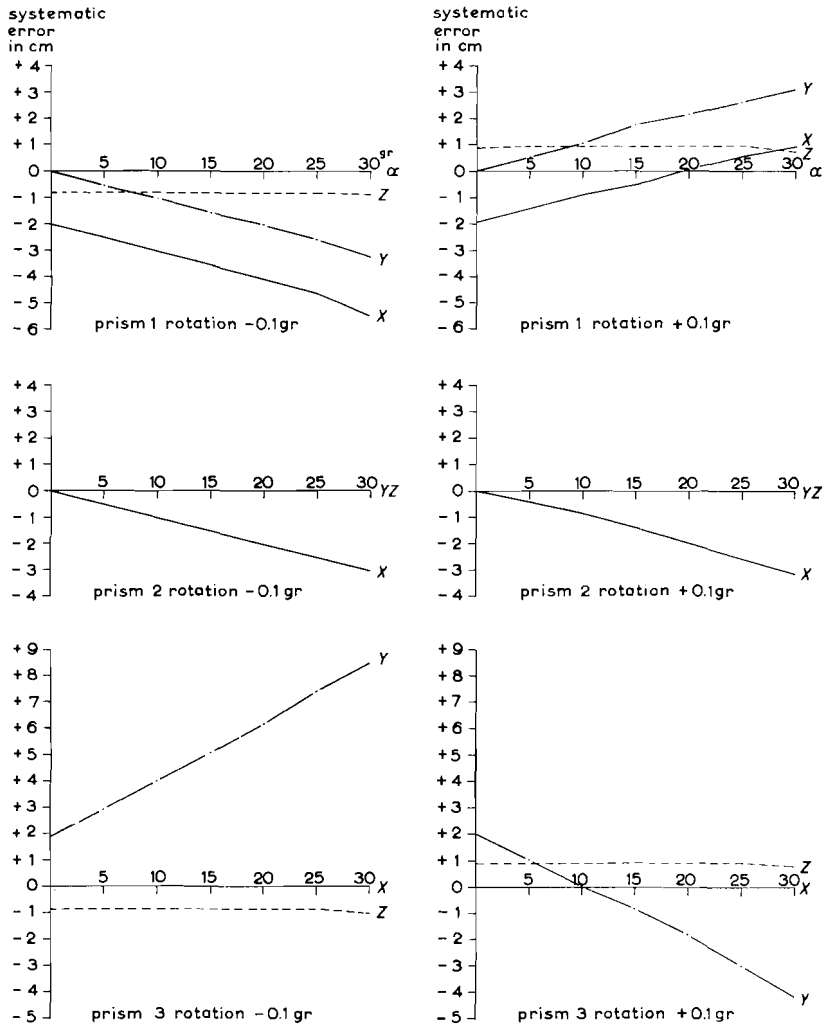


Fig. 3.28

Also for answering the question in how far the prisms may have a certain deformation, several calculations were carried out. In table 3.2 the errors are indicated for a distance of 40 m. These errors are approximately directly proportional to the distance. Each of the 10 planes (see figure 3.24) is given a rotation of $+0.01$ and -0.01 grade around the three axes. It is found that rotation of a plane around the Z axis has by far the greatest effect. Such rotation directly causes an increase or decrease of the multiplication constant.

It is further evident from the table that if the dihedral angle between the reflecting surfaces remains at 50 grades and the dihedral angle between the refractive surfaces is 100

Table 3.2 Systematic error in cm (distance 40 m)

face number	α gr	rotation on X-axis		rotation on Y-axis		rotation on Z-axis	
		-0.01 gr	+0.01 gr	-0.01 gr	+0.01 gr	-0.01 gr	+0.01 gr
1	0	0.0	0.0	0.0	0.0	64.0	- 62.0
	15	0.1	0.0	0.1	0.1	65.8	- 63.6
	30	0.0	-0.3	- 0.1	- 0.1	71.6	- 69.4
2	0	0.0	0.0	0.0	0.0	-345.0	416.8
	15	-0.4	0.4	0.2	- 0.1	-353.7	429.7
	30	-1.0	0.7	0.2	- 0.5	-382.4	472.4
3	0	0.0	0.0	0.0	0.0	416.7	-344.8
	15	0.2	-0.1	- 0.3	0.5	429.5	-353.5
	30	0.2	-0.5	- 0.9	0.7	472.2	-382.3
4	0	0.0	0.0	0.0	0.0	- 61.2	63.9
	15	0.1	0.1	0.1	0.0	- 63.5	65.7
	30	-0.1	-0.1	0.0	- 0.3	- 69.3	71.5
5	0	0.0	0.0	0.0	0.0	63.8	- 61.9
	15	0.2	-0.1	-15.0	15.3	63.8	- 61.7
	30	0.1	-0.4	-32.0	32.2	63.5	- 61.8
6	0	0.0	0.0	0.0	0.0	- 61.9	63.8
	15	0.1	0.0	15.3	-15.0	- 61.7	63.8
	30	-0.1	-0.2	32.2	-32.0	- 61.8	63.5
7	0	0.0	0.0	0.0	0.0	63.6	- 61.6
	15	0.1	0.1	0.0	0.1	65.5	- 63.3
	30	-0.1	-0.1	- 0.3	0.0	71.2	- 69.0
8	0	0.0	0.0	0.0	0.0	-343.0	414.4
	15	-0.2	0.3	0.6	- 0.4	-351.7	427.3
	30	-0.6	0.3	0.9	- 1.1	-380.4	470.0
9	0	0.0	0.0	0.0	0.0	414.2	-342.8
	15	0.3	-0.2	- 0.1	0.2	427.1	-351.5
	30	0.5	-0.7	- 0.4	0.1	469.8	-380.3
10	0	0.0	0.0	0.0	0.0	- 61.5	63.5
	15	0.0	0.1	0.1	0.1	- 63.2	65.4
	30	-0.3	0.0	- 0.1	- 0.1	- 69.0	71.2

grades, the errors are largely eliminated by the joint rotation of these surfaces. This property can be turned to account in the manufacture of the prisms.

Lastly, an answer is given in table 3.3 to the question what influence is exerted by shifting the triangular prism along the base rail. The errors were calculated in centimetres for distances of 20, 40 and 60 m. The triangular prisms are shifted through distances of 0, 2, 5, 10 and 15 cm. Such shift causes in the first instance an addition constant equal to the shift, but this can be corrected by a simple adaption of the target. This correction has been applied in table 3.3.

Table 3.3

systematic error in distance	α gr	translation of wedge-type prism				
		0 cm	2 cm	5 cm	10 cm	15 cm
20 m	0	0.0 cm	0.0 cm	0.0 cm	0.0 cm	0.0 cm
	10	0.0	0.0	-0.1	-0.1	-0.2
	20	0.0	-0.1	-0.2	-0.5	-0.8
	30	-0.1	-0.3	-0.7	-1.2	-1.7
40 m	0	0.0	0.0	0.0	0.0	0.0
	10	0.0	0.0	0.0	-0.1	-0.2
	20	0.1	0.0	-0.2	-0.4	-0.7
	30	-0.1	-0.3	-0.7	-1.2	-1.8
60 m	0	0.0	0.0	0.0	0.0	0.0
	10	0.1	0.0	0.0	-0.1	-0.1
	20	0.1	0.0	-0.1	-0.4	-0.6
	30	-0.1	-0.4	-0.7	-1.2	-1.8

3.4 Height measurement

Measurement of height differences can also be carried out in a simple manner by means of the instrument. For this purpose it is necessary that the triangular prisms shall be rotated through an angle of 100 grades, so that the refractive edges come into a horizontal position (see figure 3.29). In the case of rotation of the pentaprisms through an angle α , the triangular prisms remain in the same position.

Furthermore the shiftable pentaprisms must be placed in the zero position, at which $\alpha = 0$ grade, at some distance from the triangular prisms. This distance has been selected in such a way that at the zero position the pentaprisms are at a distance of 30 cm from each other. This is necessary because in the case of a negative angle of inclination these prisms have to be moved inwards. In this case two targets (on one staff) at a distance of 30 cm from each other are required for the height measurement.

As can be seen from figure 3.5, the height difference h is equal to $l_x \sin \alpha$, that is $h = A \cdot x_x \sin \alpha$. If on the base rail the pentaprisms are shifted from the zero position over a

distance $x_\alpha \sin \alpha$, then this quantity may be multiplied by the same constant A which applies in the case of distance measurement, in order to obtain the height difference h .

In figure 3.29 the points R and T represent the targets. For the zero position we have: $RT = UW$. If we assume that the triangular prisms are not in the instrument, the rays of light, even in the case of measurement at an angle of inclination α , will still pass through R and T . If the triangular prisms are placed in the instrument in such a manner that the refractive edges form an angle α with the horizontal, the points R and T are each shifted downwards over a distance $\frac{1}{2}x_\alpha$ to S_1 and S_2 respectively.

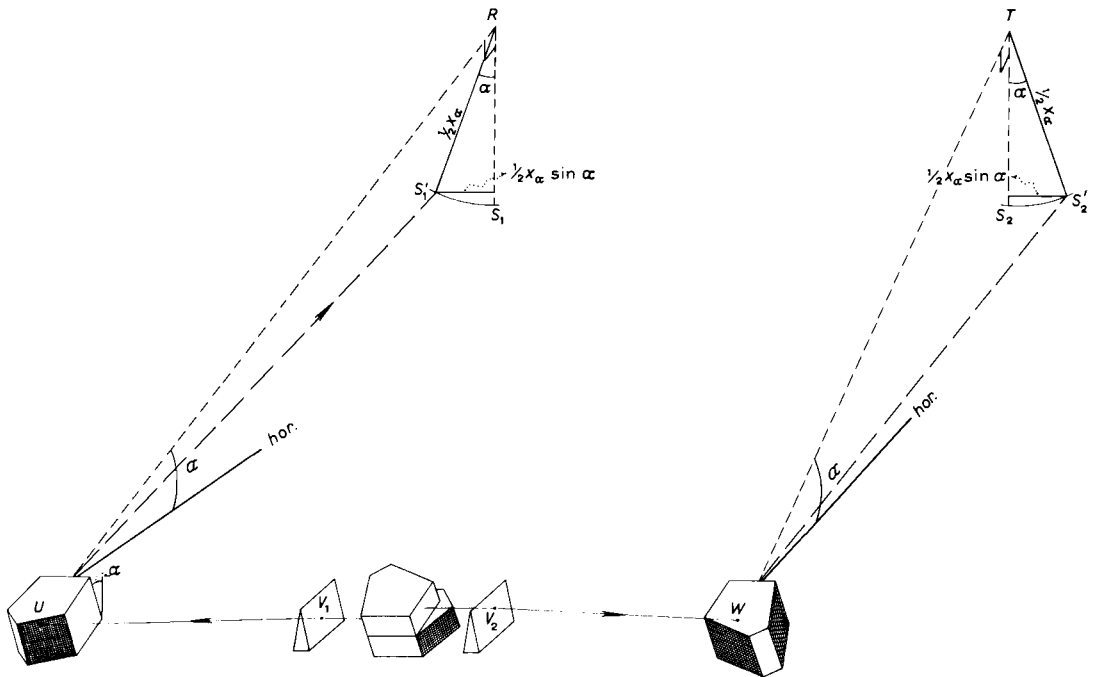


Fig. 3.29

If the refractive edges are placed horizontally, which means that the prisms are rotated through an angle α , then points S_1 and S_2 will come into positions S_1' and S_2' via an arc of a circle. In order to make S_1' and S_2' coincide, the pentaprisms must be shifted over a distance $2 \times \frac{1}{2}x_\alpha \sin \alpha = x_\alpha \sin \alpha$. The height measurement has thus in principle been effected. In the case of a negative angle of inclination α points S_1' and S_2' come to lie at the same distance from S_1 and S_2 , but this time on the other side.

As is the case with the reduced distances, the loci of U and W will here again be shifted laterally when the optical system is rotated through an angle α . This displacement will furthermore be adversely affected because, for the reduced distance measurement, a correction of 44 dmgr was made on one of the sides of the two fixed pentaprisms (see figure 3.27).

As the provision for the height measurement was added to the instrument at a rather late stage and as there was in any case an extensive computing programme for the path of the rays through the basic model, a mathematical derivation for the deviations in the height differences was not necessary.

With the aid of the computing programme the deviations in the measuring result were found which are reproduced in figure 3.30. The deviations hold good for a multiplication constant $A = 100$.

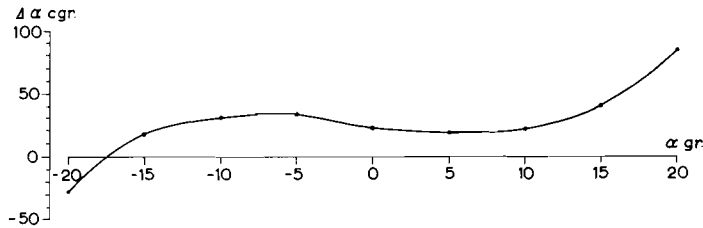


Fig. 3.30

The error $\Delta\alpha$ in the angle of inclination α in figure 3.30 has a systematic trend. This renders it possible to correct a height measurement for this error in the computer. This is done with the aid of the formula $h + \Delta h = l_\alpha \sin(\alpha - \Delta\alpha)$. This gives $\Delta h = l_0 \Delta\alpha$.

The curve that gives the best correspondence with the error curve of $\Delta\alpha$ is of the third degree and is represented in the following formula:

$$c_{gr} = +0.000117\alpha_{gr}^3 + 0.000097\alpha_{gr}^2 - 0.018139\alpha_{gr} + 0.261 \dots \dots \dots (3.79)$$

The residual error c is given in the following table 3.4 for different angles of inclination α .

Table 3.4

α grades	c grades
-20	-0.006
-15	+0.007
-10	-0.001
- 5	+0.006
0	-0.009
5	0.000
10	-0.004
15	+0.010
20	0.000

3.5 The telescope and image separation

No special form of telescope has been designed for the instrument. As the tube of the telescope must be as short as possible, use was made of the objective system with central focussing lens of a Kern telescope level type GK1. As a telescope level generally has a small visual field, an eye-piece of a Zeiss Jena Teletop was used. For image separation use was made of a biprism and of a diaphragm in the exit pupil. This system is also used, i.a., in Wild's RDH and in the Teletop.

The principle of image separation is represented in figure 3.31a and 3.31b. The entrance pupil of the telescope is situated in the objective, i.e. directly behind the two fixed pentaprisms. See Nos. 3 and 4 in figure 3.2a. The biprism is situated in the focal plane of the objective.

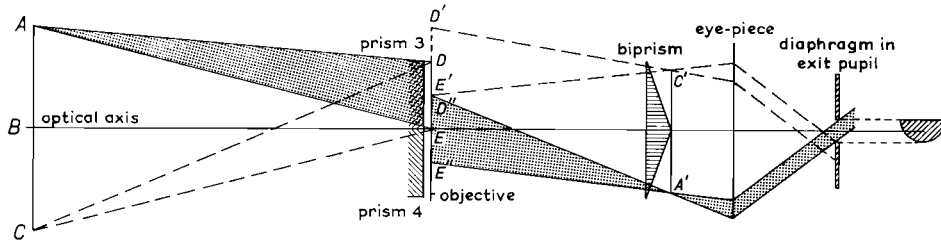


Fig. 3.31a

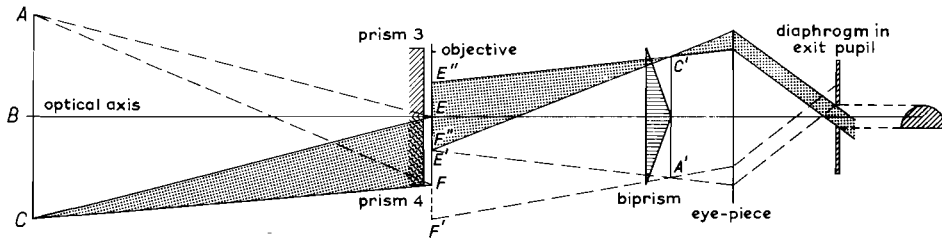


Fig. 3.31b

In figure 3.31a the path of the rays is shown as passing through the upper pentaprism No. 3 for a point A above and a point C below the optical axis. The exit pupil for this is DE . The strength of the biprism was selected in such a way that the entrance pupil of C is apparently shifted to $D'E'$ and from point A to $D''E''$. Similarly in figure 3.31b, in which the path of the rays is shown as passing through the lower pentaprism No. 4 the entrance pupil of point A is apparently shifted to $E'F'$ and from point C to $E''F''$. In figure 3.31a the entrance pupil $D'E''$ coincides with the entrance pupil $E''F''$ in figure 3.31b. The corresponding exit pupils thus also coincide. It is now possible to mount a diaphragm in the exit pupil in such a way that only the rays from this exit pupil can reach the eye. Screened from the eye are the beams falling from object points below the optical axis through the upper pentaprism and the beams falling from object points above the optical axis through the lower pentaprism.

4 SOME CONCEPTS IN SWITCHING ALGEBRA

This chapter will deal with certain concepts in switching algebra which are of importance to the subject-matters described in chapters 5 and 6.

Switching algebra is based on the scientific work of GEORGE BOOLE, and is therefore sometimes termed Boolean algebra. Switching algebra is quite a simple form of algebra, as the computing is done in the binary system (digits 0 and 1) and because only the operations of adding, multiplying and inverting occur. This algebra is termed dual because a distinct symmetry is perceivable in it. The formulae are transformed into themselves when the 0 and the 1 are interchanged as well as the addition and multiplication signs.

In switching operations we work with contacts which may be either open or closed. The assessments for these positions are: contact closed = 1 and contact open = 0. A parallel connection is represented by a + relation and a series connection by a \cdot relation.



Fig. 4.1

The system of connection $S = a + b$ is called an OR-function, and $S = a \cdot b$ and AND-function.

The elements a, b , etc. may be 1 or 0.

The undermentioned formulae and computation rules are proved in [10]. The proof of a formula is, moreover, quickly recognized by drawing the circuit concerned or by plotting the corresponding truth table.

Formulae:

Commutative law:

$$a + b = b + a$$

Dual:

$$a \cdot b = b \cdot a$$

Associative law:

$$(a + b) + c = a + (b + c)$$

$$(a \cdot b) \cdot c = a \cdot (b \cdot c)$$

Absorption law:

$$a + a \cdot b = a$$

$$a \cdot (a + b) = a$$

Distributive law:

$$a + b \cdot c = (a + b) \cdot (a + c)$$

$$a \cdot (b + c) = a \cdot b + a \cdot c$$

Other formulae:

$a + a = a$	$a \cdot a = a$
$a + 0 = a$	$a \cdot 1 = a$
$a + 1 = 1$	$a \cdot 0 = 0$
$a + \bar{a} = 1$	$a \cdot \bar{a} = 0$

(\bar{a} is the inverse of a)

By substitution of $a = 0$ or $a = 1$ in the formulae we obtain some further important computation rules:

$0 + 0 = 0$	$1 \cdot 1 = 1$
$1 + 0 = 1$	$0 \cdot 1 = 0$
$0 + 1 = 1$	$1 \cdot 0 = 0$
$1 + 1 = 1$	$0 \cdot 0 = 0$

An important formula in switching algebra is given by DE MORGAN's theorem. This is:

1. The complement of a sum is equal to the product of the complements of the variables.
 2. The complement of a product is equal to the sum of the complements of the variables.
- Expressed as formulae:

$$\left. \begin{array}{l} 1. \quad \overline{a+b+c} = \bar{a} \cdot \bar{b} \cdot \bar{c} \\ 2. \quad \overline{a \cdot b \cdot c} = \bar{a} + \bar{b} + \bar{c} \end{array} \right\} \dots \dots \dots (4.1)$$

The conclusion to be drawn from this theorem is that when converting switching functions into logical circuits we may confine ourselves to parallel connections with the possibility of inversion (NOR gates) or to series connection with the possibility of inversion (NAND gates).

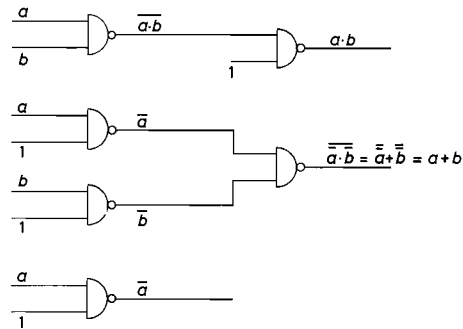


Fig. 4.2

An important aspect that presents itself in switching algebra is the simplifying of extensive circuits. This simplifying is possible with the algebraic formulae, but this is often very difficult to survey. The simplification of the circuits designed can be carried out by means of the so-called KARNAUGH maps. This method is dealt with in detail in [39].

In the electronic part of the instrument use is made of NAND gates produced by the firm of MOTOROLA. NAND means NOT-AND, i.e. the inversion of an AND circuit.

The three elementary operations: multiplying, adding and inverting, with NAND circuits are given in diagram form in figure 4.2.

An operation of rather frequent occurrence in switching algebra is that of addition according to modulo two system.

In this operation the formula for the switching function is:

$$S = \bar{a} \cdot b + a \cdot \bar{b} \dots \dots \dots (4.2)$$

If the circuit is to be executed with NAND gates the formula must be adapted somewhat.

$$\begin{aligned} S &= \bar{a} \cdot b + a \cdot \bar{b} \\ &= \bar{a} \cdot a + \bar{a} \cdot b + a \cdot \bar{b} + b \cdot \bar{b} \\ &= (\bar{a} + \bar{b})(a + b) \end{aligned}$$

These circuits which add modulo two are used in the instrument when converting the progressive code into the pure-binary code. See section 5.2.

5 CODED DISKS

By means of the instrument we have to measure three analogous quantities, viz. angle, distance and height difference. These measurements have to be registered automatically in digital memory elements. For this reason the observations must undergo analogous-digital conversion.

The distance and height measurements are effected by determining the distance between the outer pentaprisms which can be slid along the base rail. This translation of the prisms is converted into a rotation of a horizontal measuring disk. As a disk of this kind is also used for angular measurements, the use of this instrument only involves an analogous-digital conversion of a rotation.

5.1 Analogous-digital conversion of a rotation

An analogous-digital converter, which is designed for converting a rotation into digital electrical signals, consists of one or more disks or drums provided with a code. A reading mechanism enables the code to be read and to be converted into a number.

These a-d converters may be divided into two categories.

- a-d conversion according to the incremental method. With this method an interval of the coded disk is measured.
- a-d conversion according to the absolute method. With this method the position of the reading index is measured with respect to the coded disk.

With the first method an angle is measured and with the second method a direction.

If a coded disk is replaced by a coded rule, we obtain an analogous-digital conversion of a translation.

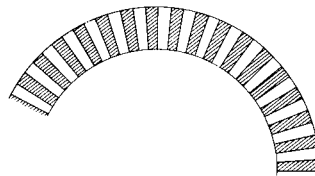


Fig. 5.1

An example of an a-d conversion according to the incremental method is afforded by an optical coded disk provided with white and black sections. See figure 5.1. With the aid of a lamp and a photo-electric cell electric signals are obtained when the sections pass the reading mechanism.

If the signals are counted by means of a counting mechanism, the difference between two positions of the circle can be measured with this a-d converter.

In order to increase the precision and speed of measurement, various possibilities are available. A coded disk may rotate several times for an angular measurement, the number of revolutions being counted as well. The disk may be equipped with several tracks, and a number of disks may be mounted one behind the other. High precision can be obtained by the use of different moiré effects.

There are considerable drawbacks to the use of an a-d converter of this category in optical distance measuring equipment:

- With angular measurement the operation of aiming at a target by means of the reading wire may be regarded as an iteration process. The a-d converter which is employed in this case must be provided with a counting device which can add and subtract. In view of the need for smallest possible dimensions and weight of the optical distance-measuring equipment it is inconvenient to equip the instrument with a reading device.
- With the incremental method intervals are determined with respect to an assumed zero point by adding up all the signals. Non-recurrent errors with respect to this zero point cannot be subsequently corrected.
- When taking each measurement it is necessary to start afresh from the zero position. This is time-consuming at a station where many targets have to be aimed at.

For these reasons an a-d converter has been decided upon which operates according to the absolute method. In the case of a-d converters which operate according to the absolute method the position of the reading index is determined. The optical coded disk is for this purpose provided with a pattern of transparent and opaque parts according to a certain code. This code is usually a variant of a binary or a decimal code or of a combination of the two. The code may also be designed for non-linear functions such as sine, cosine, etc.

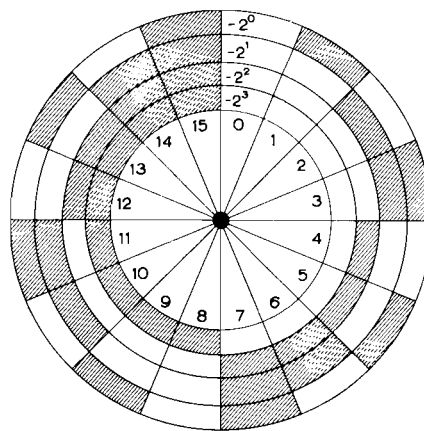


Fig. 5.2

Figure 5.2 shows a coded disk provided with a pure-binary code. The disk has four tracks with values of 2^0 , 2^1 , 2^2 and 2^3 . In this way sixteen sectors are obtained. The dark parts on this disk represent a 1 and the light parts a 0. The disk is numbered from 0000 to 1111 inclusive in the binary system and hence from 0 to 15 inclusive in the decimal system. Increase of the number of code tracks increases the resolution of the disk.

According to the nature of the reading mechanism and the material of which the coded disk is made, we differentiate between the following types of a–d converters.

– Electro-mechanical converters.

In this case the coded disk consists of conductive and non-conductive parts. With these converters there are numerous problems of a mechanical nature, the greatest of which is noise. This type of a–d converter is probably the most current. However, they practically always operate according to the incremental method.

– Magnetic converters.

Magnetic converters are provided with coded disks in which the material of the different parts is either magnetic or non-magnetic. These a–d converters are designed for comparatively high speeds of axial rotation. Their resolution is comparatively low.

– Optical converters.

These converters are expensive, but their resolution is very high, so that they lend themselves for a–d conversion according to the absolute method. The coded disk consists of material which is alternately transmissive and non-transmissive to light. The reading mechanism is formed by a battery of lamps and photo-electric cells.

5.2 The use of a progressive-binary code (Gray code)

If a disk is provided with a pure-binary code, very serious errors may occur in reading. Incorporated in the instrument are three coded disks. If the disk by means of which the distance measurement is registered is provided with a pure-binary code, figure 5.3 indicates what error may occur if for instance the photo-electric cells are not in good alignment. The disk is provided with 13 tracks.

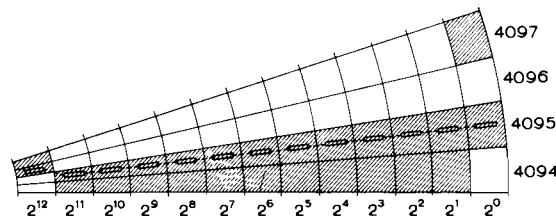


Fig. 5.3

If in the inner track representing the value 2^{12} the photo-electric cell is slightly ahead of or behind the correct position, an error will be made in passing from sector 4095 to sector 4096. In figure 5.3 it is not the binary number $011111111111 = 4095$ which is read, but $111111111111 = 8191$, i.e. an error of 100% of the number.

There are a few methods of avoiding such errors when passing from sector to sector.

- By adapting the reading mechanism it is possible to avoid errors. For this purpose two photo-electric cells are used for each track, except on the most finely divided track. The photo-electric cells are usually positioned V-shape on the disk. As a rule this method affords more liberty in the choice of the code. The method of reading, however, is complicated and necessitates a large number of additional circuits. See [41]. This solution does not meet the requirements of simplicity, small dimensions and low weight which are specified for a surveying instrument. Therefore, this solution was not chosen.

- The second possibility for the avoidance of errors consists in taking care that reading is not effected in the vicinity of a black-to-white transition. This possibility has been selected for angular measurement. The rather complicated equipment which is needed for this purpose will be further dealt with in section 5.3.

- Adaptation of the code by making it progressive is the simplest way of avoiding errors. All the coded disks are provided with a progressive code of this kind.

With a progressive code the pattern from light to dark or vice versa in course of passage from one sector to another changes on one track only.

If the errors in alignment of the slit through which the rays of light fall on the photo-electric cells are not too serious, no greater errors than one unit of a decimal number can occur during passage from one sector of the disk to another. The advantage is that only one photo-electric cell is required for each track. Owing to this, one is somewhat more restricted in the choice of the code. Figure 5.4 gives illustrations of some progressive-binary codes in comparison with the pure-binary code. Among the progressive-binary codes the Gray code has been selected for this instrument on account of the easy possibilities it affords for conversion into the pure-binary code.

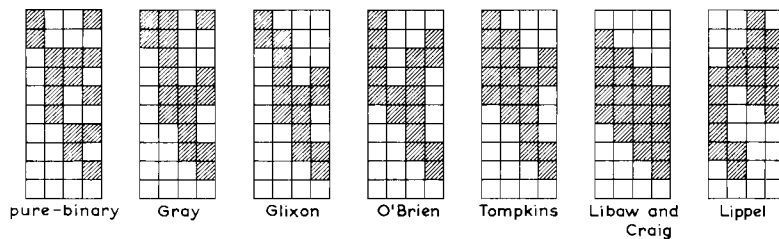


Fig. 5.4

The Gray code is named after one of its three inventors H. J. GRAY, P. V. LEVONIAN and M. RUBINOFF, who have published an article on this code [11].

The code owes its other name “reflected binary” to the fact that it is formed by reflection of the pure-binary code. Figure 5.5 shows how this reflection takes place. On the track with value 2^0 the sections are reflected around the axes 0, in the direction indicated. On the track with value 2^1 the sections are reflected around the axes 1, etc.

The Gray code possesses some important properties.

- In the Gray code the representations of each pair of consecutive numbers A and $A+1$ differ only in one column.
- The parity of a number in the Gray code is either even or odd according to whether the least significant digit in the corresponding number in the pure-binary code is 0 or 1.

The theses are proved, e.g. in the above-mentioned article [11].

The measuring results obtained by means of the coded disks are in the Gray code. In this code the number may safely be stored in the memory of the instrument. In processing the measuring data in the computer these numbers are converted via a computer programme into decimal numbers. In dealing with the electronic part of the instrument in chapter 6 it will be found necessary to be able to incorporate a checking instrument by means of which the observations in the field can be directly read. In this instrument the Gray code is converted into the pure-binary code.

The relations between the codes may be indicated in different ways. See [1], [11], [30] and [41]. The difference lies in the fact that either the most significant or the least significant of the digits in the numbers may be taken as basis. Moreover, the instruments required for conversion vary on account of the possibility of using series or parallel connections involving different logical switching elements (flip-flops, AND gates, NOR gates, etc.).

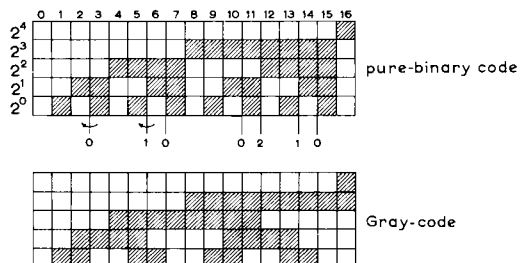


Fig. 5.5

A number in the pure-binary code is represented by $b_n b_{n-1} \dots b_2 b_1$. A number in the Gray code is represented by $g_n g_{n-1} \dots g_2 g_1$.

For the relation between the two codes use is made of the addition according to modulo two system as described in chapter 4.

In the notation of switching algebra the relation between the codes reads as follows:

$$\left. \begin{aligned} b_n &= g_n \\ b_j &= g_j \cdot \bar{b}_{j+1} + \bar{g}_j \cdot b_{j+1} \quad (j = 1, \dots, n-1) \end{aligned} \right\} \dots \dots \dots (5.1)$$

In [41] this relation is indicated by the following theorem: Each digit in the Gray code must be inverted as many times as there are ones preceding this digit.

The conversion in the instrument is effected in parallel with the aid of NAND gates. This conversion is new insofar as it is not found in literature on the subject.

5.3 Angular measurement

The measurement of distance by means of the instrument will not be more accurate than about 2 to 3 cm per 100 m. Taking as basis the rule of thumb according to which a deviation in the direction of one centigrade gives a point at a distance of 60 m a deviation of 1 cm perpendicular to the direction of measurement, it is not necessary to carry out the angular measurement with greater accuracy than to within centigrades. This means that at least 1/40,000 part of the circumference of the circle must be read. As $2^{15} < 40,000 < 2^{16}$, the horizontal circle will have to be given 16 tracks, so that 1/65,532 part of the disk can be read.

The size of the disk must be restricted as otherwise the instrument becomes too bulky, but also because the disk is coupled to the vertical spindle of the instrument. The radius of the disk should preferably not be greater than 7 to 8 cm.

The reading mechanism consists of two lamps and of a photo-electric cell for each of the 16 tracks. For these cells the BPY 10 of Philips has been selected. As a result of the breadth

of the photo-electric cells, the width of the tracks has been taken as 3 mm. A space of 1 mm has been left open between the tracks, as a photo-electric cell must not react to light impinging upon an adjacent track. As a result of this, the radius of the inner track is not greater than 2 cm. The accuracy of 1 centigrade with which the inner track has to be read corresponds in linear measure to 3 μ . This measure not only makes high demands upon the manufacture of the coded disk, rendering it very expensive, but in addition almost insuperable difficulties are encountered in connection with the reading mechanism. A geodetic instrument makes particularly high demands upon the reading mechanism, since an instrument of this kind may be subjected to a variety of atmospheric conditions. Moreover, an optical distance-measuring appliance is exposed to shocks, as the instrument is frequently transported and mounted.

As a coded disk with 16 tracks involves difficulties, a different mode of solution has been selected. Incorporated in the instrument are two coded disks, the parts of the most finely divided track of the first disk being measured by means of the second disk. This solution is similar to the reading of the circle of a theodolite, a circle of which, having a scale division with rather large intervals, is read with the aid of a micrometer.

The main disk in the instrument is provided with 10 tracks, whilst the micrometer consists of a segment of a coded disk with a size of about 40 grades provided with 6 tracks. With this micrometer it is possible to read $2^6 = 64$ units.

In figure 5.6 the position is given of a part of the main disk with respect to the reading line. In the tenth track the distance a should be measured with a micrometer. This is no problem in the case of an ordinary theodolite, because with this instrument the reading line is set in coincidence with a graduation of the scale division with the aid of the micrometer. This is not possible with a coded disk, as in that case the reading line, i.e. the photo-electric cells, are positioned on a black-to-white transition, so that it is uncertain what will be read. One unit of the 10th track corresponds to 0.1 grade, and an error of this magnitude is not permissible.

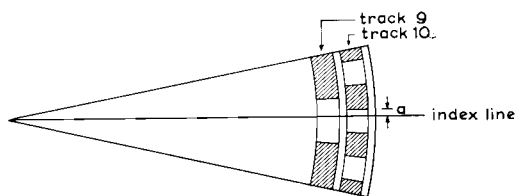


Fig. 5.6

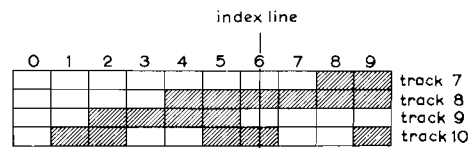


Fig. 5.7

In the case of the main disk steps have been taken to ensure that in reading the micrometer the row of 10 photo-electric cells is as far distant as possible from any black-to-white transition. This mode of solution offers the greatest possible certainty that the main disk will not be erroneously read.

In order to ascertain how the position of the reading line with the row of 10 photo-electric cells should be in the case of an observation of a direction, a part of the coded disk is depicted in figure 5.7 as a rectangle. This section of the disk is provided with four tracks and ten sectors, each of which represents a decimal number.

It can be seen from the figure that if during registration the photo-electric cells are to be

as far distant as possible from all black-to-white transitions, then the reading line must run midway across a sector. As on the track with the finest division a white and a black section each have the breadth of two sectors, the reading line must fall along the line which is situated at a distance of $\frac{1}{4}$ of the length of a section from a transition on this track.

In order to achieve this a track of lines is placed along the 10th track. These lines are situated at the boundaries of the sectors of the coded disk. The distance between the lines is about 0.38 mm.

Moreover, a new reading line is incorporated in the instrument which, like the reading line with the photo-electric cells, passes through the centre of the disk. The two reading lines form a constant angle with each other, the size of which is an integral number of sectors plus half a sector. This second line is provided with a reading wire. As the reading mechanism may be turned somewhat out of position, it is possible to set the reading wire in coincidence with one of the lines on the track of lines. In this way the reading line with the photo-electric cells occupies the ideal position.

High demands are made upon the accuracy of the lines. By means of these lines an accuracy of one centigrade must be obtained by coincidence with the reading wire.

The advantage of this method of reading is that the precision with which the scale division of the Gray code must be marked on the disk need not conform to very high demands. During reading the photo-electric cells are always situated a few tenths of a millimetre from the black-to-white transitions.

Similarly, the precision of the black-to-white transitions on the micrometer disk need not

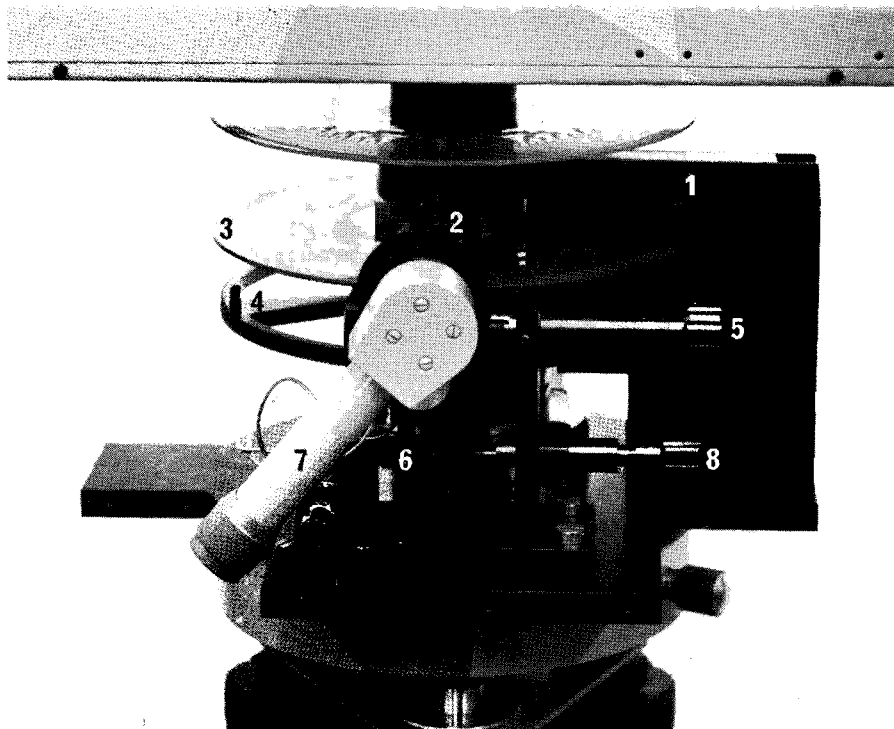


Fig. 5.8

conform to extremely high standards. This disk was originally provided with 9 tracks, so that the number of sectors was $2^9 = 512$. One sector corresponds to $400/512 \approx 0.8$ grade. The smallest unit to be measured for horizontal directions which, as set forth in the beginning of this section, is somewhat less than 1 centigrade, corresponds on the micrometer to an interval of approximately 0.8 grade.

The mechanical part of the coded disk together with the micrometer is represented in figure 5.8. The reading mechanism for the main disk and for the micrometer disk is fixed to arm No. 1.

The main disk 3, which is rigidly coupled to the vertical spindle, and the large toothed wheel 4 in which the micrometer disk is placed, turn through this reading mechanism. Arm 1 is rigidly connected to another arm 2. Connected to this latter is a rotatable telescope 7 in which a reading wire is incorporated. This telescope will in due course be replaced by a piece of image-transmitting fibre-glass optics. The reading wire forms with the slits in the reading mechanism an angle which is equal to an integral number of times plus a quarter of the smallest interval of the main disk. The reason for this has already been stated by reference to figure 5.7. Arms 1 and 2 are to some extent rotatable around the vertical spindle of the instrument in order to make the reading wire coincide with one of the lines on the track of lines of the main disk. This coincidence is brought about by rotating knob 5, thereby enabling arm 2 and hence arm 1 to be moved horizontally with the aid of a worm wheel. By rotating knob 5 the vertical spindle 6 is at the same time rotated via two conical toothed wheels, by means of which spindle the large toothed wheel 4 together with the micrometer disk is turned through the reading mechanism.

Knob 8 in figure 5.8 is separate from the micrometer part. This knob serves only for fine adjustment of the rotation of the vertical spindle in order to facilitate precise aiming at the target.

5.4 Measurement of distance and height

For registering the observations in connection with the measurement of distance and height it was decided to select a coded disk and not a coded rule. An advantage of the use of a coded disk is, e.g., that this disk, together with the coded disks for angular measurement, can be stored in a practically dust-tight casing. This is important because each photoelectric cell in the reading mechanism is covered with a thin plate in which a slit of only 80μ breadth is provided. Moreover, the reading mechanism together with the wiring can now remain stationary when the instrument is rotated.

The displacement of the shiftable pentaprisms, which is a measure both for the distance and for the height difference, must be converted into a rotation of the coded disk. The toothed wheel 1 in figure 5.9 is rigidly connected with the coded disk. They can together rotate freely around the vertical spindle of the instrument.

The instrument is designed in principle for measuring distances up to 100 m. With the aid of a special staff this distance can, moreover, be extended without undue difficulty to 200–300 m. Reading must be effected in units of 1 cm. The number of binary units into which the coded disk can best be divided is $2^{13} = 8192$. The disk is therefore divided into 13 tracks. The size of the disk is adapted to that required for angular measurement, so that the radius of the outer track is 7 cm. A unit on the disk corresponds to approximately

0.05 grade. This means that the accuracy with which the reading should be taken is $\frac{1}{20}$ mm for the outer track and $\frac{1}{40}$ mm for the inner track. The method of reading the coded disks is further dealt with in section 6.1. Reading with the aid of a lamp and photo-electric cells is rather difficult. It is therefore desirable that the coded disk should continue to rotate in a horizontal direction even if the distance and the height difference are measured at an angle of inclination of α .

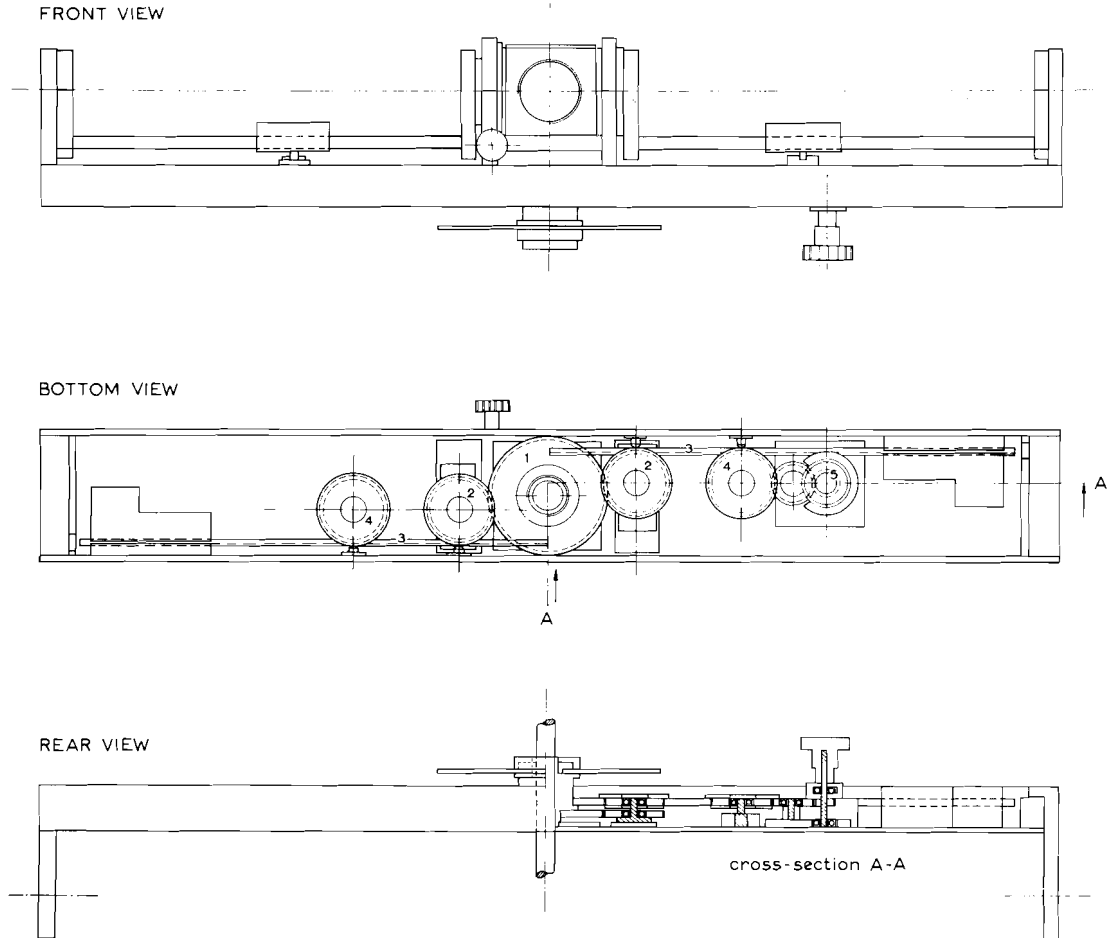


Fig. 5.9

The toothed wheel 1 must rotate in the same horizontal position as the coded disk. If during measurement at an angle of inclination α the spindle of the toothed wheel 1 forms this same angle with the vertical axis, then the toothed wheel and the coded disk will no longer rotate conformally.

Figure 5.10 indicates what influence the angle α exerts upon the angular rotation φ of the vertical axis of the coded disk and upon the angular rotation ψ of the oblique spindle of toothed wheel 1.

From the figure we find: $\tan \varphi = a/OP$; $\tan \psi = a/OQ$ which gives:

$$\frac{\tan \psi}{\tan \varphi} = \frac{OP}{OQ} = \cos \alpha \dots \dots \dots (5.2)$$

Hence $\tan \psi = \tan \varphi \cos \alpha$.

Systems are known by means of which conformal couplings for two intersecting spindles can be made. For instance, in the case of two Hooke's joint mechanisms and an intermediate spindle the angular error of the first Hooke's joint transmission is compensated by that of the second.

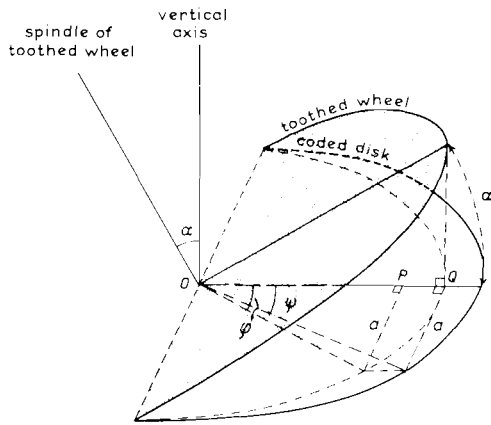


Fig. 5.10

In order not to render the construction of the instrument unnecessarily complicated it has been decided to keep the toothed wheel 1 and the system providing for propulsion horizontal. A bottom view of this mechanism is given in figure 5.9.

The horizontal shifting of the pentaprisms is effected by means of two short spindles which are rigidly coupled to the toothed racks 3. These toothed racks are shifted by rotating knob 5 in such a way that the images of the targets are made to coincide in the visual field of the telescope. The toothed racks bring about rotation of the toothed wheels 2 and hence of toothed wheel 1.

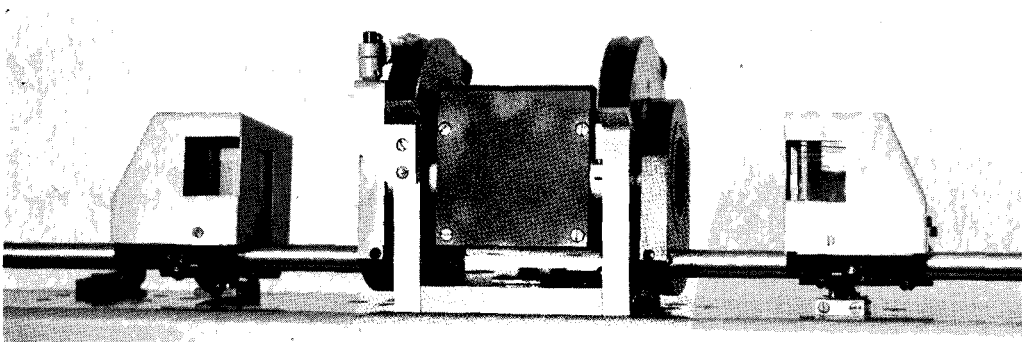


Fig. 5.11

In order to permit measurement at an angle of inclination α by means of the shiftable pentaprisms, they are mounted on two carriages, each of which can be slid along two rails. This assembly can be rotated around the optical axis of the prism system. See figure 5.11.

A further difficulty in the measurement of distance and height is caused by the toothed wheel system represented in figure 5.9. When the telescope is directed on to a detail point the entire arm of the instrument rotates until it is positioned perpendicular to the direction of measurement. During this rotation there must in principle be no shifting of the pentaprisms. This means that toothed racks 3 and all the toothed wheels must occupy the same position with respect to each other. In this way toothed wheel 1 and the coded disk coupled to it will rotate to the same extent as the instrument. The reading on the coded disk will thus consist of the sum of the angular measurement and of the measurement of distance or height. From this value, the known angular measurement can straight away be deducted in the computer. In 400 grades, there are 65,536 units available for the angular measurement and 8192 units for the distance or height measurement. This correction is made in the pre-programme of tacheometry.

5.5 Production of the coded disks

Many manufacturers make coded disks according to their own particular process. The accuracy of these disks sometimes varies considerably. The prices are difficult to compare, since one group of manufacturers calculates the price per coded disk, whilst the other group calculates a high price for the first coded disk and a very low price for subsequent identical disks.

The price depends upon the number of tracks and is about Dfl 2000.— for a disk with ten tracks in a current code (pure-binary or Gray code). The delivery time is generally at least three months. Should one desire a coded disk with a special division or deviating dimensions, or a disk with a track of lines such as the coded disk for angular measurement, the price is considerably higher and one has to reckon with a delivery time of at least one year.

For this reason a system has been developed within the framework of this research for the production of special coded disks in a comparatively cheap manner, and with a fairly short period of manufacture. It was possible to undertake this manufacture because electronic drawing machines have for some years been ready-installed in Holland at a number of geodetic institutions. On these machines it is possible to plot points on a drawing surface of at least 1.50 m by 1.20 m with a fairly high degree of accuracy (standard deviation < 0.05 mm) and at a fairly high speed.

The manufacture of the coded disks is as follows. The polar coordinates of all the angular points of the black-to-white transitions on the disk can be calculated according to a simple formula. On a computer, in this case the TR-4 of the Delft University of Technology, the Cartesian coordinates of these angular points are calculated according to the formulae $x = r \cos \varphi$ and $y = r \sin \varphi$. Here φ is the polar angle of the point in question with respect to the value zero on the disk.

The radius r is multiplied in the computer by a certain factor, as the points of the coded disk have to be plotted on a larger scale on the electronic coordinatograph.

Moreover, the punched tape with the Cartesian coordinates must be provided with drawing instructions in the computer for the machine by means of which plotting is effected. After

the points have been plotted by the drawing machine on dimensionally stable drawing material, the blocked distribution of the Gray code is applied as accurately as possible by a draughtsman.

A photographic reduction of this drawing is made on a dimensionally stable reversing film or directly on to a glass negative by means of a cartographic precision camera. If the process of the reversing film is followed, a negative of the latter is made on a glass photographic plate. This glass negative with the code upon it is the coded disk. The final processing operations to be performed on this square plate are the grinding of the disk to a circular shape and providing it with a hole into which the vertical spindle of the optical distance-measuring equipment fits.

5.5.1 *Production of the micrometer disk*

In order to ascertain whether a sufficiently accurate coded disk can be made according to the process described above, a disk with nine tracks was made first.

With this disk a trial set-up was made in order to find out what lamps, photo-electric cells and photo-electric amplifiers could most suitably be used in the reading mechanism. In course of testing for accuracy it was ascertained which parts had to be improved in the production process.

For calculation of the polar coordinates of the angular points of the blocked distribution the following data were used.

There are nine tracks, whilst on one track the number of black-to-white transitions is $i + 1$.

For the polar angle on track p ($p = 2, \dots, 9$) the following formula is applicable:

$$\varphi_1 = \frac{2\pi}{2^p}; \quad \varphi_i = \frac{2\pi}{2^{p-1}} + \varphi_{i-1} \quad \text{or} \quad \varphi_i = (i-1)\frac{2\pi}{2^{p-1}} + \varphi_1 \quad \dots \dots \dots (5.3)$$

For track 1 (inner track) on which there are two black-to-white transitions the applicable equations are $\varphi_1 = \pi$ and $\varphi_2 = 2\pi$.

For the radii (r) of the tracks, we have:

- track 9: $r = 300$ mm and 280 mm
- track 8: $r = 275$ mm and 255 mm, etc.
- track 1: $r = 100$ mm and 80 mm

The Cartesian coordinates of these points were calculated on the TR-4 and punched into a tape. This tape served as input for an electronic drawing machine (Zuse Graphomat). The drawing material on which the points were plotted was the dimensionally stable correctostat. The entire distribution of the Gray code was marked with Indian ink between these points.

A fivefold reduced diapositive of this drawn coded disk was made on the dimensionally stable Kodolith material with the cartographic precision camera Littlejohn. As the image of this disk on the film is identical with the original drawing, the diapositive obtained in this way is a reversing diapositive. Negatives of these were made on Ilford "Special Lantern" photographic glass plates by means of contact copy. One of the glass negatives was ground to a circular shape and provided with a hole. In this way the first coded disk was obtained.

Figure 5.12 shows the image produced by the reversing diapositive. The hatched part has been cut out of this disk. This part, on which there are 63 black-to-white transitions, is used in the instrument for the micrometer of the horizontal circle.

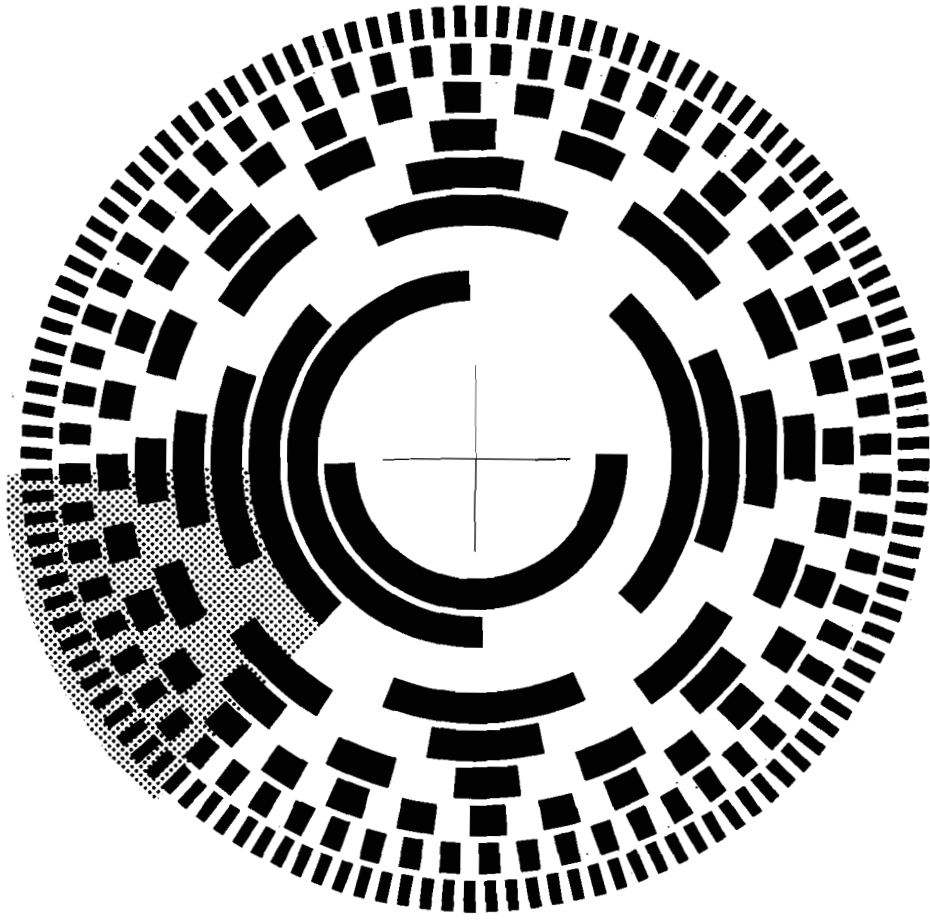


Fig. 5.12

5.5.2 Production of the main disk for angular measurement

The reversing diapositive of the main disk for angular measurement is shown in figure 5.13. The manufacture of this diapositive resolves itself into two items:

- The tracks of the Gray code.
- The track of lines.

The marking of the ten tracks of the Gray code on the main disk is practically identical with the process followed in the case of the micrometer disk. As has been shown in section 5.3, the standards specified for the black-to-white transitions of the main disk are not made too rigorous, because in registering the observations the photo-electric cells are situated as far away as possible from all black-to-white transitions. Nevertheless, in order to eliminate in advance any errors which might occur through bad marking of the transitions, more care

has been taken in drawing the blocked distribution than in the case of the micrometer disk.

The Cartesian coordinates of the angular points of the division of the disk were plotted by means of an electronic coordinatograph (Coradomat).

The drawing material used for this purpose was the dimensionally stable Stabilene Y 466 H of the firm of Keuffel and Esser Co. The contours of the blocked division were engraved

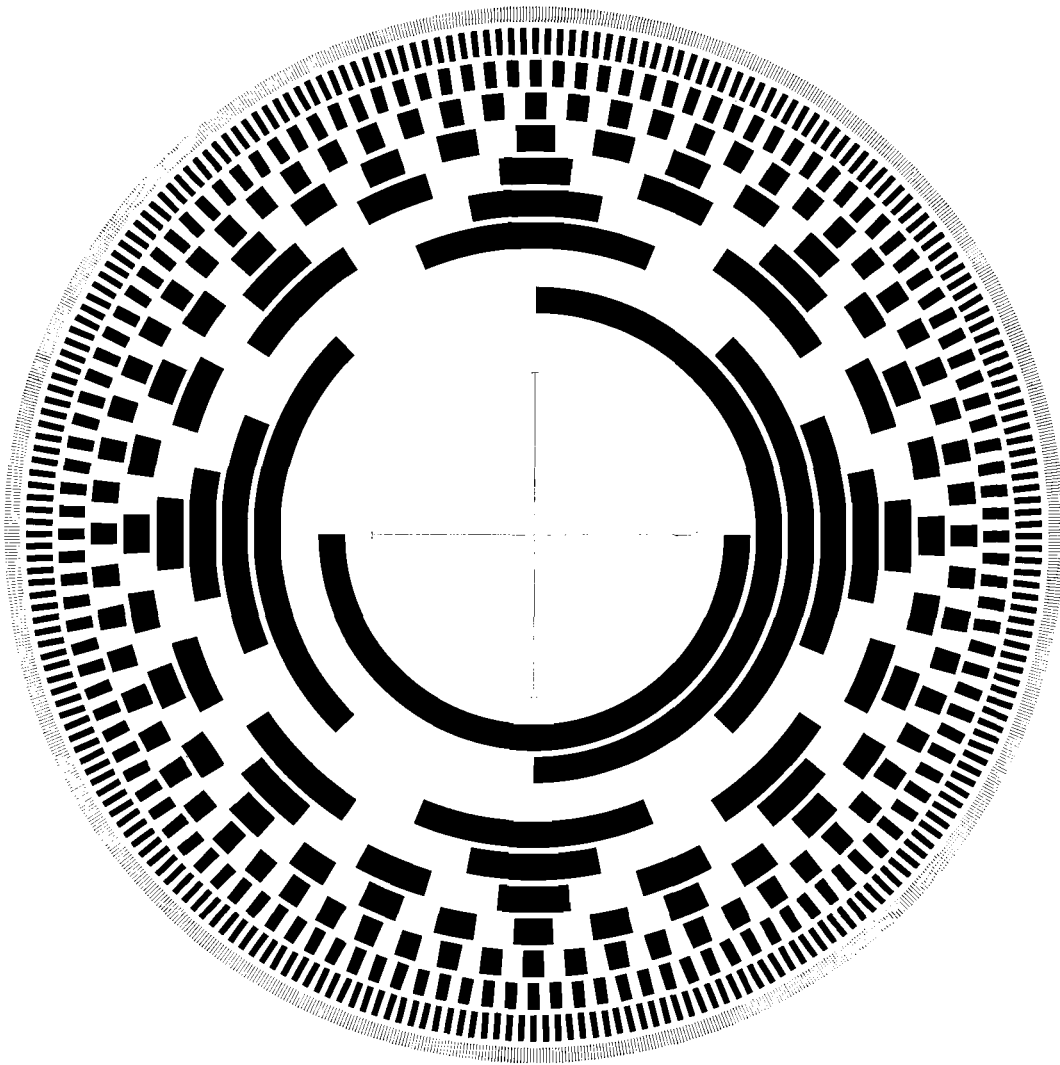


Fig. 5.13

upon this material with the utmost precision by a draughtsman of the Delft Geodetic Institute. The diapositive, which was manufactured at a later stage, was a sevenfold reduction of this drawing.

Some difficulty was experienced in making the track of lines on the coded disk. The lines on the coded disk have in reality a breadth of approximately 0.03 mm. For a sevenfold enlargement these lines are engraved with a line thickness of 0.2 mm. It was hardly feasible

to make the middle of such a line coincide with its plotted initial and final points. For this reason a different method was adopted for making the track of lines. If the enlargement is 21 times instead of 7 times it is possible to engrave a line as a small block. Inside the contour lines of the block, the engraving layer was removed as has been done with the blocks of the Gray code.

On account of the size of existing electronic coordinatographs it is not possible to plot the coordinates of the angular points of the track of lines on a drawing all at once in the case of a 21-fold enlargement. For this reason only $\frac{1}{8}$ of the track of lines was plotted and engraved on the Stabilene engraving film Y 466 H. Eight prints of this drawing were made with a threefold reduction and glued together as satisfactorily as possible, after which they were affixed to the drawing of the Gray code. A sevenfold reduction of this drawing was made on Kodolith by means of the cartographic precision camera of Littlejohn.

5.5.3 *Production of the disk for distance measurement*

In the test for the accuracy of the coded disks, which test is described in section 5.6, it was found that the precision of the black-to-white transitions in the case of the main disk was not up to expectations. This was a result of halation, as a result of which the white and black blocks were not equal in size. Moreover, this halation was not regular, but was distributed very erratically over the disk.

The disk for distance measurement is provided with 13 tracks. This means that $2^{13} = 8192$ black-to-white transitions were marked on the disk. One sector on the disk corresponds to $400/8192 \text{ gr} = 5 \text{ cgr}$. As the inner track has a radius of about 3 cm, this means that the transitions have to be marked with an accuracy of at least 25μ . It was found on remeasuring the main disk that this degree of accuracy was not reached at certain locations. Efforts were made to increase the degree of accuracy in all phases of manufacture of the disk for distance measurement.

In the first place use was made of the Cut'n Strip engraving material 0.13 mm in thickness as produced by the firm of Keuffel and Esser. The blocked division was cut out in this material with a sharp knife after the angular points of the blocks had been plotted by means of an electronic coordinatograph (Coradomat).

In the second place the best camera obtainable in Holland was used, viz. the large Klimsch Commodore camera of the Ministry of Public Works in The Hague. As this camera is used almost exclusively for cartographic purposes, little was known about the effect of halations in different parts of the visual field. Before the final photographs could be taken, a thorough investigation of this halation effect was carried out.

In this investigation the following questions were posed:

- What is the effect of different kinds of developer?
- What is the difference according to whether the light falls upon or through the drawing?
- May a reversing diapositive be used or should a photograph be taken directly on a glass negative?
- What photographic plates are most suitable?

In order to answer these questions several photographs were taken under different conditions and with different exposure times. It was necessary for all the coded disks made in

this manner on glass plates to be minutely examined at different locations with a comparator.

It is not possible to go thoroughly into this investigation within the framework of the present thesis, so that a statement of the results must suffice.

The kinds of developer which were used gave a good result in every case. The freshness of the developer was an important consideration. When a given quantity had been used once for a glass plate, halation of the order of 20 μ occurred if this developer was used a second time.

Practically all the tests were carried out with transmitted light, because with impinging light a bad result was obtained. In the case of directly transmitted light it was found that the halation on a plate was not constant. The correct exposure times varied between the side edges and the top and bottom edges by about 20 seconds over an average exposure time of 30 seconds. The best result was obtained by making the light fall on a pearl screen. This reflected light was transmitted via a frosted glass disk through the drawing.

Unfortunately it was found that with these photographs it was not possible to use reversing diapositives. If this had been possible a large number of coded disks of the same quality could have been obtained with these plates by means of contact copying. The tests showed that if all other conditions were identical the exposure times for good reversing diapositives varied too greatly. A reliable result could not therefore be predicted beforehand.

For the photographic plates the choice was in the first instance in favour of MR plates (maximum resolution) of Kodak. Owing to the long delivery times, however, it was decided to incorporate in the prototype of the instrument a coded disk of one of the available Gevaert plates having a resolution of 225 lines per mm.

As it was found that the correct exposure time was somewhere about 60 seconds, a series of five glass negatives with exposure times of 55, 57.5, 60, 62.5 and 65 seconds was ultimately produced. Figure 5.14 gives the average halations for the outer track 13. A block on this track is on an average 105 μ in breadth.

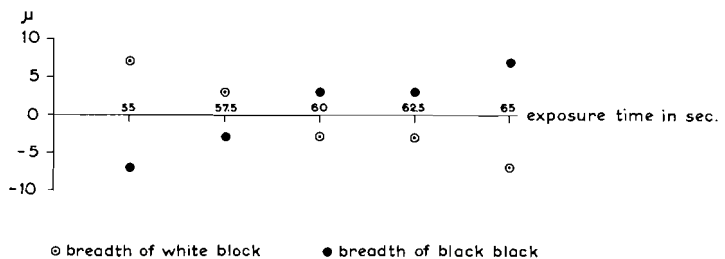


Fig. 5.14

From this series the disk with an exposure time of 60 seconds was selected. This disk as viewed in its entirety was the most satisfactory in regard to halation. On grinding this glass negative to a circular shape the disk was broken. The second choice was in favour of the plate with an exposure time of 62.5 seconds. The halations were in some places slightly larger than on the disk of 60 seconds. The deviations of this disk were still within tolerable limits as will be seen in the next section.

An illustration of the coded disk for distance measurement is given in figure 5.15.

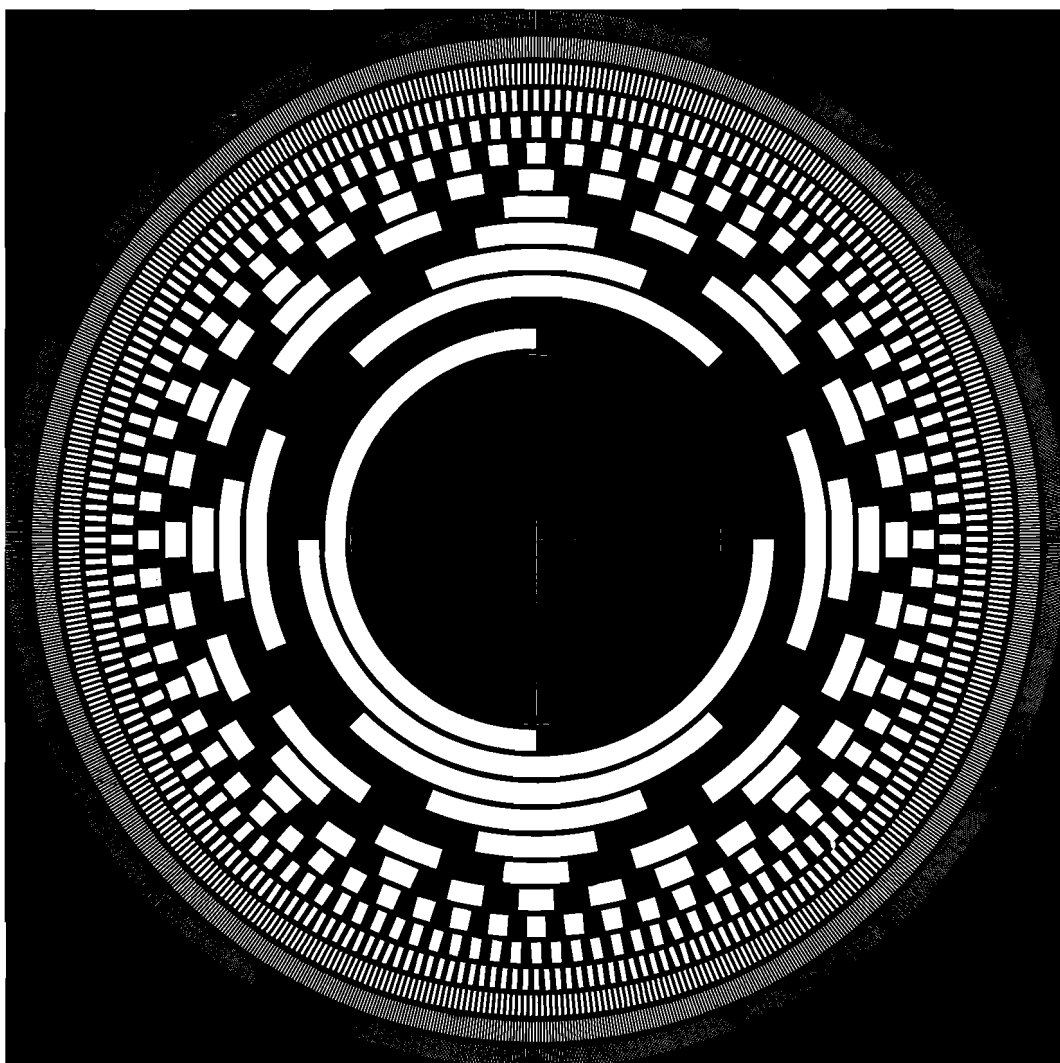


Fig. 5.15

5.6 Investigation of the accuracy of the coded disks

Before the coded disks were incorporated in the instrument measurements were made directly upon them in order to verify their accuracy. The measurements on the disks were carried out on the Wild stereocomparator. This instrument was used in this case as a monocomparator. The standard deviation in the coordinates measured is 2 to 3 μ . It will be shown in this section that this degree of accuracy is sufficient for the different measurements to be carried out.

The investigation as to the accuracy of coded disks resolves itself into three items:

- Investigation as to the accuracy of the track of lines on the main disk for angular measurement.
- Investigation as to halation in the Gray code on the main disk.

- Investigation as to the accuracy with which the division in the Gray code is marked on the disk for distance measurement.

5.6.1 *Investigation regarding the track of lines on the main disk for angular measurement*

The object of this investigation is not only to ascertain with what degree of accuracy the track of lines was marked on the disk, but also to ascertain whether, in the case of excessively large deviations, these latter can be corrected by means of a simple formula during the calculations in the computer.

As set forth in section 5.3, the accuracy of the track of lines on the main disk is the decisive factor for the degree of accuracy with which angular measurement can be effected. Over the entire circle $2^{16} = 65,536$ units can be measured by means of the micrometer disk. This corresponds to approximately 0.006 gr. The track of lines has a radius of 6.9 cm, which means that a measurement perpendicular to the radius with a standard deviation of from 2 to 3 μ corresponds to an accuracy of 0.002 to 0.003 grade, so that measurement with a Wild stereocomparator gives a sufficiently accurate result.

For measurement of one of the lines the target of the stereocomparator was set in coincidence with the line at two positions. In figure 5.16 these two positions are points *a* and *b*.



Fig. 5.16

This was done not only to increase the accuracy of measurement, but also to make sure the lines were properly directed towards the centre of the disk. All the lines of the disk were measured, because on account of the manufacturing process it was considered quite possible that short-period errors might occur. This assumption did prove correct, because at the locations where the eight segments of the track of lines were welded to each other rather large differences of at times 1.5 centigrade were found to exist.

As it has already been shown by the foregoing test measurements that the stereocomparator had a very slight but regular shift of position, a fresh orientation was measured on the disk after each measurement of about 60 lines, which orientation consisted in measuring the centre and the zero line of the coded disk.

For the purpose of measurement a hole had already been drilled for the vertical spindle of the instrument. The measurement of the centre consisted of observations on the four arms, *l*, *m*, *n* and *p* of the cross which marked the centre *s* on the disk. See figure 5.17.

The points were measured in the following order:

$$l-m-n-p-t-1a-1b-2a-2b- \dots -na-nb-l-m-n-p-t, \text{ etc.}$$

The measurement of $n \approx 60$ lines took about half an hour. By this method of measurement it was possible to correct the observations for the slight regular shift in position of the comparator.

The theoretical value φ_i ($i = 0, \dots, 1023$) of the differences between the directions $s-1a, s-1b, s-2a$, etc. as compared with the orientation $s-t$, is a multiple of $400 \text{ gr}/1024$, because there are 1024 lines over the entire circle. ($\varphi_1 = 1 \times 400/1024, \varphi_2 = 2 \times 400/1024$,

etc.). If the measured angles corresponding to φ_i are called α_{ia} and α_{ib} , the differences v_{ia} and v_{ib} can be calculated.

$$v_{1a} = \varphi_1 - \alpha_{1a}; \quad v_{1b} = \varphi_1 - \alpha_{1b}; \quad v_{2a} = \varphi_2 - \alpha_{2a}; \quad \text{etc.} \quad \dots \quad (5.4)$$

With the aid of this formula we can calculate the mean deviation per line by the formula:

$$v_i = \frac{1}{2}(v_{ia} + v_{ib}) \quad \dots \quad (5.5)$$

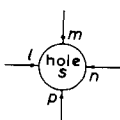


Fig. 5.17

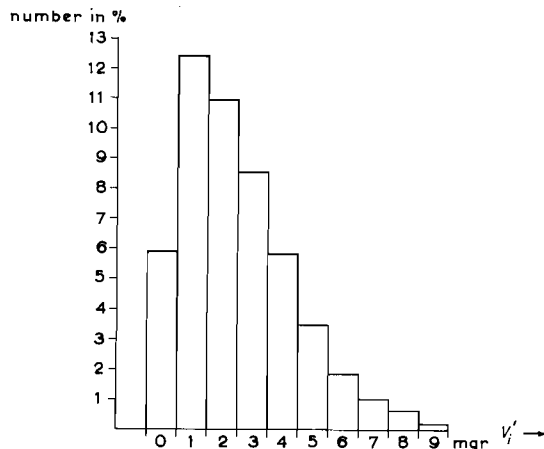
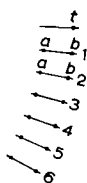


Fig. 5.18

In order to make sure all the lines are properly directed towards the centre, a calculation was also made of:

$$v_i' = v_{ia} - v_{ib} \quad \dots \quad (5.6)$$

Of the 1024 lines measured, the differences v_i' may be expressed in milligrades. A histogram of the v_i' is shown in figure 5.18.

As set forth in section 5.5.2, the track of lines was made by welding eight segments of 128 lines each to each other. In the first measurements carried out on the coded disk it was already found that the deviations of the lines were of the order of a few milligrades. At the positions of the welds, however, there were deviations of 15 milligrades.

In order to obtain a good approximation to such variations of sudden occurrence by means of a Fourier series, a large number of terms have to be included in the series.

In this section a comparison will be made between the standard deviation of the residual differences if a correction is made for:

1. a Fourier series with 2 terms
2. a Fourier series with 16 terms
3. a Fourier series with 24 terms
4. straight horizontal lines per segment
5. straight non-horizontal lines per segment

In the case of a Fourier series for the entire circle the observation equation reads as follows:

$$v_i + \varepsilon_i = a_0 + \sum_{r=1}^{\infty} a_r \cos r\varphi_i + \sum_{r=1}^{\infty} b_r \sin r\varphi_i \quad \dots \dots \dots (5.7)$$

In this formula ε_i is the residual error, whilst $a_0 = \sum_{i=0}^{1023} v_i / 1024$.

To permit calculation of the Fourier series without the terms a_0 , new variates w_i are introduced, for which the following applies:

$$w_i = v_i - \frac{\sum v_i}{1024} \quad \dots \dots \dots (5.8)$$

The deviations v_i depend upon the deviation in line 0, for which we take $v = 0$, whereas for the variates w_i this no longer applies.

The observation equation for the Fourier series used for calculation is:

$$w_i + c_i = \sum_{r=1}^n a_r \cos r\varphi_i + \sum_{r=1}^n b_r \sin r\varphi_i \quad \dots \dots \dots (5.9)$$

In this equation the values for the three series are $n = 1, 8$ or 12 .

As the deviation for the circle divisions are approximated by straight horizontal lines, an average deviation p_j ($j = 1, \dots, 8$) can be determined for each segment in which 128 lines occur. The simple observation equation is in this case:

$$w_k + c_k = p_j \quad (k = 1, \dots, 128) \quad \dots \dots \dots (5.10)$$

The straight non-horizontal lines for each segment for which the deviations at the circle divisions can be corrected, were also calculated by means of the adjustment problem with observation equations. For each of the eight segments the observation equation is as follows:

$$w_k + c_k = a + b(\varphi_k - \varphi_1) \quad (k = 1, \dots, 128) \quad \dots \dots \dots (5.11)$$

In this formula, φ_1 is the circle position of the first line of each segment.

Table 5.1

type of curve for wich correction was made	number of redundant observations	estimated standard deviation of residual differences
fourier series with 2 terms	1022	4.0 mgr
fourier series with 16 terms	1008	3.4
fourier series with 24 terms	1000	3.4
straight hor. lines per segment	1016	5.7
straight but not hor. lines per segment	1008	2.8

Table 5.1 gives a survey of the estimated standard deviations of the residual differences c if correction is made for the different curves.

On account of the large number of redundant observations there is a significant difference between the calculated standard deviations. On this account it was decided to correct the observations in the computer for straight non-horizontal lines per segment. As in consequence of the above the accuracy of the division on the track of lines was brought below 1 centigrade, no further calculations were carried out. Incidentally, it may well be expected that

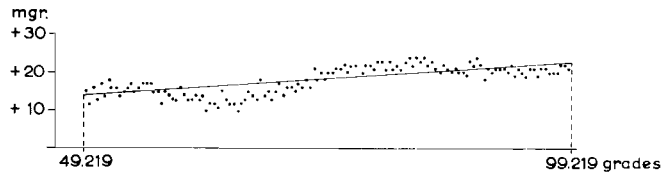


Fig. 5.19

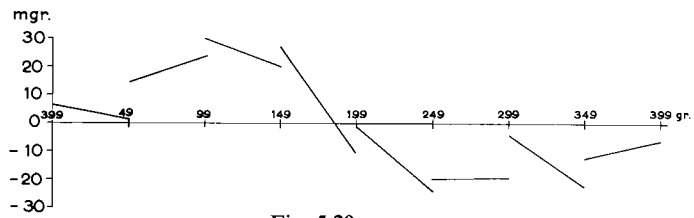


Fig. 5.20

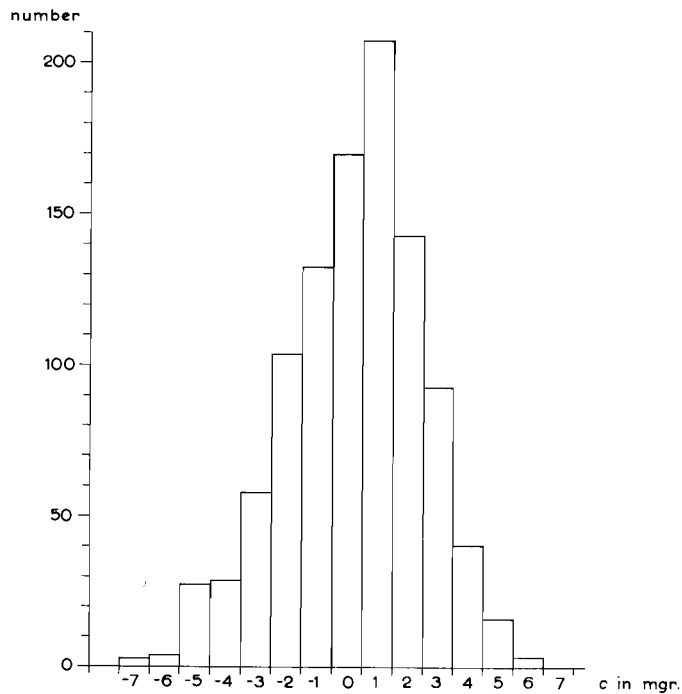


Fig. 5.21

approximations by means of quadratic or higher degree curves would have yielded a considerable improvement per segment. The correction for this, however, would have been a far more laborious process.

An example of the correction line in the second segment is given in figure 5.19.

Figure 5.20 gives a survey of the eight non-horizontal lines for which a correction has to be made. Lastly, figure 5.21 shows the histogram of the residual deviations c as corrected for the lines in figure 5.20.

5.6.2 *Investigation as to halation in the code on the main disk*

As already shown in section 5.3, the Gray code on the main disk for angular measurement need not be marked with the same degree of accuracy as the track of lines. Nevertheless, on the three outer tracks 10, 9 and 8 of this disk the halation was measured at various locations on the disk. Table 5.2 gives the halation in terms of the quantity w/z , where w is the breadth of a white block and z that of a black block.

Table 5.2

number of track	position on disk	w/z	average overradiation per track
10	0 gr	1.021	1.009
	100	0.994	
	200	1.010	
	300	1.011	
9	0	1.022	1.012
	100	0.995	
	200	1.016	
	300	1.017	
8	0	1.002	1.000
	100	0.996	
	200	1.001	
	300 gr	1.002	

On the strength of the measuring results, from which it was found that the halation on the disk shows considerable local variations, extensive measurements were carried out in connection with the manufacture of the disk for distance measurement in order to keep the effect of this halation as slight as possible.

5.6.3 *Investigation as to accuracy of the disk for distance measurement*

On the disk for distance measurement there are $2^{13} = 8192$ black-to-white transitions. For the purpose of determining the accuracy of division about 2000 of these transitions were measured with the Wild stereocomparator.

All the 512 transitions of the inner tracks 1 to 9 were measured. On the remaining tracks 10, 11, 12 and 13 measurements were taken of a number of transitions which in each case were situated in the vicinity of 0, 100, 200 and 300 grades. On each of the tracks 10 and 11 about 250 transitions and on each of the tracks 12 and 13 about 500 transitions were measured. As in the case of the measurements on the track of lines, the values v_i were determined for all the transitions measured (see figure 5.17), but only one point was measured at each transition. For the purpose of orientation the zero transition of track 13 was selected for each track.

The values v_i were plotted in a graph for each track as a function of the corresponding φ_i . A study of the graph, which is too large to be illustrated owing to the roughly 2000 values of v_i , shows that for each track the points plotted follow the same sinusoidal line. This means that the centre of the disk which was used in each case for orientation and which was measured in the same way as the track of lines, did not fall into the correct position but shows a certain eccentricity. Subsequent measurements on the original with a coordinatograph confirm this conclusion.

In order to determine the accuracy of the disk the variates v_i were corrected for this eccentricity because, when the disk is incorporated in the instrument, it will probably be possible to eliminate this eccentricity. The effect of the eccentricity upon the values of v_i will be further dealt with by reference to figure 5.22.

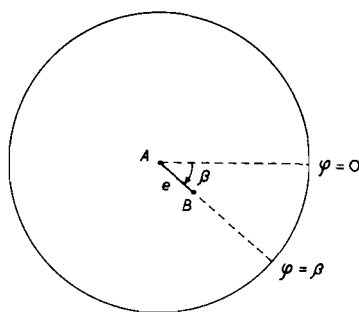


Fig. 5.22

A is the centre of the 13 tracks on the disk, B the point of intersection of the diameters marked on the disk. The unknowns e and β must be solved by means of the observations v_i . In formulating the observation equation the same unknown a_0 occurs which is a measure for the incidental deviation at the zero transition which was used for orientation.

For the purpose of calculating the sinusoidal line with the aid of the adjustment problem with observation equations, the observation equation may now be formulated as follows:

$$v_i + \varepsilon_i = a_0 + e \frac{q}{R} \sin(\varphi_i - \beta) \dots \dots \dots (5.12)$$

In this formula R depends upon the track number. R varies from 68 mm to 27 mm. Since v_i is expressed in milligrades, $q = 63662$. The variates in formula 5.12 are further elucidated in figure 5.23 in the drawing of the sinusoidal line.

The approximate values of a_0 , e and β were determined from the graphs: $a_0 = 0$; $e_0 = +0.025$ mm and $\beta_0 = 200$ gr.

In the calculations in the adjustment problem with observation equations different weights were assigned to the variates v_i on the different tracks. The higher the track number, the more was read from this track and the better the sinusoidal line could be adapted to it. On track 13, for instance, half (4096) of the total number of transitions of the entire disk are to be found.

In the diagonal matrix of the weights the diagonal elements are: 1 for tracks 1 to 9; 2 for track 10, 4 for tracks 11 and 12; 8 for track 13. The calculated variates a_0 , e and β are stated in table 5.3.

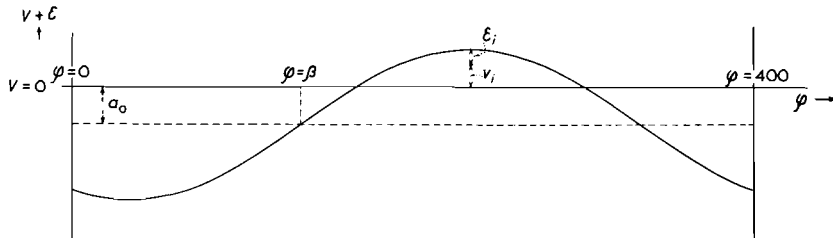


Fig. 5.23

Figure 5.24 gives the histogram in which the residual circle errors ϵ of the coded disk were processed for distance measurement. In this processing a correction of the sinusoidal line was made which gives the best possible correspondence with all the tracks from 1 to 13 inclusive. The variates a_0 , e and β which were used in this processing are listed in table 5.3 and are respectively 0.67 mgr, 0.023 mm and 197 gr.

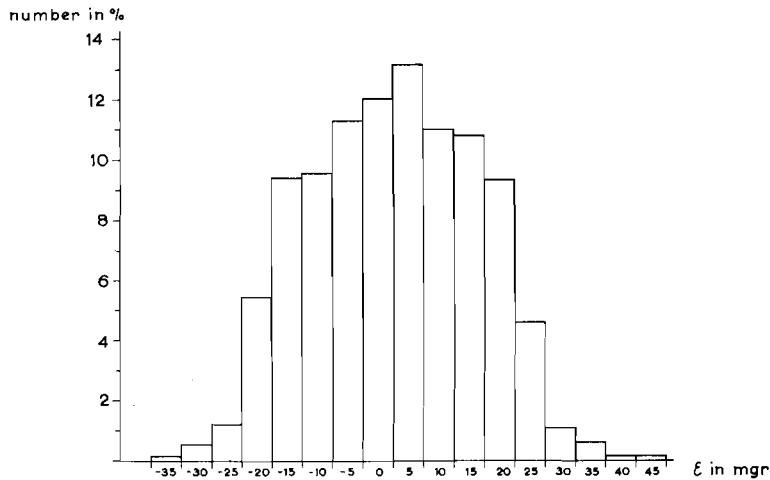


Fig. 5.24

The disk for distance measurement is divided into 8192 units. Such a unit corresponds to approx. 50 milligrades. The standard deviation of the circular errors in the black-to-white

transitions whose histogram is shown in figure 5.24, is 14 milligrades. The accuracy of the disk is therefore sufficient for distance measurement.

Table 5.3

No. of track	a_0	e	β
1 to 7	-6.20 mgr	0.011 mm	204 gr
8	-3.75	0.014	189
9	-8.37	0.013	192
10	-5.50	0.019	201
11	-7.43	0.017	209
12	1.09	0.028	213
13	4.22	0.026	184
1 to 13	0.67 mgr	0.023 mm	197 gr

6 ELECTRONIC SECTION

6.1 Brief survey of the electronic section

As set forth in chapter 5, the distance and bearing measurements are carried out with the aid of three coded disks. The position of each coded disk is measured with a reading mechanism. For this the blocked division on the disk is subject to the rule that the black portions represent a "1", and the transparent portions a "0". Figure 6.1 gives a side view of the reading mechanism for the main disk (10 tracks) and the micrometer disk (6 tracks).

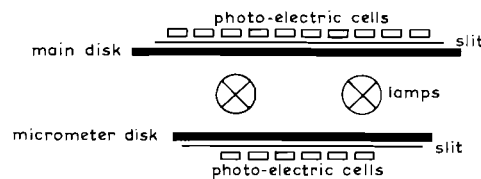


Fig. 6.1

The illumination consists of two frosted glass lamps of 4.5 volts. Situated at a distance of 0.1 mm from the disk, there is a slit 60 μ in breadth in front of each photo-electric cell. These slits were formed in a single line in a thin metal plate by the process of spark erosion. In front of each track of the disk a Philips photo-electric cell BPY 10 is positioned at a distance of 0.1 mm from a slit.

Associated with each photo-electric cell is a photo-electric pre-amplifier which is provided with a discriminating element. Although the correct combination of lamp, slit, photo-electric cell and photo-electric pre-amplifier was only found after a great deal of experimenting, the result is better than was strictly necessary for an optical distance-measuring instrument. The position of one black-to-white transition can be measured by means of the reading mechanism with a standard deviation of less than 1 μ . On a radius of 6.4 cm this corresponds to a precision in the circle reading which is better than 0.001 grade. A reading mechanism of this kind may in future also be used in a theodolite provided with an automatic registration system.

In each measurement 29 bits from the coded disks must be registered in Gray code. Prior to registration, the signals may first be fed into a check unit in which the distance measured, the height difference and the bearing can be read and in which it is verified whether the reading mechanism of the coded disks is still working properly.

It is advisable to use the check unit at set times for checking the measurement of a given bearing and distance. As this instrument will only be used to a small extent it is of the simplest possible construction. The numbers in the Gray code are converted in parallel into the pure-binary code. In section 5.2 the relation is given between a number in the Gray code and in the pure-binary code.

$$\left. \begin{aligned} b_n &= g_n \\ b_j &= g_j \cdot \bar{b}_{j+1} + \bar{g}_j \cdot b_{j+1} \end{aligned} \right\} \dots \dots \dots (6.1)$$

In figure 6.2 it is indicated for the micrometer disk how the conversion in parallel is effected by means of NAND gates. The signals $\bar{g}_6, \bar{g}_5, \bar{g}_4, \bar{g}_3, \bar{g}_2, \bar{g}_1$ are presented at the input

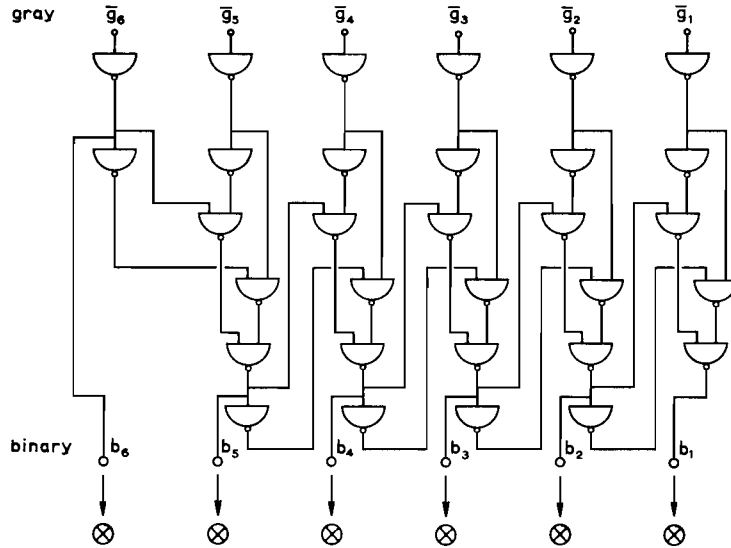


Fig. 6.2

terminals. The front panel of the check unit carries 29 lamps (lamp "on" is "1") which indicate the readings of the three coded disks in pure-binary form. See figure 6.3.

2^{12}	2^{11}	2^{10}	2^9	2^8	2^7	2^6	2^5	2^4	2^3	2^2	2^1	2^0	binary octonary
2^0	2^2	2^1	2^0	2^2	2^1	2^0	2^2	2^1	2^0	2^2	2^1	2^0	
⊗	⊗	⊗	⊗	⊗	⊗	⊗	⊗	⊗	⊗	⊗	⊗	⊗	
			⊗	⊗	⊗	⊗	⊗	⊗	⊗	⊗	⊗	⊗	
							⊗	⊗	⊗	⊗	⊗	⊗	

Fig. 6.3

The numbers are too great to permit easy calculation of the decimal value. For this reason the bits were arranged in groups of three. A binary number of three digits can be converted into the decimal system in a simple manner, and in this way numbers in the octonary system are obtained. These numbers are converted by means of a table into the decimal system.

Example: 1011101000111 (binary) = 13507 (octonary) = 5959 (decimal).

Along with the measuring data, distance, height and bearing, which are obtained by

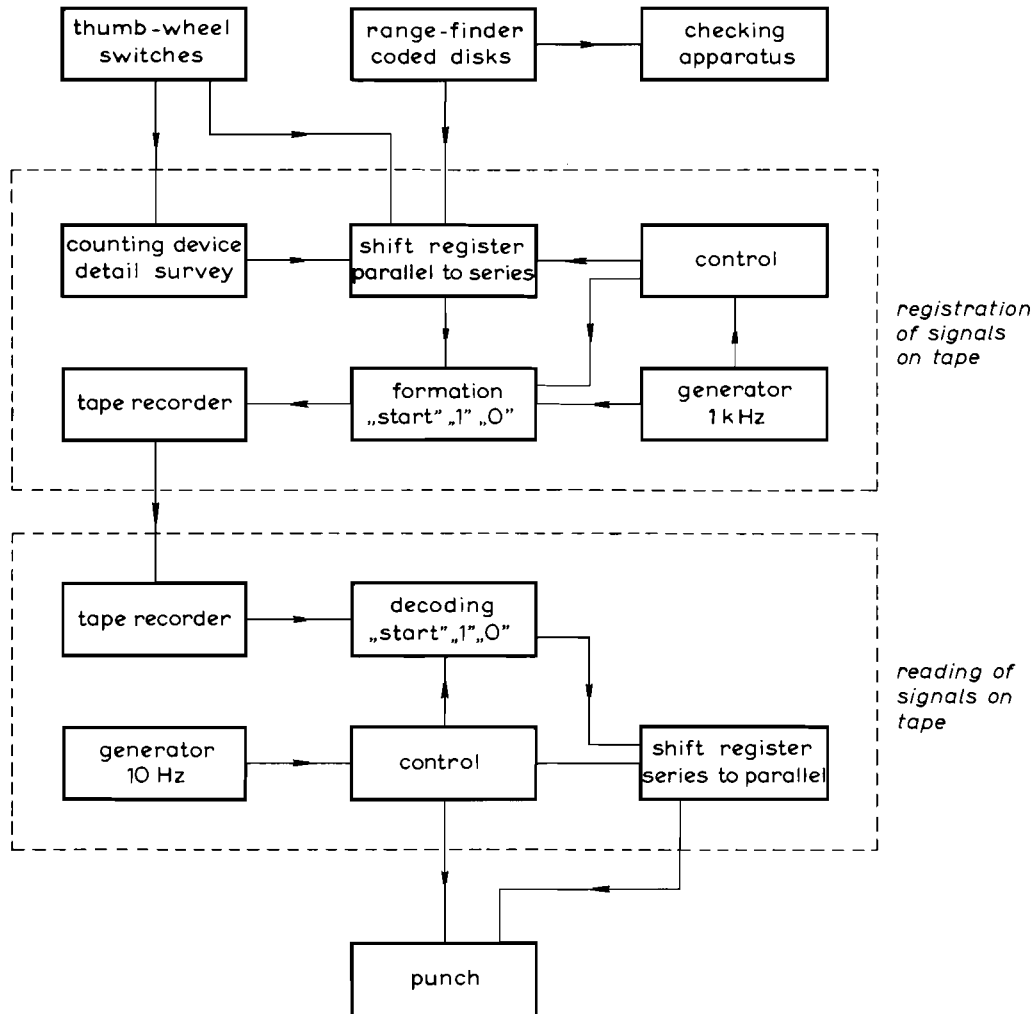
SURVEY OF ELECTRONIC SECTION

Fig. 6.4

means of the coded disks, other data of the station and of the point to be determined must be registered in the memory. These data, such as station and target number, category of measurement, etc. are collected with the aid of nine thumb-wheel switches. (See section 6.3). These data are in the binary-decimal code.

Figure 6.4 gives a diagrammatic survey of the processing of the signals from the thumb-wheel switches and the photo-electric pre-amplifiers. The signals are registered in the field on the magnetic tape of a Philips cassette recorder. This part of the apparatus is dealt with in section 6.4.

The most important part of the recording section is the 80-bits shift register in which the signals presented in parallel are converted into series. These 80 bits are distributed as follows:

29 bits from the coded disks, 36 bits from the thumb-wheel switches, 8 bits from the counting mechanism for detail measurement in which the detail points are automatically numbered, 3 bits for the starting and finishing signs and 4 bits as reserve. The shift pulses for the register are produced by means of a 1 kHz generator in a control unit. By means of the elements in this unit three signals can be formed, depending on the output reading of the shift register.

- The starting signal consists of 35 pulses of 1 kHz. This signal is given before each measurement.
- The 1-signal consists of 24 pulses of 1 kHz.
- The 0-signal consists of 8 pulses of 1 kHz.

See figure 6.5.

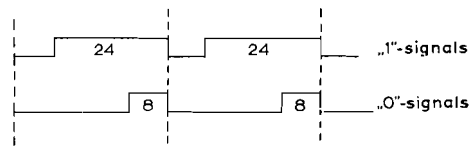


Fig. 6.5

There invariably occurs on the magnetic tape a starting signal followed by 79 zero or one-signals. The “0” and “1”-signals consist of three parts. Both end with 8 pulses, whilst the middle data section of the “1”-signal contains 16 pulses and that of the “0”-signal 0 pulses.

The tapes used in the field cannot be directly processed in the computer. The data registered on them have to be converted into punched cards. This is done in an apparatus that is installed at the office. This conversion unit will be dealt with more fully in section 6.5.

The most important part in this unit is an 80-bits shift register in which the signals which are in series on the tape, are converted into parallel for processing in the punch. Before the signals enter the shift register the starting signals and the “1” and “0”-signals must be decoded. By means of the starting signal a “1” is punched into the first two columns of the punched card. The 80 parallel output terminals of the shift register are connected with the 80 punch coils of the punch. Furthermore, a control unit for the punch is incorporated in the apparatus. This control unit ensures that the ones and the noughts are punched in turn in the cards and that each card is passed through the machine in four stages.

6.2 The logical switching circuits used

In the electronic section of the instrument a number of logical switching circuits are incorporated in the form of integrated circuits.

The internal structure of these circuits will not be further dealt with here. Only the signals that are delivered in the case of certain input combinations will be considered. Use will be made in the instrument of NAND gates and bistable multivibrators of Motorola and Texas Instruments.

The principle of NAND gates has already been described in chapter 4, so that it will not be further dealt with here. In the case of gate circuits, voltage losses may occur in case of high loads at the output terminals. This drawback is surmounted by using power gates at

critical points. The NAND gates belong to the so-called combinatory circuits. These are circuits in which the condition of the output terminals depends directly upon the state of affairs at the input terminals.

In another category of circuits one set of input conditions may cause several sets of output conditions, depending upon the state in which the circuit itself happens to be. An example of such a circuit with a memory function is the bistable multivibrator, usually called a flip-flop. A flip-flop has two output terminals which are usually each other's inverses.

Flip-flops can be divided into two groups according to the way in which the signals are fed into them.

- In the first group the outputs adopt a position depending upon the inputs, when a clock pulse is presented. These flip-flops operate synchronously.
- In the case of asynchronous flip-flops the input signals are fed directly into the memory element without a clock pulse.

In the instrument frequent use is made of the flip-flop MC 845 of Motorola (see figure 6.6).

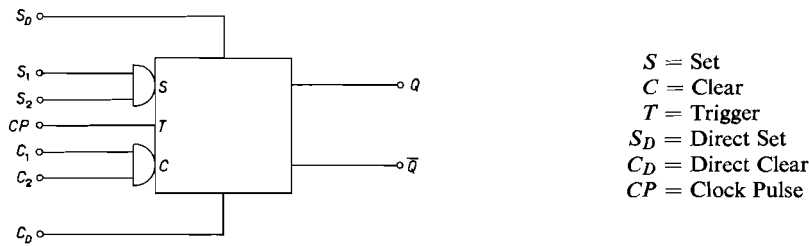


Fig. 6.6

The various applications will be examined on the basis of this figure.

The inputs S_1 and S_2 , C_1 and C_2 are connected with two AND gates, so that: $S_1 \cdot S_2 = S$ and $C_1 \cdot C_2 = C$.

The following flip-flops, among others, can be made with this circuit. Among them, the R-S and the J-K flip-flops operate according to the clock pulse system. In this case Q does not change if T does not change. If T passes from "1" to "0", then Q assumes a position which depends upon the condition of S and C before T passed from "1" to "0". In the truth tables below, n indicates the moment just prior to negative clock transition and $n + 1$ the moment after.

The J-K flip-flop shows the characteristic that S_2 is connected with \bar{Q} and C_2 with Q . As Q

Table 6.1

S_n	C_n	Q_{n+1}
0	0	Q_n
0	1	0
1	0	1
1	1	undetermined

R-S flip-flop

S_{1n}	C_{1n}	Q_{n+1}
0	0	Q_n
0	1	0
1	0	1
1	1	\bar{Q}_n

J-K flip-flop

S_D	C_D	Q	\bar{Q}
0	0	1	1
0	1	1	0
1	0	0	1
1	1	no change	

asynchronous flip-flop

and \bar{Q} cannot simultaneously possess the value 1, the combination $S = 1$ and $C = 1$ will automatically be ruled out.

The flip-flop that operates without a clock pulse system is called an asynchronous flip-flop. This flip-flop is in the rest position when both $S_D = 1$ and $C_D = 1$. Q and \bar{Q} do not change unless in the previous condition $S_D + C_D = 0$. In the rest position Q and \bar{Q} are also inverse.

6.3 The input of basic data by means of thumb-wheel switches

An important point in the automatic registration of measuring data is the registering of the basic data belonging to a given measurement. The basic data may be arranged in three groups.

- data which remain constant for an entire network of traverse points.
- data which occur in traversing.
- data which are of importance for the detail survey.

The data which remain constant for an entire network of traverse points are: a network number; numbers and coordinates of given points; addition and multiplication constants. These data need not be registered during measurement. They are punched into cards and are fed into the computer together with the measurement data for the purpose of automatic processing.

In traversing, the number of the station and the number of the target point must be noted. In automatic processing it is important to know whether the measurement was carried out in a normal traverse side, to a distant bearing, from and to a lateral point (offshoot) or as a check bearing measurement. In numbering the points one may, in the case of branching traverses, assign several numbers to one and the same point. Two or more of these numbers then indicate the same point; such indication will in future be referred to as an equivalence. In regard to this it may be observed that in the reverse measurement of an offshoot no traverse angle need be measured and, in the case of measurement to a distant bearing and in the case of traversing with check bearings, no distance measurement is necessary. In the case of an equivalence there is no distance measurement nor angular measurement. As this is no obstacle to the computing programme, in all these cases the position of all the coded disks will nevertheless be registered as well.

As shown in section 3.1, in the case of a distance measurement several marks on the survey staff may be set in coincidence. Although in principle the automatic registration of these measurements can be effected by means of the position of the central focussing lens, these data too will be fed into the instrument by hand. In the measurement it must be possible to differentiate between distance and height measurement. It is possible that the measurement to a given point may have to be repeated one or more times to increase the precision of measurement and to provide a check. In this case it is desirable that there is a possibility to indicate how many measurements have been made to one and the same point.

In the detail survey the points measured are numbered per station. This numbering is effected automatically in the computer and need not be separately registered. As in traversing it must be indicated also in distance measurements which marks coincide on the survey staff and whether a distance measurement or an angular measurement is being effected. Here again, the possibility must be afforded of measuring several times to the same point.

As a detail point to be measured may be inaccessible, it should be possible to position the target not only at the point itself but also one or two metres before or behind the point.

Lastly, it should be possible to indicate which measurements have to be cancelled in the automatic processing. This may be due for instance to rapid dismantling of the measuring set-up on account of bad weather conditions or because the numbering of the points on the sketch of the partyleader is no longer synchronous with the number of detail points measured, etc.

The registering of these basic data will be effected with the aid of so-called thumb-wheel switches. These switches have only been introduced in recent years, but have since then found widespread acceptance. They can be set at the desired position by a simple movement of the fingers, whereupon the digit or symbol appears in a window. A number of these switches may be connected to each other to form a compact block, thus affording an easy survey of the whole number.

For the basic data registered in course of measurement, use was made of 9 thumb-wheel switches having a BCD (binary coded decimal) output. Each of these switches can occupy 10 different positions. Figure 6.7 shows how the switches are arranged.

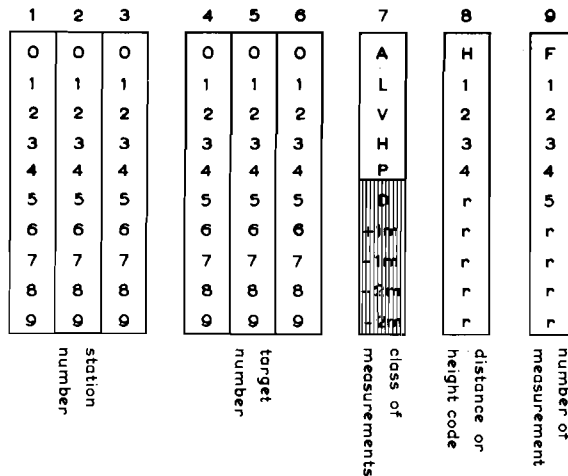


Fig. 6.7

Switches 1, 2 and 3 are used for the number of the station. Switches 4, 5 and 6 are used in traversing for indicating the target number and, in the case of detail survey, the number of the point serving as orientation. The first five positions of switch No. 7 are used for the various possibilities in traversing. The code A indicates the equivalence between the numbers of the switches 1, 2 and 3 and those of 4, 5 and 6. L indicates measurement from and to an offshoot, V denotes a bearing measurement to a distant point and H traversing with check bearings. Position P indicates that the measurement relates to an ordinary traverse side. The last five positions of the switch are used for detail surveying.

The position D is used if the target can be placed on the detail point, whilst the remaining positions indicate how far this target lies before or behind the point.

Positions 4, 3, 2 and 1 on switch 8 indicate what marks coincide on the staff, whilst position H denotes that a height measurement is being carried out.

The positions marked r on switches 8 and 9 are kept in reserve. Positions 1, 2, 3, 4 and 5 on switch 9 indicate the number of repetition measurements. The topmost position is used for an error signal. In the case of erroneous registration of a traverse measurement it may be indicated by means of code F and code P which measurements are given in the calculations. An erroneous detail survey is indicated by F and D, whilst the detail point number is noted at the position of the target number.

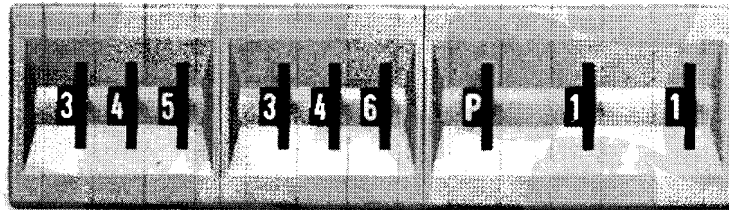


Fig. 6.8

In figure 6.8 the switches are illustrated with station number 345 and target number 346. We have here an ordinary traverse measurement in which the target coincides with itself in the visual field of the telescope. This is the first repetition measurement.

6.4 The registering section and the magnetic-tape memory

A punched card is made of each measurement to a point that is to be determined. Noughts and ones only are punched into this card in the same order in which they are presented in parallel in the electronic section of the field apparatus. The lay-out of the punched card is shown in figure 6.9.

1-2	3-14	15-26	27-34	35-38	39-42	43-46	47-50	51-63	64-73	74-79	80
start	station number	target number	number of detail point	reserve	class of measurements	code number	number of repetition	distance height	bearing	micrometer	finish
	thumb-wheel switches 1-6				thumb-wheel switches 7-9		coded disks				

Fig. 6.9

A diagrammatic survey of the registering section is given in figure 6.10 (see page 84). The most important item in this figure is the 80-bits shift register. The purpose of this register is to convert into series the signals that are presented in parallel with the aid of the thumb-wheel switches and coded disks, to enable their registration on magnetic tape. The 80 parallel input terminals of the shift register correspond to the 80 columns of the punched

card. A "one" (= +5 volts) is constantly presented at the input terminals 1, 2 and 80. The input terminals 3 to 26 inclusive and 39 to 50 inclusive are connected to the thumb-wheel switches. Input terminals 51 to 79 inclusive are connected with the output terminals of the 29 photo-electric pre-amplifiers of the reading mechanism of the coded disks. The input terminals 35 to 38 inclusive are for the time being not connected but remain in reserve.

The eight input terminals 27 to 34 inclusive are intended for the numbering of the detail points. This numbering is effected automatically by means of the counting device for detail points which is shown on the extreme right in the diagram of figure 6.10. This will be further dealt with later on in this section. The output terminals of the counting device are connected with input terminals 27 to 34 inclusive of the shift register.

The registering section is started by pressing the starting button as a result of which a brief downward pulse is produced at the input terminal S_D of ff 87. At the commencement of a series of measurements the batteries are switched into circuit so that ff 86, ff 87 and the two single-shot delays already have a power-supply before the starting button is pressed. The power is supplied by six rechargeable batteries of 1.2 volts each.

The tape recorder is started by means of signal Q_{87} , whilst \bar{Q}_{87} serves for switching on the power-supply of the photo-electric cells and amplifiers, of the lamps for illumination, of the photo-electric cells and of all the further digital circuits.

Signal \bar{Q}_{87} starts the single-shot delay I which has a delay time of 800 msec. There are three reasons for the adoption of this delay time:

- During the reading of the photo-electric cells the lamps for illumination must be burning at full strength.
- During registration of the signals the tape recorder must be running at full speed.
- In converting the measuring data into punched cards sufficient space must be provided between two separate measurements on the tape to enable the punch to complete its punching programme.

By means of the signal \bar{b} the shift register is read in. This signal is obtained by means of the output terminal "a" of single-shot delay I and signal s . The value of "s" depends upon the contents of the entire shift register. As a rule $s = 1$, since „s" is only equal to "0" if the entire shift register is empty, that is if $\bar{Q}_1 = \bar{Q}_2 = \dots = \bar{Q}_{79} = \bar{Q}_{80} = 1$

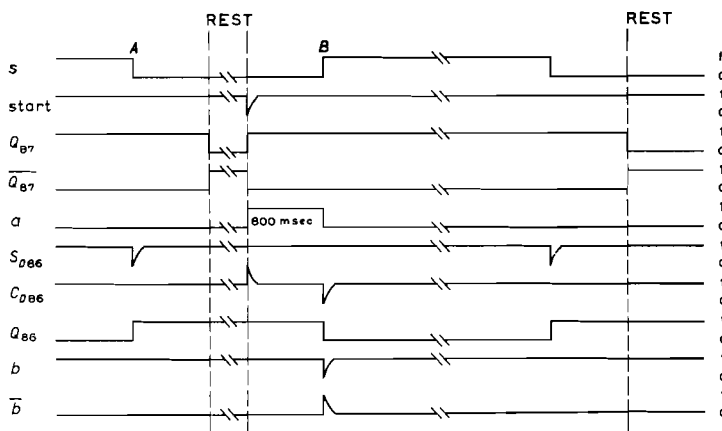


Fig. 6.11

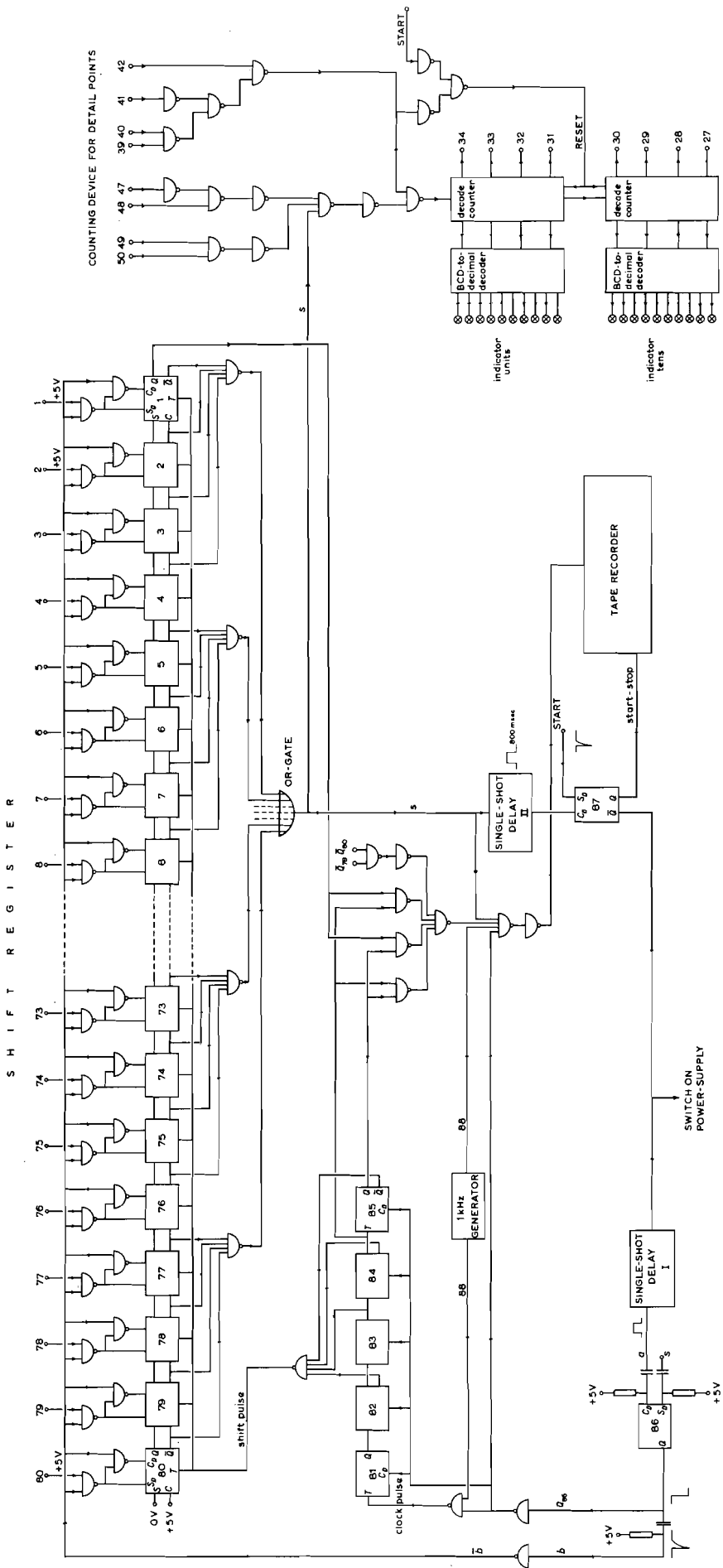


Fig. 6.10

$$s = \overline{Q_1 \cdot Q_2 \cdot \dots \cdot Q_{79} \cdot Q_{80}} \dots \dots \dots (6.2)$$

Figure 6.11 shows the relation existing between the signals which contribute towards producing signal \bar{b} .

The figure shows the state of the signals during a measurement and also the state of affairs at the end of the previous measurement. A is the moment at which the contents of the shift register become nil and B the moment at which the shift register is read in. The output terminal of the single-shot delay II, which corresponds to the input terminal C_D of ff 87, is not shown in the figure. The delay of 800 msec is manifested in the difference in time between the negative transition of “ s ” and of Q_{87} .

The delay time of single-shot delay II serves to stop the recorder only when it is certain that all the signals have been registered on the tape. In figure 6.11 a state of rest is indicated which may be of unlimited duration.

It is shown in figure 6.12 how the n -th signal in the n -th element of the shift register is read in by means of signal \bar{b} , which during a brief period assumes the value “1”.

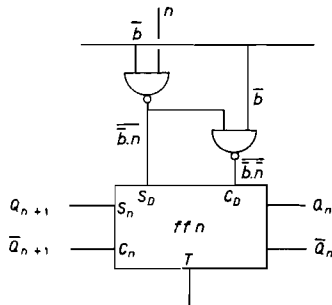


Fig. 6.12

In table 6.2 the relation is indicated which exists between the signals \bar{b} and n and the output signals of flip-flop n .

Table 6.2

\bar{b}	n	S_D	C_D	Q_n	\bar{Q}_n
0	0	1	1	no change	no change
0	1	1	1	no change	no change
1	0	1	0	0	1
1	1	0	1	1	0

It can be seen from this truth table that the value of Q_n is equal to that of the signal n if $\bar{b} = 1$. If $\bar{b} = 0$, then “ n ” cannot exert any influence whatever upon the position of the flip-flop. As the value 1 is constantly presented at the input terminals 1, 2 and 80, it follows that $Q_1 = Q_2 = Q_{80} = 1$, if $\bar{b} = 1$. Hence “ s ” will be equal to 1. When all the signals in the particular elements of the shift register have been read in, the shifting process can commence. This is effected by means of shift pulses, which act as clock pulses for all the

elements of the shift register. A shift pulse is a “1”-signal with short “0” periods. At the moment when the shift pulse passes from “1” to “0”, the output terminals Q_n and \bar{Q}_n of flip-flop n acquire the values of the output terminals Q_{n+1} and \bar{Q}_{n+1} respectively of flip-flop $n + 1$. This means that the contents of flip-flop $n + 1$ is in fact taken over by the next flip-flop n .

For the formation of the shift pulse use is made of 5 JK flip-flops Nos. 81, 82, 83, 84 and 85. See figure 6.10. As in this operation the output signal of one flip-flop invariably acts as a clock pulse for the next flip-flop, the frequencies of these signals are divided by two.

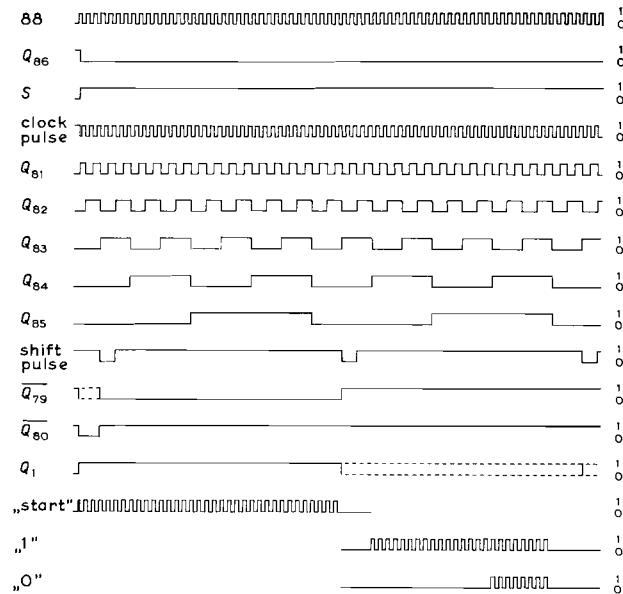


Fig. 6.13

Compare the signals Q_{81} , Q_{82} , Q_{83} , Q_{84} and Q_{85} in figure 6.13. The clock pulse of ff 81 is formed by the signal $\bar{Q}_{86} \cdot 88$, signal 88 being the output of a generator with a frequency of 1 kHz. The shift pulse is governed by the equation:

$$\text{shift pulse} = \overline{\bar{Q}_{82} \cdot Q_{83} \cdot \bar{Q}_{84} \cdot \bar{Q}_{85}} \dots \dots \dots (6.3)$$

In figure 6.13 the three types of signals “start”, “1” and “0” to be registered on the magnetic tape are also indicated. These three signals are obtained by means of \bar{Q}_{79} , \bar{Q}_{80} , Q_{85} , Q_{84} , Q_1 , S, 88 and \bar{Q}_{86} .

By means of a number of NAND gates (see figure 6.11), the signal that is registered on the tape must satisfy the condition:

$$\text{“start”, “1” or “0”} = \overline{Q_1 \cdot Q_{84} \cdot Q_1 \cdot Q_{85} \cdot \bar{Q}_{84} \cdot Q_{85} \cdot \bar{Q}_{79} \cdot \bar{Q}_{80} \cdot \bar{Q}_{86} \cdot S \cdot 88} \quad (6.4)$$

In each measurement the starting signal is first registered on the tape, this being followed by 79 noughts or ones. The starting signal consists of 35 pulses of 1 kHz; the “1”-signal consists of 24 pulses and the “0”-signal of 8 pulses.

The magnetic tape memory selected was the Philips cassette recorder on account of its light weight, compactness and easy interchange of tapes.

Two students of Electrical Engineering at the Delft University of Technology made an investigation, within the framework of a study assignment, as to whether, in the registration of signals on the magnetic tape of the cassette recorder, interfering phenomena might occur as a result of which the data might wholly or partly fail to be included in such registration. The investigation was carried out in the "Switching Technique and Information Processing Laboratory".

The measurements were effected with sinusoidal signals in the frequencies of 2, 3, 4, 5 and 6 kHz. The number of bits measured amounted to a total of 16,500,000, whilst the number of pulses per bit varied from 2 to 5. During this investigation it was found that only one bit was erroneous, which in the opinion of the researchers was purely incidental and not due to the quality of the tape or recorder. As in the final embodiment of the electronic equipment the "0" signal consists of 8 pulses of 1 kHz, see figure 6.13, it may be concluded that the registration of the observations on a magnetic tape of a cassette recorder is very reliable.

The total number of measurements (of 80 bits each) that can be registered on one tape is at most 1200.

In the registering section a further provision has been made for automatically numbering the detail points per station. This facilitates the observer's task as it is now practically unnecessary to use the thumb-wheel switches in detail measurement.

A measurement is only provided with a new detail point number if thumb-wheel switch 7 occupies the position D, +1, -1, +2 or -2 and if at the same time thumb-wheel switch 9 indicates that this is the first measurement to the point. The detail numbers are punched in columns 27 to 34 inclusive, which possess the values of respectively 10×2^3 , 10×2^2 , 10×2^1 , 10×2^0 , 2^3 , 2^2 , 2^1 , 2^0 .

Table 6.3

T_7	T_9	2^3	2^2	2^1	2^0	
A	F	1	1	1	1	
L	1	1	1	1	0	
V	2	1	1	0	1	
H	3	1	1	0	0	
P	4	1	0	1	1	
D	5	1	0	1	0	
+1		1	0	0	1	
-1		1	0	0	0	
+2		0	1	1	1	
-2		0	1	1	0	
card		42	41	40	39	T_7
column		50	49	48	47	T_9

It is necessary for the detail numbers to be made visible in decimal form, as during measurement these numbers are also marked by the party leader on the sketch of the field situation. The detail numbers are made visible by means of two indicators fixed to the panel in which the thumb-wheel switches are also fitted. Situated in each of the indicators are 10 lamps with the aid of which the digits 0 to 9 inclusive can be projected on a frosted glass window. In this manner 99 detail points per station can be numbered. As the numbering is effected by means of thumb-wheel switches 7 and 9, the values of the various positions are indicated in table 6.3. Below the truth table is indicated in which card column the noughts and ones are punched, regardless of the position of the switches. Columns 39 to 42 inclusive are intended for thumb-wheel switch 7, by means of which the category of measurement is indicated. Columns 47 to 50 inclusive are intended for thumb-wheel switch 9.

As can be seen from the truth table, the equation

$$(39 \cdot 40 + 41) \cdot 42 = 0 \dots \dots \dots (6.5)$$

is applicable to positions D, +1, -1, +2 and -2 of thumb-wheel switch 7. When switch 9 is at position 1 the applicable equation is:

$$\overline{50} + \overline{49} + \overline{48} + 47 = 0 \dots \dots \dots (6.6)$$

Use is made of these two equations in the counting device for detail points, which is shown on the extreme right in figure 6.10.

Counting proceeds only when the counting pulse passes from "1" to "0". It is found from figure 6.10 that:

$$\text{counting pulse} = \overline{s \cdot (\overline{47 + 48 + 49 + 50}) \cdot (39 \cdot 40 + 41) \cdot 42} \dots \dots \dots (6.7)$$

If $s = 0$, then the counting pulse = 1, so that no counting is done. At the moment when the shift register is read in, $s = 1$ (see formula 6.2). At that moment counting may proceed if at the same time the conditions of formulae (6.5) and (6.6) are fulfilled.

The eight BCD-coded output signals of the counting device are fed to the input entrances 27 to 34 inclusive of the shift register.

The delay time of these signals from the moment of the counting pulse until the moment of feeding them to the shift register, is of the order of 10^{-7} seconds. Since the read-in pulse of the shift register \bar{b} (see figure 6.11) has at least a duration of $5 \cdot 10^{-4}$ sec, the eight output signals of the counting device will certainly be received in good time in the shift register. The resetting of the counting device may only be effected during traversing, i.e. when the thumb-wheel switch 7 is in position A, L, V, H or P.

The starting pulse is included in the reset in order to prevent the counting mechanism from being straight away reset in the event of the thumb-wheel switch 7 being accidentally set at the wrong position.

The equation for the reset pulse is:

$$\text{reset} = \overline{(39 \cdot 40 + 41) \cdot 42} + \text{start} \dots \dots \dots (6.8)$$

6.5 The reading section and the punch

Figure 6.14 (see page 90) gives a diagrammatic survey of the section in which the signals on the magnetic tape are converted for processing in the punch.

The signals are fed from the tape recorder into a selective amplifier. This is an RC-circuit in which the 1 kHz square-wave signals with voltage levels 0 and 300 mV are separated from the accompanying noise and changed into sinusoidal signals of 2 V. These signals make their way into a Schmitt trigger in order to regain their square-wave form, so that two decidedly logic levels are obtained. At the same time the trigger also detects whether the signals registered are at the correct levels of 0 and 2 V. The output signals of the Schmitt trigger serve as clock pulse for the J-K flip-flops 81 to 86 inclusive, with the aid of which the signals “start”, “1” and “0” are distinguished.

Furthermore, these signals are fed into an integrator which is connected with a second Schmitt trigger. The object of the integrator is to eliminate single spikes which may occur on the tape. The switching level of the Schmitt trigger is not reached until after about three pulses. As long as this level has not been reached, the output of the trigger is nil.

Of the six J-K flip-flops, $C_D = 0$ and $S_D = 1$, so that $Q_{81} = Q_{82} = \dots = Q_{86} = 0$ (continuous reset).

If C_D assumes the value 1 (S_D remains 1), the position of each flip-flop alters only in case of variations in input of the synchronous part.

On the top line in figure 6.15 (see page 91) pulses are shown which have voltage levels of 0 and 5 V, originating from the output of the first Schmitt trigger. Below them the six signals Q_{81} to Q_{86} are indicated. As set forth in section 6.4, a “0” signal consists of 8 pulses, a “1” signal of 24 pulses and a “start” signal of 35 pulses. A certain safety margin will have to be observed in detection. As can be seen from figure 6.15, a number of pulses between 6 and 11 is considered as a “0”-signal, a number between 20 and 31 corresponds to a “1”-signal, whilst a “start” signal lies between 32 and 39 pulses. It is shown in figure 6.14 how this is achieved by means of NAND gates.

$$\left. \begin{aligned} \overline{Q_{82} \cdot Q_{83} \cdot \overline{Q_{84}} \cdot \overline{Q_{83}} \cdot Q_{84}} + \overline{Q_{85} \cdot \overline{Q_{86}}} &= \text{“0” signal} \\ \overline{\overline{Q_{83}} \cdot \overline{Q_{84}} \cdot Q_{85} \cdot \overline{Q_{86}}} &= \text{“1” signal} \\ \overline{Q_{84} \cdot \overline{Q_{85}} \cdot Q_{86}} &= \text{“start” signal} \end{aligned} \right\} \dots \dots \dots (6.9)$$

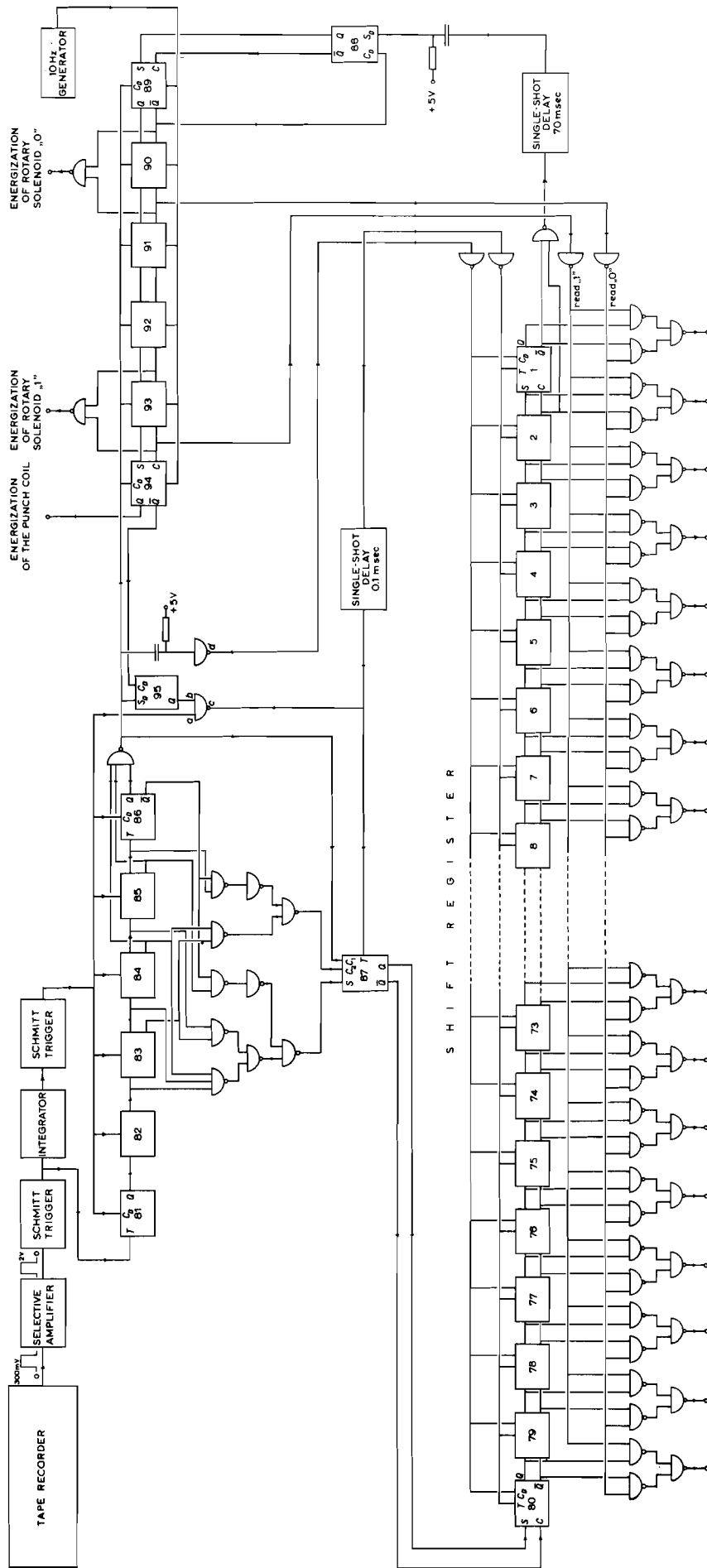
These three signals are fed into the RS flip-flop 87. The “0” signal is connected with S , the “1” signal with C_1 and the “start” signal with C_2 .

The following three cases are distinguished:

- “0” signal: $C_1 = 1, C_2 = 1, S = 0 : Q_{87} = 0$
- “1” signal: $C_1 = 0, C_2 = 1, S = 1 : Q_{87} = 1$
- “start” signal: $C_1 = 1, C_2 = 0, S = 1 : Q_{87} = 1$

Flip-flop 87 provides the input of the 80-bits shift register. In the latter the signals presented in series are converted in parallel for processing in the punch.

The “start” signal is fed into ff 87 in order to punch a “1” in the first column of each



ENERGIZATION OF THE 80 RELAY COILS OF THE PUNCH

Fig. 6.14

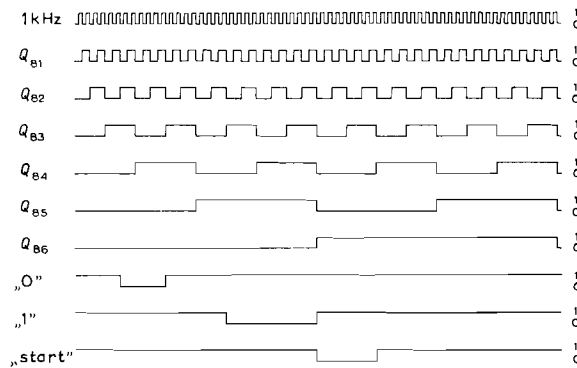


Fig. 6.15

card. The clock pulse of ff 87 is determined by the output of ff 95 of the second Schmitt trigger.

During the punching of a card the punch coil is energized. This means that $\bar{Q}_{94} = 0$. This signal resets ff 95 ($C_D = 0$). The "start" signal is connected with S_D of ff 95. S_D and C_D cannot simultaneously become equal to nil. Here again three cases can be distinguished:

- $C_D = 0, S_D = 1 : Q_{95} = 0$
- $C_D = 1, S_D = 1 : \text{no change}$
- $C_D = 1, S_D = 0 : Q_{95} = 1$

The last situation occurs during the "start" signal.

Supposing the output signal of the second Schmitt trigger is a and $Q_{95} = b$, then the applicable equation for the output of the corresponding NAND gate is $c = \overline{a \cdot b}$.

Flip-flop 87 is set and the single-shot delay with a delay time of 0.1 msec is started when "c" passes from "1" to "0". Before the "start" signal is presented $a = 0$ and $b = 0$, so that $c = 1$. During this signal $a = 1$ and $b = 1$, so that $c = 0$. If S_D of ff 95 again becomes equal to "1" at the end of the "start" signal, then $S_D = C_D = 1$, so that "b" does not change. Only if "a" changes does the value of signal "c" also change.

There is a variation of "a" at the end of each "0" and "1" signal. In this way the pulse "c" is obtained (every 32 msec, which is the duration of a "0" or "1" signal). Pulse "c" is the clock pulse for ff 87 and the shift pulse for the 80-bits shift register. The single-shot delay with a delay time of 0.1 msec is incorporated in order to ensure that the shift pulse is not effected until the signal concerned has reached the input of the shift register.

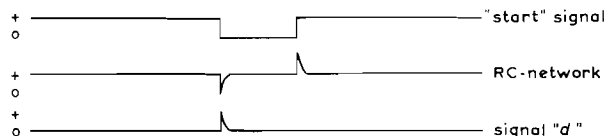


Fig. 6.16

At the commencement of each "start" signal the 80-bits shift register is reset. This is done by means of the signal "d". Figure 6.16 indicates how "start" and "d" are related.

Signals “c” (delayed) and “d” are finally reversed by means of power gates.

The diagrammatic survey in figure 6.14 shows along with the 80-bits shift register a shift register consisting of flip-flops 89 to 94 inclusive. This latter register controls the punch. The clock pulse of the second register is provided by a 10 Hz generator. The relation between all the signals which are discussed in connection with the shift register are reproduced in figure 6.17. The input S_D of ff 88 is connected via an RC network with the output of the single-shot delay with a delay time of 70 msec. This is started by means of the last two elements of the 80-bits shift register, using the signal $\overline{Q_2} \cdot \overline{Q_1}$.

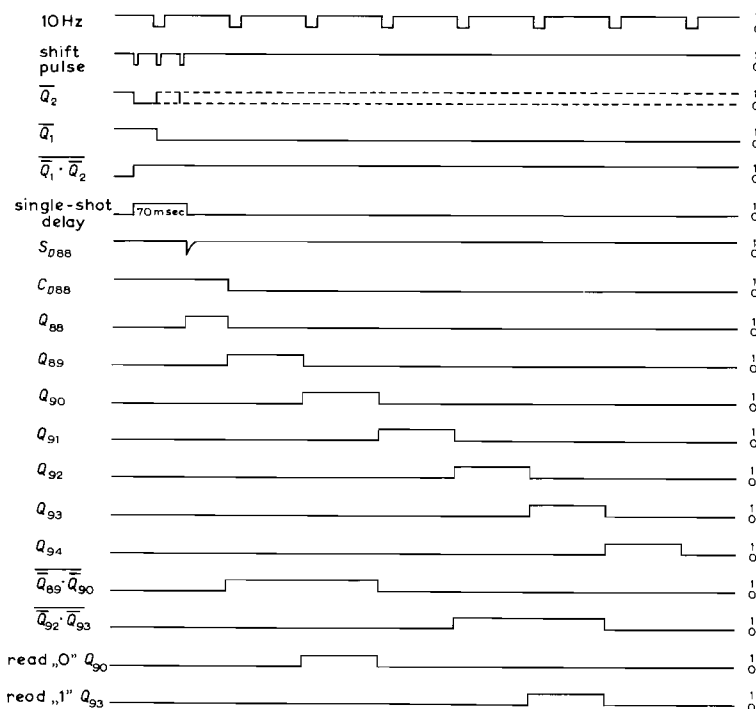


Fig. 6.17

As a rule $\overline{Q_2} = \overline{Q_1} = 1$, so that $\overline{\overline{Q_2} \cdot \overline{Q_1}} = 0$.

After 79 shift pulses, $\overline{Q_2} = 0$ because the “start” signal (that is converted into a “1”) is the first pulse that is fed into the shift register.

Consequently $\overline{Q_2} \cdot \overline{Q_1}$ becomes equal to 1 and the single-shot delay starts. During the waiting time of the monovibrator the last shift pulse occurs and $\overline{Q_1}$ becomes equal to 0. The waiting time has been made such that in any case a shift pulse will occur. Should one of the 80 bits get lost as a result of a possible interference, then $\overline{Q_1}$ remains equal to 1, but in that case Q_{88} nevertheless becomes equal to 1.

The flip-flops 88 and 89 are connected with each other in the following manner: $Q_{88} = S_{89}$, $\overline{Q_{88}} = C_{89}$, $\overline{Q_{89}} = C_{D88}$. By means of $\overline{Q_{89}}$, ff 88 is reset. Figure 6.17 shows the relation between the signals Q_{89} to Q_{94} inclusive. By means of $\overline{Q_{94}}$ the start ff 95 is reset, so that the “start” signal is necessary before a new series of shift pulses can be presented. The register, consisting of the flip-flops 89 to 94 inclusive, controls a punch type

Bull PC 80. By means of this punch only noughts and ones are punched into the cards. In this way the cards are indeed used uneconomically, but this punch provides a temporary solution and serves only to show that the measuring data which have been automatically registered on the tape of the cassette recorder can be processed in the computer without undue difficulty. It is probable that the punch will in future be replaced by a digital tape recorder whose tapes can be fed directly into the computer.

The punch is provided with a punch block having 960 cutters arranged in 12 rows. The punching of the noughts and ones is effected by means of two rotary solenoids. These latter, when energized, release in turn the rows which are to punch the noughts and the ones. As can be seen from the diagrammatic survey in figure 6.14, the energization of the rotary solenoid "0" is effected by means of the signal $\overline{Q_{89}} \cdot \overline{Q_{90}}$ and that of rotary solenoid "1" by means of signal $\overline{Q_{92}} \cdot \overline{Q_{93}}$.

The relation with the further signals is represented in figure 6.17. Which ones or noughts will be punched, depends upon the voltage levels of the 80 parallel output terminals of the shift register.

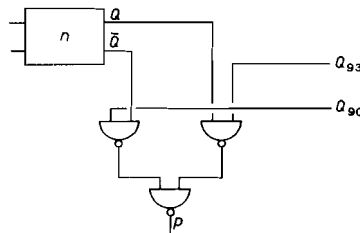


Fig. 6.18

During the energization of rotary solenoid "0", when $\overline{Q_{89}} \cdot \overline{Q_{90}} = 1$, those of the 80 output terminals first become equal to "1" whose corresponding bit in the shift register was a "0". This is effected with the aid of signal $\overline{Q_{90}}$, which is inverted via a power gate. Afterwards, during the energization of rotary solenoid "1", when $\overline{Q_{92}} \cdot \overline{Q_{93}} = 1$, those output terminals become equal to "1" whose corresponding bit in the shift register was a "1". This is effected by means of signal $\overline{Q_{93}}$, which is likewise inverted via a power gate.

The example taken is the *n*-th element of the 80-bits shift register. See figure 6.18. The equation for the output *p* is:

$$p = \overline{\overline{Q_n} \cdot Q_{90}} \cdot \overline{\overline{Q_n} \cdot Q_{93}} \cdot \dots \dots \dots (6.10)$$

The cutters, which are to provide punchings in the two rows, are set in the punching position at the correct time by the outputs *p*, via transistors and relay coils.

Lastly, the punch coil of the punch is energized by Q_{94} . This energization initiates four operations of the punch.

- A punched card from the hopper is fed into the punch.
- A card already fed to the punch is punched.
- The card that was punched in the previous cycle is passed on.
- The passed-on card of the previous cycle is placed in the stacker.

7 COMPUTING PROGRAMMES

In this chapter the four computing programmes which were dealt with in section 1.1 will be further discussed by reference to greatly simplified flow diagrams. These computing programmes will be used for processing the measuring data.

7.1 The pre-programme of tacheometry

An altogether new pre-programme has been drawn up for processing the measuring data obtained with the new optical distance-measuring instrument. It was not possible to make use of the existing pre-programmes because, among other reasons:

- the input cards have been greatly altered. The measuring data are arranged differently on the cards and are, moreover, punched in the binary system. See section 6.4.
- special corrections have to be made in the angular measurement. See section 5.6.
- the reading of a distance measurement or a height measurement must be diminished by the observed value of the corresponding angle. See section 5.4.

The numbering of the traverse points will not be further dealt with here. For this purpose the system described in the article by WITT [42] will be applied.

The lay-out of the punched cards which are to serve as input for the pre-programme of tacheometry has been dealt with in section 6.4. By means of this pre-programme the data are converted in such a manner that they can be processed directly in the main programme of tacheometry. Figure 7.1 shows a greatly simplified flow diagram of the pre-programme. The basic data obtained with the aid of the nine thumb-wheel switches are indicated in the diagram by codes T1 to T9 inclusive.

For each card read it is first investigated whether an error signal was detected with the aid of the 9th thumb-wheel switch. See figure 7.1. If so, the data on this card will not be further processed.

If no error has been recorded, then the basic data of the thumb-wheel switches will be converted from the binary system into the system used for punched cards. After this it is first investigated whether the card is an equivalence card. This means that several point numbers are assigned to a traverse point at which two or more traverses branch off. Should this be the case, the equivalence card can at once be punched, as the data for angle, distance or height are superfluous.

For all other categories of cards the circle reading is composed. For this purpose the data of the main disk and the micrometer disk are taken together. For the observations with the prototype, the data of the main disk have to be corrected for the deviations indicated in figure 5.20. Moreover, for each circle reading the orientation which is indicated per station in a detail card with detail point number 0 must be deducted.

For measuring a bearing to a given distant point and for traversing with check bearings,

PRELIMINARY PROGRAMME TACHEOMETRY

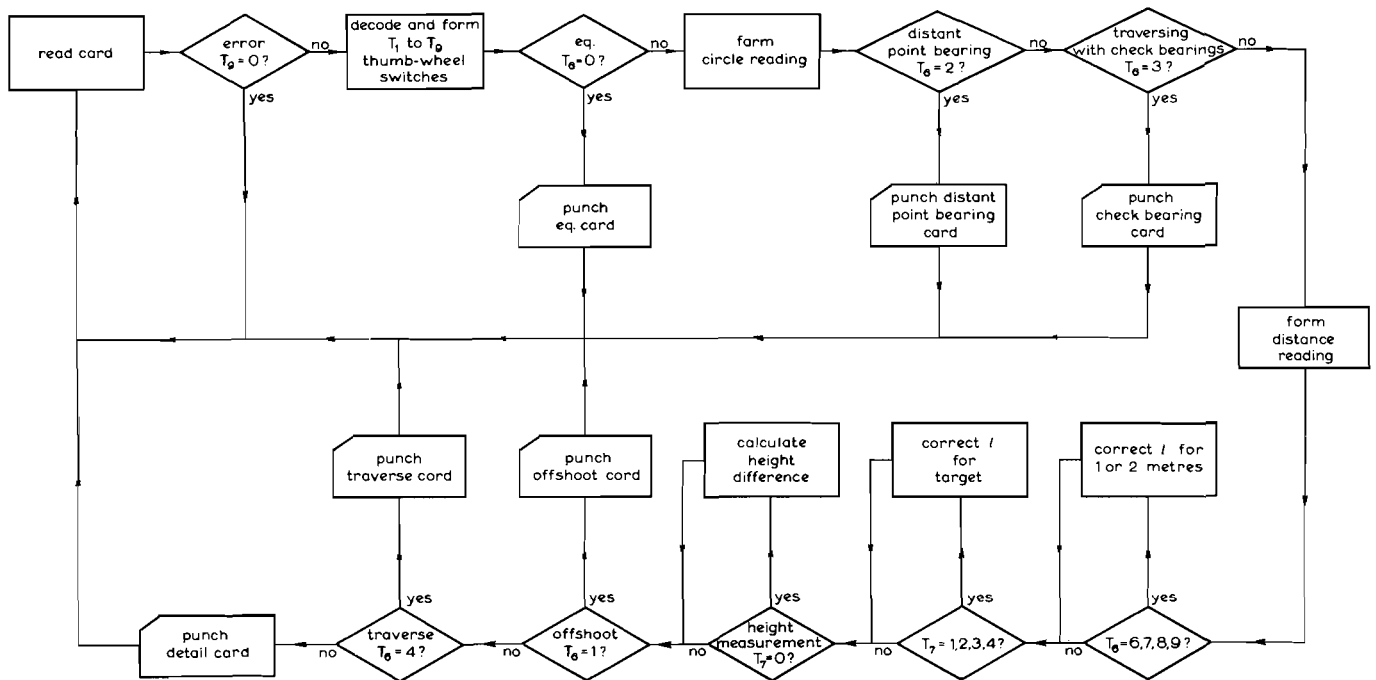


Fig. 7.1

the distance and height measurements are superfluous data, so that the cards may already at this stage be punched for this category of measurements.

Next, the distance reading is composed. For this one has to consider that the data of the coded disk for distance measurement must be diminished by those of the coded disk for angular measurement. This principle is dealt with in section 5.4.

It is necessary to indicate for an entire network of traverse points whether the reduced distance or the unreduced distance, has been measured. After this the distance may be corrected on possible detail cards if the measuring mark has been erected 1 or 2 metres before or behind the detail point to be measured. Moreover, each distance is corrected for the measuring mark that has been used and that is indicated by code 1, 2, 3 or 4 of the 7th thumb-wheel switch.

Next, the height difference is calculated. As the same coded disk was used for this purpose as for distance measurement, the same rules of computation hold good. Moreover, the height difference has to be corrected for the deviations indicated in figure 3.30.

A special measurement is the so-called offshoot, for which a card provided with a code has to be punched.

If none of the special cases, equivalence, distant bearing, traversing with check bearings or offshoots, have occurred, then finally either a traverse card or a detail card will be punched, after which a new card can be read.

7.2 The main programme of tacheometry

Of the main programme of tacheometry there exist one SPS version and two FORTRAN versions. First a FORTRAN programme was written for the IBM-1620. As the programme was highly complicated, the maximum number of traverse points in a network which could be calculated in one single operation with an IBM 1620, was 200. On this account an SPS version of this programme was made in which, for the same computer, this number of traverse points was increased to 999. These programmes were drawn up by IBM on behalf of the Delft Geodetic Institute.

On adoption of the computer IBM 360 a new FORTRAN version was prepared at the computation centre of the Netherlands Land Development and Reclamation Society. Thanks to the high capacity of this computer the programme was supplemented and improved in some of its essentials.

In the main programme, coordinates of the points measured are calculated and, if

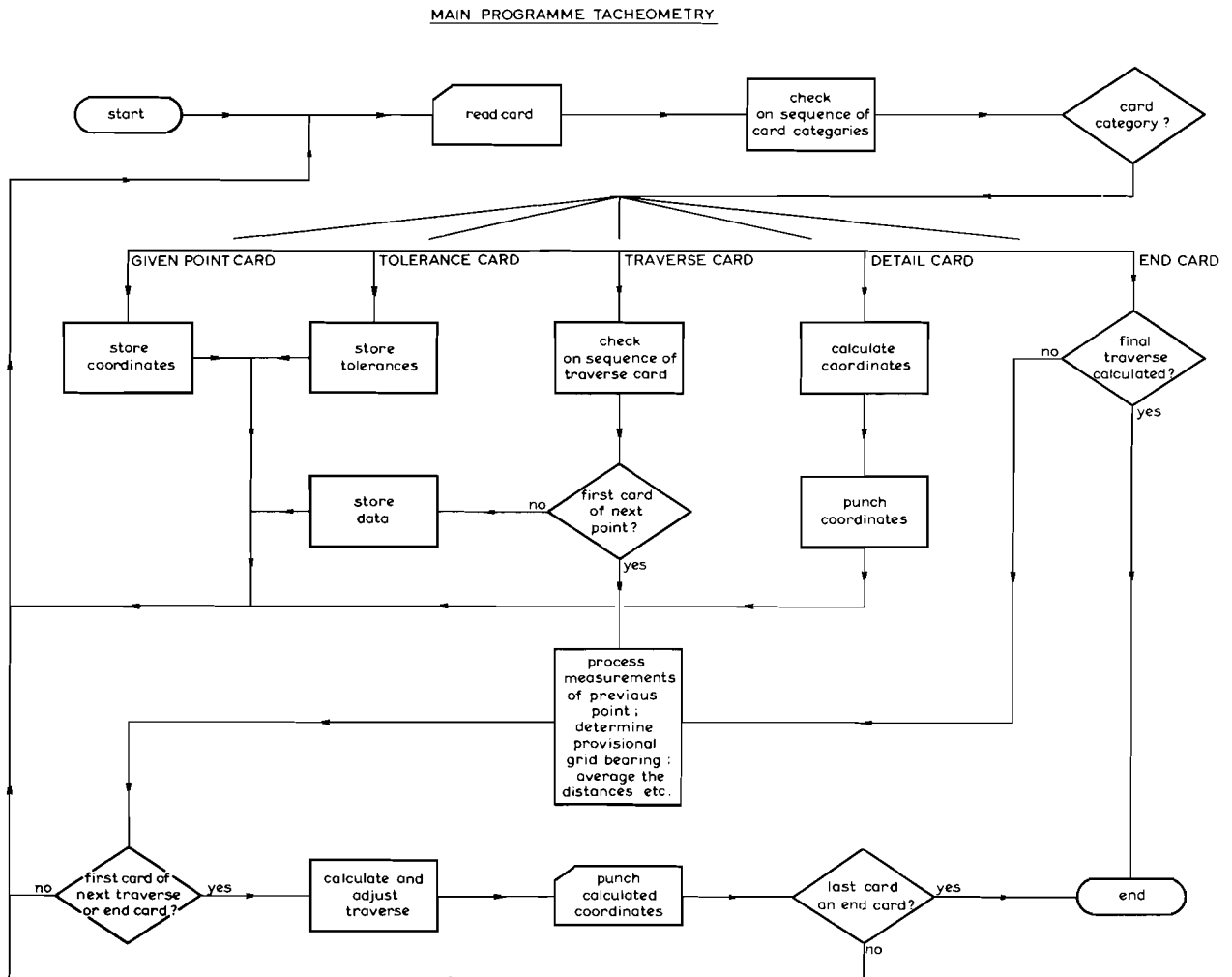


Fig. 7.2

desired, also the map coordinates for use in special electronic drawing instruments. The input of the computing programme may consist of 9 different categories of cards, of which categories 5 to 8 inclusive contain the measuring data originating from the pre-programme.

The card categories 1 to 4 inclusive contain the basic data for calculating a traverse network. Of these basic data, card category 1 bears the given points of which only the Z coordinate is known, card category 2 the given points with only the X and Y coordinates, whilst card category 3 bears the given points with X , Y and Z coordinates. Punched into card category 4 are the tolerances ruling for distance and height measurement to and from a traverse side and for angular measurements face left and face right.

Card category 5 is used for traverse measurement. Special measurements that may occur in this connection are measurements from and to offshoots, traversing with check bearings and measurements to distant point bearings. Card category 6 is used in the special case in which only the height of the traverse points has to be measured. Card category 7 contains the data for the equivalences. Should one or more traverses branch off at a particular traverse point, such point is assigned several numbers which are indicated by equivalences. Card category 8 comprises all detail measurements. Lastly, card category 9 is an end card which indicates that no further measurements occur in the traverse network.

In the computing programme a check is made for a great variety of errors relating mainly to the numbering of the traverse points. The errors detected by the computer are printed on a list on which the misclosures in the traverses are also stated.

Along with this list, the output of the programme consists of the point numbers together with their coordinates which, if desired, are recorded in punched cards, magnetic tape and/or on a list.

In the flow diagram of figure 7.2 a comprehensive survey is given of the trend of the calculations in the main programme of tacheometry.

7.3 The programmes for checking the detail survey, for the area calculation and mapping

After the calculations in the main programme of tacheometry, we have at our disposal the X and Y coordinates of the points measured. These data may be stored for instance in a magnetic tape. We also possess sketches in which the situation is outlined, in which each measured point is indicated by its number and in which the tape measures are indicated. As a rule a further three operations have to be performed with these data.

1 *A check on the detail survey*

The detail survey of a tacheometric recording can be checked in various ways. An example of this is the bearing measurement to detail points that were measured at other stations. A further check is the taking of tape measures. This second method is to be preferred in the case of a high degree of automation, because in this way difficult coding of the points to be measured is avoided. Moreover, it is often necessary to delimit in advance for a survey, so that then there is ample opportunity for taking tape measures. The check on the tape measures must be effected in the computer, because as a rule large numbers are involved. In this check the tape measurements are compared with the distances calculated from coordinates.

In preparing the map there is a possibility for a final visual check on the survey.

2 Area calculation

After the measurements have been effected one will usually wish to determine the area of one or more plots by making use of the measuring results. As the coordinates of the angular points of the plots are available, the area calculation can obviously be effected by means of these coordinates. As a check one may calculate blocks of adjacent plots. These computations, too, must be carried out in the computer.

3 Drawing

The drawing of the situation measured can be carried out with the aid of an electronic drawing instrument. The major part of the input for this instrument viz. the point numbers and the coordinates of the points measured, have already been collected on a magnetic tape.

During the survey the traverse points are numbered progressively in the order of calculation. The numbering of the detail points is effected per traverse point. For the purpose of carrying out the above-mentioned three operations the points are no longer in the correct order. This is evident from the example I used in a paper read at a meeting of the Netherlands Geodetic Federation. See [32].

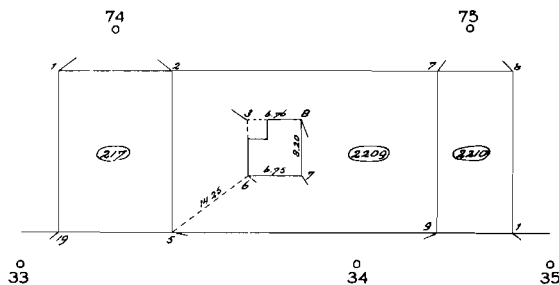


Fig. 7.3

Five traverse points together with some of the corresponding detail points are shown in figure 7.3. If it is desired to determine the area of plot number 2209, the calculation begins for instance with 34-05 and runs according to 74-02; 75-07; 34-09 back to 34-05. The order of the point numbers has thus become purely arbitrary. The same applies to the calculation of the tape measures and the drawing of the plot.

An advantageous circumstance is that the order of the point numbers to be stated per plot for the tape measures, for the area calculation and for drawing, is approximately the same. This order has to be communicated to the computer, after which the corresponding coordinates have to be called from the memory.

For the above-mentioned three operations a data sheet has been designed for the I.B.M. 1232. As already set forth in the introduction, data sheets are used in order to avoid the time-consuming operation of punching and the errors involved.

In the aforementioned article [32] the classification and the method of filling up these sheets were discussed at length.

The calculations are carried out in two parts, the reason being that a number of coordinates of detail points must be corrected because the check by means of the tape measures has shown them to contain errors. Only after this, one can proceed to the area calculation

and the preparation of the input of the electronic drawing machine. The two computing programmes, which will be discussed on the basis of greatly simplified flow diagrams, were written in FORTRAN IV and can be calculated on the IBM 360.

CHECK PROGRAMME OF TAPE MEASUREMENTS

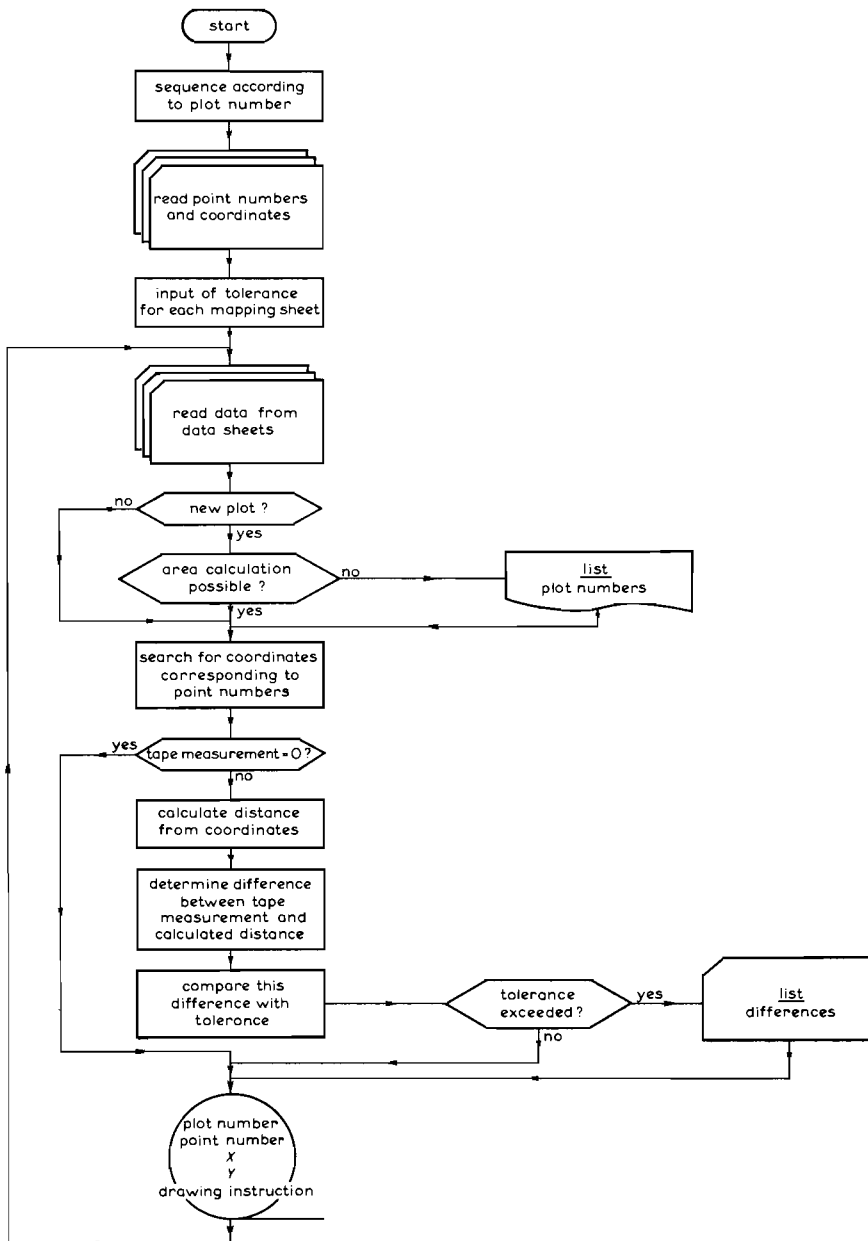


Fig. 7.4

7.3.1 *The "check programme of tape measurements"*

Prior to calculation the particulars from the data sheets in the IBM 1232 are converted into punched cards which are afterwards sorted. See figure 7.4. These punched cards, into which the data of the sketches have been punched, serve as input for the 'check' programme of tape measurements". Besides this, two further particulars are required for the calculation:

- the magnetic tape with the point numbers and coordinates.
- for each magnetic tape, a punched card stating the tolerance allowed for the difference between the measured and the calculated tape measures.

At the reading-in of each punched card this programme checks whether a fresh plot is being started with. If this is the case, then it is investigated whether the area calculation of the previous plot will be possible. If not, then the number of this plot is printed on a list.

Next, it is investigated at each point number whether a tape measure has been punched. This tape measure refers to the distance between the point number concerned and the previous point number. If a tape measure has been punched, it is calculated from coordinates and the difference is determined between the calculated and the measured tape measure. This difference is compared with the tolerance stated. Should this tolerance be exceeded, then the difference between the calculated and the measured tape measure is punched into a card. When all these operations have been performed, the plot number, the point number, the coordinates and the drawing instructions belonging to this point are recorded on a magnetic tape.

The output of the "check programme of tape measurements" thus comprises the following parts:

- a list of plot numbers whose area calculation for some reason or other cannot be effected.
- a list of differences between the calculated and the measured tape measures.
- a magnetic tape with plot numbers, point numbers, coordinates and drawing instructions.

On the basis of this output the erroneous coordinates can be corrected. These new coordinates are punched into cards.

7.3.2 *The programme "area calculation and drawing"*

The input of the programme "area calculation and drawing" consists of two parts (see figure 7.5):

- the output tape of the "check programme of tape measurements".
- the punched cards bearing the corrected coordinates.

The areas of the plots have to be calculated by means of these data, and a magnetic tape, a punched tape or a set of punched cards with drawing instructions have to be made. At each point number is investigated whether corrected coordinates of that number are available. If so, work is continued with these new coordinates. If a given point number proves to be the first point of a new plot, then the area of the previous plot is calculated and printed on a list.

The next operation in the programme is the preparation of the input of the electronic drawing machine. The data for this, consisting of point numbers, X and Y coordinates, drawing instructions and plot numbers, can be recorded on a magnetic tape, in a punched tape or in punched cards.

PROGRAMME OF AREA CALCULATION AND DRAWING

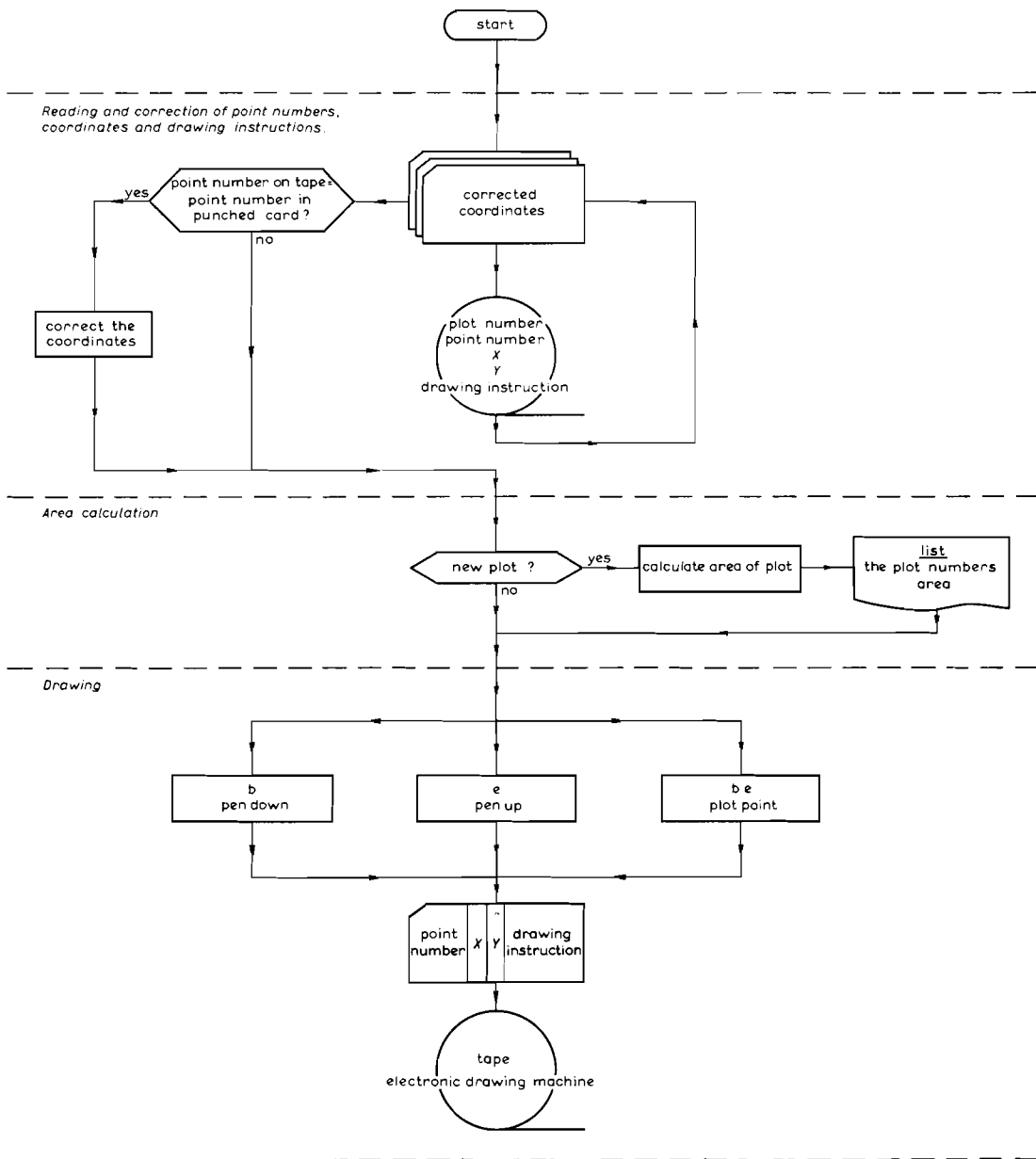


Fig. 7.5

8 CONCLUSIONS

No extensive measurements were carried out with the prototype of the instrument for the determination of accuracy in the distance and angular measurements under all weather conditions. The reason for this was that in all probability other materials will be used in the final embodiment and that a number of improvements will be made. Still, it may well be expected on the basis of the measurements carried out so far that the accuracy in distance measurement will be approximately 3 cm per 100 m. This corresponds to the accuracy of another range-finder, the BRT-006 of Zeiss-Jena, in which the standard deviation in distance measurement is about 6 cm per 100 m, but in which the multiplication constant is 200. The accuracy of bearing measurement is slightly better than 1 centigrade.

An important aspect of the instrument is that it can be used very well when computed data have to be set out in the field. For this purpose, however, the measuring results must be directly visible in decimal form. A reading unit is now being made to this end on which the distance, the bearing and the height difference can be read on a number of indicators.

The most important improvements which may be made on the instrument at this stage are as follows:

- Simplification of the reading apparatus of the coded disks. This can be achieved by making use of very narrow photo-electric cells (breadth approx. 70 μ), evaporated on to a glass plate. The elements of the photo-electric pre-amplifiers may similarly be evaporated on to this glass plate. The advantages of this are that two heavy reading units are eliminated and that the diameters of the coded disks may be smaller, or that while maintaining the same diameter a larger number of tracks may be formed per disk.
- The use of image-transmitting fibre glass optics, with the aid of which the main disk and the micrometer disk can be set at the correct position for angular reading at any position around the instrument.
- The adoption of a different bearing for the vertical spindle, as a result of which a substantial saving in weight can be effected.
- The adoption of new integrated circuits, with four flip-flops embodied in one block. This represents a considerable reduction in the bulk of the electronic section.

In spite of the fact that no large-scale measurements have so far been carried out with the prototype, a fair estimate of its serviceability can nevertheless be obtained. In 1965 a comparative test was made between the conventional survey-line method (using ranging poles, tape and optical square) and the bearing and distance method in a re-survey of a 450 hectare plot in the Frisian village of Suawoude. The measuring data of the latter method were automatically processed according to the computing programmes described in chapter 7.

In a report presented by Prof. Ir. G. F. WITT and the Engineer-Examiner to the Head of the Land Registry all the operations were enumerated in detail, stating the number of hours worked. A comprehensive survey of the results of this investigation is given in [32]. A total survey of the costs for the re-survey of 450 hectare is given in table 8.1.

Table 8.1

	conventional method	bearing and distance method
field operations	Dfl 13,115.—	Dfl 15,038.—
processing of measuring data	Dfl 8,000.—	Dfl 7,838.—
total	Dfl 21,115.—	Dfl 22,876.—

A survey of the number of man-hours worked is given in table 8.2.

Table 8.2

	conventional method	bearing and distance method
field operations	1642 hours	1717 hours
processing of measuring data	1000 hours	548 hours
total	2642 hours	2265 hours

Some reserve should be exercised however in drawing conclusion from these figures.

In the test only two measuring teams were compared with each other. Of these two teams, the survey-line team was highly experienced and the tacheometer team was not. The latter, a large team, was led by a fourth-year student of surveying. The bearing and distance method is the more efficient one in the case that there are many small plots. In Suawoude, however, there were large plots and few buildings.

The advantage of the bearing and distance method is clearly shown in the automatic processing of the measuring data. With this method only about half the number of hours is employed as compared with the processing of the data with the conventional method.

For the cost calculation the rates of the Land Registry were taken as basis, whilst in the automatic processing the rates applied were those of I.B.M. and the Netherlands Land Development and Reclamation Society.

If an optical distance-measuring instrument is used, which is provided with an automatic registration system, no booker need be included in the measuring team, so that in this way the task of the partyleader is simplified.

In the figures for the field operations according to the bearing and distance method in tables 8.1 and 8.2 a working time of 197 hours was reckoned at a rate of pay of Dfl 12.— per hour for the work of the booker. With the new instrument the bearing and distance method for 450 hectare would have been Dfl 2364.— cheaper and would have saved 197 man-hours. As 270 traverse points and 4455 detail points were measured in this region, the use of an optical distance-measuring equipment provided with an automatic registration system would have yielded here a saving of about Dfl 0.50 per point measured.

The foregoing considerations will serve to show that this thesis may contribute its quota towards further developments in automation, which is making increasingly rapid progress in geodetic surveying as in other fields of technique.

REFERENCES

- [1] BERGMANS, H. J., Een analoog-digitaal omzetter werkend met een optische codeschijf. Department of Applied Physics, Delft University of Technology, 1958.
- [2] BOGAERTS, M. J. M., Een methode voor het registreren van meetgegevens. Tijdschrift voor Kadaster en Landmeetkunde, 1965, p. 257.
- [3] BUJVELD, W. J., en TOORN, A. J. v. D., Methoden voor het met de hand invullen van automatisch te lezen getallen. De Ingenieur, 1964, p. A 693.
- [4] CASTELIJS, H., Tellers en kodes. Symposium: Digitale technieken in de automatisering. Antwerp, 1966.
- [5] DAVIDSON, A., Handboek van de fijnmechanische techniek, part 1. Philips, Eindhoven, 1966.
- [6] EVERSDIJK, C. H., Het overbrengen en verwerken van digitale informatie. Symposium: Digitale technieken bij meten en regelen. Utrecht, 1958.
- [7] FLÜGGE, J., Leitfaden der geometrischen Optik und des Optikrechnens, Vandenhoeck und Ruprecht, Göttingen, 1956.
- [8] GENT, H. L. VAN, Some remarks on automatization in Surveying and Mapping. Invited paper XIth F.I.G. Congress. Rome, 1965.
- [9] GERLACH, O. H., C. VAN HOLTEN, A. SNIJDERS, Digitale registratie van meetgegevens, afkomstig van een vliegtuig. De Ingenieur, 1963, p. E 157.
- [10] GOVAERTS, R., Inleiding tot de logische functies en de Boolean algebra. Symposium: Digitale technieken in de automatisering. Antwerp, 1966.
- [11] GRAY, H. J., P. V. LEVONIAN and M. RUBINOFF, An Analog to Digital converter for serial computing machines. Proceedings of the I.R.E., 1953.
- [12] GUILD, J., Diffraction gratings as measuring scales. Oxford University Press, London, 1960.
- [13] HEEL, A. C. S. VAN, Inleiding in de Optica. Martinus Nijhoff, 's-Gravenhage, 1964.
- [14] HEREMANS, J., In- en output apparatuur. Symposium: Digitale technieken in de automatisering. Antwerp, 1966.
- [15] HUTH, P., Das Filmumsetzgerät Zuse Z 84. Vermessungstechnische Rundschau, 1963, p. 209.
- [16] I.B.M., General Information Manual. Introduction to I.B.M. Data Processing Systems, 1960.
- [17] KNOESTER, C. J., Analooq-Digitaal Omzeters. Symposium: Digitale technieken bij meten en regelen. Utrecht, 1958.
- [18] LATOUR, P. L., Elektronische rekenmachines. Het Spectrum, Utrecht, 1964.
- [19] LANG, E., Die Automatisierung der technischen Arbeiten der Flurbereinigung in Hessen unter besonderer Berücksichtigung des selbstregistrierenden Code-Theodoliten. Tijdschrift voor Kadaster en Landmeetkunde, 1963, p. 190.
- [20] LEITZ, H., Eine elektronische Winkelmess-einrichtung mit automatischer Registrierung der Messwerte. Thesis, Technische Hochschule Hannover, 1966.
- [21] MEINES, VAN, Logische schakelingen met relais. Symposium: Digitale technieken in de automatisering. Antwerp, 1966.
- [22] MUNCK, J. C. DE, Elektronica. Geodetic Institute of the Delft University of Technology, 1963.
- [23] OBERMAN, R. M. M., Binaire- en spiegelbinaire codering. Symposium: Digitale technieken bij meten en regelen. Utrecht, 1958.
- [24] PERKIN-ELMER Corporation, A new shaft encoder principle.
- [25] PHILIPS, Circuit blocks for ferrite core memory drive. Eindhoven, 1965.
- [26] POEL, W. L. v. D., Afgeven en bewaren van digitale informatie. Symposium: Digitale technieken bij meten en regelen. Utrecht, 1958.
- [27] SCHERMERHORN, W. en H. J. VAN STEENIS, Leerboek der Landmeetkunde. Argus, Amsterdam, 1965.
- [28] SMITH, T., On systems of plane reflecting surfaces. Opt. Soc. 1928-29 p. 68.
- [29] SNIJDERS, A., Schakeltechniek I. Department of Electrical Engineering, Delft University of Technology, 1968.
- [30] SPAULDING, C. P., How to use shaft encoders. Datex Corporation, 1965.

- [31] SUSSKIND, A., Notes on Analog-Digital Conversion Techniques. Chapman and Hall, London, 1957.
- [32] UNIVERSITY OF TECHNOLOGY, Delft, Een vergelijkend onderzoek tussen de meetlijnenmethode en de voerstraalmethode in vlak land (proef Dinther-Suawoude). 1966.
- [33] VANDEVELDE, W., Logische bouwstenen met magneetkernen. Symposium: Digitale technieken in de automatisering. Antwerp, 1966.
- [34] VEELTURF, L. P. J., Micro-elektronica. Tijdschrift van het Nederlands Elektronica- en Radiogenootschap, 1966, p. 195, 211, 233.
- [35] VEER, J. D. DE, Some optical devices for testing alignment and flatness. Thesis, Delft University of Technology, 1966.
- [36] VERHAGEN, C. J. D. M., Metingen deel I en II. Department of Applied Physics, Delft University of Technology, 1965.
- [37] VERSTRAELEN, R., Getransistoriseerde logische bouwstenen. Symposium: Digitale technieken in de automatisering. Antwerp, 1966.
- [38] VOSSEN, G. H. VAN DER, Ervaringen met het mechanisch verwerken van opnamegegevens bij de Koninklijke Nederlandse Heidemaatschappij. Geodesia, 1965, p. 141.
- [39] VROMAN, J., Methodes voor synthese van logische problemen. Technological Institute, Antwerp, 1965.
- [40] WELY, G. A. VAN, Kwalitatieve en economische beoordeling van afstandmeters. Tijdschrift voor Kadaster en Landmeetkunde, 1967, p. 185.
- [41] WESTERWEEL, J. PH., Analoog-digitaal omvorming. Symposium: Digitale technieken in de automatisering. Antwerp, 1966.
- [42] WITT, G. F., Automatisering bij de verwerking van waarnemingen, verkregen met optische afstandmeters. Tijdschrift voor Kadaster en Landmeetkunde, 1965, p. 3.
- [43] WITTKÉ, H., Automatische Winkel-Registrierung mit dem Fotoelektrischen Winkel-schrittgeber von Leitz. Vermessungstechnische Rundschau, 1963, p. 253.
- [44] ZETSCHÉ, H., Die Bildung der Sekundenschritte beim Digitaltheodolit Digigon. Zeitschrift für Vermessungswesen, 1968, p. 22.
- [45] ZWICKERT, E., Der Fennel-Code-Theodolit F.L.T., Vermessungstechnische Rundschau, 1964, p. 397.

SUMMARY

In the present thesis a description is given of a new self-reducing range-finder by means of which both reduced and unreduced distances, height differences, and bearings can be measured. The thesis also deals with the way in which measuring data and the further data regarding the points to be measured are automatically registered on a magnetic tape. This is followed by the description of an electronic apparatus by means of which the data are transferred from the magnetic tape to punched cards, needed for carrying out the calculations with the measuring data in a computer.

Lastly, four computing programmes are described which are necessary for effecting a check upon the measurements, calculating the areas of the plots measured, and producing the input for the electronic drawing machine to permit of automatically mapping the survey.

The optical section of the range-finder is dealt with in chapter 3. The measurement of the reduced and the unreduced distance and of the height difference to a point to be determined is effected by measuring the distance between two pentaprisms which can be shifted along a base rail. In order to obtain the parallactic triangle, two triangular prisms are mounted between the shiftable pentaprisms. For the purpose of measuring at an angle of inclination of α grades the pentaprisms are rotated through α grades with respect to the triangular prisms in determining the reduced distance, whereas in determining the height difference this rotation is $(100-\alpha)$ grades.

For the determination of the deviations in the measuring result a computing programme was prepared. By this means it was determined at the same time what effect is exerted upon the measuring result by disadjustments and deformations of the optical elements. The result of the calculations was, inter alia, that the slight systematic deviation occurring in the distance measurement is compensated by giving one of the refractive faces of the two non-shiftable pentaprisms, which likewise belong to the optical system, a rotation of 50 dmgr. The measured height difference is corrected in the computer for the systematic deviation that may occur by means of a third degree equation in terms of the angle of inclination α .

The distance between the shiftable pentaprisms is measured with the aid of an optical coded disk. This disk has thirteen tracks in the Gray code, which are read with the aid of two sources of light and thirteen photo-electric cells.

Angular measurement is effected by means of two coded disks, the first of which is divided into 1024 sectors. By means of the second disk, which acts as a micrometer, $\frac{1}{64}$ part of one sector can be measured. An additional advantage of this construction is that the pattern of the code need not be marked so very accurately upon the disks. It is thus possible to use cheap coded disks.

In chapter 5 attention is paid to measurement by means of the coded disks, the production of these disks and the method of determining their accuracy.

Besides the measuring data that are collected by means of the coded disks a number of further data are registered: point numbers, code numbers for various categories of measurements, possible error signals, etc. These additional data are set on 9 thumb-wheel switches.

In chapter 6 there follows a description of the electronic section of the equipment. All the measuring data are registered in an easily accessible memory, viz. a small cassette tape recorder.

Some electronic equipment has been added, since the signals of the coded disks and the thumb-wheel switches are presented in parallel and have to be converted into series for the purpose of registration.

The numbering of the detail points per station runs automatically and is rendered visible on the instrument by means of indicators. The observations collected in the memory by means of the field equipment have to be made suitable for automatic processing in the computer. The equipment required for this purpose consists of a reading unit for the magnetic tape and a card-punching machine.

In this way the incoming data from a large number of field instruments can be successively processed by means of automatic registration.

SAMENVATTING

In dit proefschrift wordt een beschrijving gegeven van een nieuwe zelfreducerende basisafstandmeter, waarmee wel en niet gereduceerde lengten, hoogteverschillen en richtingen kunnen worden gemeten. Tevens wordt behandeld hoe deze meetgegevens en de andere gegevens betreffende de op te meten punten automatisch worden geregistreerd op een magneetband.

Hierna volgt de beschrijving van een elektronisch apparaat waarmee de gegevens van de magneetband worden overgebracht in ponskaarten, die nodig zijn om de berekeningen met de meetgegevens in een elektronische rekenmachine te kunnen uitvoeren.

Tenslotte worden vier rekenprogramma's beschreven, die noodzakelijk zijn voor het uitvoeren van controle op de metingen, het berekenen van de grootten van de opgemeten percelen en de vervaardiging van de invoer voor de elektronische tekenmachine teneinde de opgemeten situatie automatisch in kaart te kunnen brengen.

In hoofdstuk drie wordt het optische gedeelte van de basisafstandmeter behandeld. De meting van de wel en de niet gereduceerde lengte en van het hoogteverschil naar een te bepalen punt geschiedt door de afstand te meten tussen twee pentagoonprisma's die verschuifbaar zijn langs een basisrail. Voor de vorming van de parallactische driehoek zijn twee driezijdige prisma's opgesteld tussen de verschuifbare pentagoonprisma's. Bij meting onder een hellingshoek van α graden zijn bij de bepaling van de gereduceerde lengte de pentagoonprisma's ten opzichte van de driezijdige prisma's gedraaid over α graden, terwijl bij de bepaling van het hoogteverschil deze draaiing $(100-\alpha)$ graden bedraagt.

Voor de bepaling van de afwijkingen in het meetresultaat is een rekenprogramma vervaardigd. Met behulp hiervan is tevens bepaald hoe groot het effect op het meetresultaat is als gevolg van ontregelingen en vervormingen van de optische elementen. Het resultaat van de berekeningen is onder meer geweest dat de geringe systematische afwijking die optreedt in de lengtemeting wordt gecompenseerd door een van de brekende vlakken van de twee niet-verschuifbare pentagoonprisma's, die eveneens tot het optische stelsel behoren, een verdraaiing van 50 dmgr te geven. Het gemeten hoogteverschil wordt in de computer gecorrigeerd voor de optredende systematische afwijking met behulp van een derdegraadsvergelijking in de hellingshoek α .

De afstand tussen de verschuifbare pentagoonprisma's wordt gemeten met behulp van een optische codeschijf. Deze is voorzien van 13 sporen in de gray-code, die worden afgelezen met behulp van twee lichtbronnen en dertien foto-elektrische cellen.

De hoekmeting geschiedt met twee codeschijven, waarvan de eerste is verdeeld in 1024 sectoren. Met de tweede schijf die als micrometer fungeert kan $1/64$ gedeelte van één sector worden gemeten. Een bijkomend voordeel van deze constructie is, dat het patroon van de code niet erg nauwkeurig op de schijven hoeft te worden aangebracht. Het is daardoor mogelijk goedkope codeschijven te gebruiken.

In hoofdstuk vijf wordt aandacht besteed aan de meting met behulp van de codeschijven, de vervaardiging en de bepaling van de nauwkeurigheid van deze schijven. Behalve de

meetgegevens die worden verzameld met de codeschijven moet nog een aantal gegevens worden geregistreerd: puntnummers, codenummers voor verschillende soorten metingen, eventuele foutmeldingen, enz. Deze bijkomende gegevens worden ingesteld op negen dekadeschakelaars.

In hoofdstuk zes volgt een beschrijving van het elektronisch gedeelte van de apparatuur. Alle meetgegevens worden geregistreerd in een gemakkelijk toegankelijk geheugen en wel in een kleine cassettebandrecorder. Enige elektronische apparatuur is toegevoegd, omdat de signalen van de codeschijven en de dekadeschakelaars parallel worden aangeboden en voor de registratie in serie moeten worden omgezet. De nummering van de detailpunten per standplaats verloopt automatisch en wordt op het instrument zichtbaar gemaakt met behulp van indicatoren. De waarnemingen die met het veldinstrumentarium in het geheugen zijn verzameld, moeten geschikt worden gemaakt voor de automatische verwerking in de computer. De apparatuur die hiervoor benodigd is, bestaat uit een leeseenheid voor de magneetband en een ponskaartmachine. Hiermee kunnen achtereenvolgens de binnenkomende gegevens van een groot aantal veldinstrumenten met automatische registratie worden verwerkt.

